International specialized medium for agricultural mechanization in developing countries

ISSN 0084-5841

AMA

AGRICULTURAL MECHANIZATION IN ASIA, AFRICA AND LATIN AMERICA

VOL.50, NO.3, SUMMER 2019

FARM MACHINERY INDUSTRIAL RESEARCH CORP.


ECHO

International specialized medium for agricultural mechanization in developing countries

ISSN 0084-5841

AMA

AGRICULTURAL MECHANIZATION IN ASIA, AFRICA AND LATIN AMERICA

VOL.50, No.3, SUMMER 2019

Edited by

YOSHISUKE KISHIDA

Published quarterly by

Farm Machinery Industrial Research Corp.

in cooperation with

The Shin-Norinsha Co., Ltd.

and

The International Farm Mechanization Research Service

TOKYO

CIRCULATION
(Tel.+81-(0)3-3291-3674)
(Fax.+81-(0)3-3291-5717)
Editorial, Advertising and Circulation Headquarters
1-12-3, Kanda Nishikicho, Chiyoda-ku, Tokyo 101-0054, Japan
URL: http://www.shin-norin.co.jp/english/
E-Mail: ama@shin-norin.co.jp

Printed in Japan

This is the 180th issue since its maiden issue in the Spring of 1971

EDITORIAL

20 years already has passed after going into the 21st century. The world's population is steadily increasing and has already reached about 7.5 billion. It is estimated to exceed 9.5 billion by 2050. China, with the largest population is expected to continue the population growth in the future by stopping the one-child policy. The world population is expected to surpass 10 billion within the 21st century. Resources are limited on the confined earth. We must survive using our limited resources well, especially the farmland. The farmland per capita continues to decrease. Therefore, it is necessary to raise the land productivity of agriculture. In order to increase land productivity, it requires timely and exact operations. Agricultural land productivity cannot be increased without the proper agricultural mechanization and should be promoted through the development of new means of mechanization in all regions. At the same time, the problem of declining agricultural labor force is emerging all over the globe.

In Japan, the population of agriculture engagement has already dropped to 1.7 million, and nearly 100,000 people are getting away from agriculture every year. More than 80% of the labor force is over 60 years old. The 80% of the labor force will be over 80 years old after 20 years. The transferring of labor force from other sectors cannot be expected. Thus, Japan is in a difficult situation where agricultural labor productivity must be increased 5 times within 20 years.

In Japan, therefore, it is necessary to increase the agricultural labor productivity by new means of mechanization. The small agricultural robot machines would play the essential role for this purpose. There are many operations in Japanese agriculture that are not yet mechanized. For example, in the case of fruit trees, it is the pruning operations that are not yet mechanized. These also have to be robotized using AI.

Currently, the word Sustainable Development Goals (SDGs) is being advocated in the world. In a word, we must do sustainable economy, sustainable agriculture in the confined earth. It is asked how to do it concretely. Among them, the development of agricultural mechanization is the most important. As for how to do it, the new agricultural machine robots are required after all, making full use of the power of AI.

For the mechanization of developing countries, we have been seeking appropriate technology and now we have to rethink what is appropriate. This possibility is greatly expected that people in developing countries will also use small, inexpensive agricultural machine robots as they use smartphones.

It is necessary to promote the research of new agricultural machine robots for farmers in developing countries. We have to make every effort to make good use of new technologies and to enable many people to live in harmony and with good health in this confined earth. The responsibility on the people involved in agricultural machinery development is extremely important.

Yoshisuke Kishida
Chief Editor
July, 2019

CONTENTS

AGRICULTURAL MECHANIZATION IN ASIA, AFRICA AND LATIN AMERICA

Vol.50, No.3, Summer 2019

Effect of Rotary Plough and Precision Land Levelling on Faba Bean Response to Organic Fertilization

by
O. T. Bahnas
Head
Researchers at Agric. Eng. REs. Inst.,
Agric. Res. Center
EGYPT
otbahnas@yahoo.com

M. Y. Bondok
Emeritus Chief
Researchers at Agric. Eng. REs. Inst.,
Agric. Res. Center
EGYPT
mohamedbondok901@yahoo.com

Abstract

This study was carried out to identify the effect of rotary plough and precision land levelling on faba bean response to organic fertilization using rice straw. The experiment was designed statistically as a split plots with three replicates. The main plots involved the rotary ploughing treatment levels i.e. rotary plough as a minimum tillage, rotary plough after chisel plough (one pass) and rotary plough after chisel plough (two passes). The sub plots were located for the precision land levelling slope treatment levels i.e. 0.01, 0.02 and 0.03%. The control treatment was the chisel plough (two passes) followed by traditional land levelling under bereaved of rice straw application. The rotary plough after chisel plough of 1 pass followed by 0.02% precision land levelling slope under rice straw application accomplished more desirable soil characteristics, required the lower total applied irrigation water amount, produced higher seed yield, terminated higher water use efficiency and achieved higher net return.

Keywords: Rotary plough, Precision land levelling, Faba bean, Rice straw

Introduction

The Egyptian annual faba bean cultivated area is about 42,522 ha which produced about 148,721 t seeds (Ministry of Agricultural and Land Reclamation, 2013). In Egypt, faba bean constitutes a major part of the diet due to the richness in seed protein content, used as a vegetable either the green, dried fresh or canned, as well as, using secondary product as animal feeding. It plays an important role in maintaining soil productivity due to fixing atmospheric nitrogen according to the symbiotic relation with rhizobium through root nodules (Abou Amer et al., 2014). So, increasing faba bean production and improving yield quality is the major target to face the demand of the increased Egyptian population. Fertilization is considered as an efficient factor in faba bean production (Abd El-Aziz (2008) and Abou-Amer et al., 2014). Excessive and continuous chemical fertilizers application creates accumulated side effects on the human and the animal health and the environment and maximizes the agricultural production costs (Savci, 2012). In Egypt, the agricultural policy directs a great attention to minimize chemical fertilizers application. There is recent attention towards utilization rice straw as an organic soil conditioner (Khider, 2004 and Ali, 2011). Abdelhameed et al. (2004) found that the composted rice straw application significantly enhanced faba bean growth and increased crop yield.

During rice harvest, the combine harvester distributes straw upon the soil surface without chopping. The long straw pieces may swing and breakdown tillage machines during the next crop soil preparation. There are available options to farmers for rice straw management including burning, baling and incorporation and surface retention. According to the high cost of rice straw assembling and transporting , the farmers choose the easy, inexpensive and rapid method through the uncontrolled burning that disposition it and save enough time to prepare the seedbed for the next crops, regardless of environmental pollution (El-Gendy, et al., 2009). The rotary plough is an appropriate implement for rice straw incorporation (Abdel-Galil, 2007 and Rusu, 2011). It imparts rotation to successive bites of the soil. Then, the chopped straw pieces fall between soil bites and mix with the soil particles, enhancing straw decomposition rate by improving contact between soil particles and straw pieces, achieving appropriate soil conditions (Ji et al., 2012).

On the other hand, faba bean responds well to irrigation as plants are not particularly susceptible to water logging. Hence, controlled irrigation is essential to produce faba bean high crop yield and quality (Hegaba et al., 2014). Faba bean is sensitive to both over and under irrigation. Beginning of the flowering period is most sensitive to water shortage. Soil water depletion in the root zone during this period should not exceed 25%. Water shortage just prior and during early flowering reduces the number of fruits (El-vendy et al., 2001 and Samiha et al., 2010). So, it is an important issue to depend on the precision land leveling as an efficient and rationalized method to manage the available water (El-Khatib et al., 2014). Meanwhile, rice straw incorporation increases soil moisture accumulation, resulting in the increased soil water-holding capacity (Lentz and Bjorneberg, 2003 and Bescansa et al., 2006). Bahnas and Bondok (2010) indicated that the precision land levelling increased faba bean response to application of the composted rice straw. Hence, the present work aimed to assess rotary ploughing and precision land levelling under organic fertilization using rice straw on faba bean crop yield.

Material and Methods

Experimental Site and Soil Characteristics:

During October 2013 to end of April 2014, a field experiment of 0.36 ha (105 × 60 m) was established at Kalabsho Region, El-Dakhlia Governorate, Egypt that is located at 31.409408 latitude and 31.478470 longitude with an altitude of 1,550 m above sea level which has an average annual rainfall of 175.00 mm, whereas the pre-seeding crop was rice which was harvested using a general purposes combine harvester. As cited by El-Serafy and El-Ghamry (2006), **Table 1** shows the soil mechanical analysis and the soil texture classification. As pointed out by El-Serafy and El-Ghamry (2006) and Garcia (1978), **Table 2** presents some soil characteristics. According the procedure of El-Serafy and El-Ghamry (2006), some rice straw characteristics are shown in **Table 3**. According to Mc Clung et al. (1985), **Fig. 1** demonstrates the experimental site survey which was measured in terms of surveying grid.

Treatments and Statistical Design:
During the experiment, the following treatments were tested:

1. Rotary ploughing which included levels of rotary plough as a minimum tillage, rotary plough after chisel plough (1 pass) and rotary plough after chisel plough (2 passes).
2. Precision land levelling slope which included levels of 0.01, 0.02 and 0.03%.

These treatments were compared with chisel plough (two passes) followed by traditional land levelling (0.01% slope and accompanied with bereaved of rice straw application (control).

Fig 1 Schematic diagram of the experimental site topography

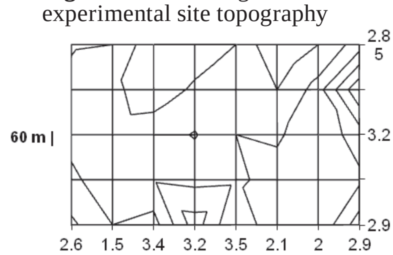

The experiment was established as a split plots statistically design with three replications. The main plots involved the rotary ploughing treatment levels and the sub plots included the precision land levelling slope treatment levels.

Agricultural Practices:
Seed bed preparation:

The seed bed was prepared as the previous mentioned treatments. The soil was tilled using a 7 shares chisel plough. Rice straw was chopped and incorporated into soil using a rotary plough with 24 L-shape blades. The traditional land levelling was carried out using a mounted hydraulic scraper of 1.26 m^3 capacity (0.60 × 3.00 × 070 m). For precision land levelling, the scraper was accompanied with a laser control equipment that consists of transmitter (Spectra-physics 1145 laser plane), control box (CB2MTD), receiver mast, receiver unit and telescoping grade rod (1084 English).

Planting:

A 4 rows pneumatic planter was used to plant the selected seeds of Giza 3 faba bean variety at row spacing of 0.60 m with 0.20 m hill

Table 1 Soil mechanical analysis of the experimental site

Sand, %			Silt, %	Clay, %	Soil texture class
Coarse, %	Fine, %	Total, %			
64.41	3.63	68.04	14.85	17.11	Sandy

Table 3 Some rice straw characteristics

Moisture content, % (d.b.)	Ash, %	Organic matter, %	Organic carbon, %	Total N, %	C/N ratio
9.00	17.79	75.21	43.46	0.482	90.16

Table 2 Some soil characteristics of the experimental site

Bulk density, g/cm^3	pH, 1:2.5 (susp.)	Available nutrients, ppm			Fieldcapacity, Wt/wt%	Wilting point, Wt/wt%	Available water, mm	nfiltration rate, mm/h
		N	P	K				
1.55	7.30	21.41	10.71	271.40	17.01	6.90	23.91	45

spacing at the same row.

The chisel plough, the rotary plough, the traditional land levelling unit and the planter were operated using a 2 WD tractor of 60 kW power. The precision land levelling unit was operated using a 4 WD tractor of 90 kW power.

Irrigation:

The border surface irrigation system was applied using an electric Archimedean screw of 252 m^3/h discharge. The irrigation was scheduled as 4, 3 and 2 irrigations with intervals of 12, 14 and 16 days to achieve 50, 60 and 70% of the available water during flowering, bud setting and maturity growing stages, respectively.

The other practices were done uniformly for all treatments according to the recommendations of Ministry of Agriculture and Land Reclamation (2005).

Measurements:

Soil characteristics:

At harvest, soil mean weight diameter, soil bulk density, soil infiltration rate and soil available macronutrients concentration were determined according to Kepner, et al. (1982), ASAE (1992), Garcia (1978) and Hesse (1971), respectively.

Total irrigation water amount:

The total irrigation water amount (TIW) is determined as follows:

$$TIW = \frac{LR + CR}{\eta A} m^3 / fea \qquad \text{....... (1)}$$

Where: *LR* is leaching requirements, m^3/ha.

CR is crop water requirements, m^3/ha.

η is irrigation system efficiency, %.

A is irrigated area, ha.

LR is estimated as outlined by Doorenbos and Prutt (1977) as follows:

$$LR = \frac{EC_i}{EC_d} \qquad \text{....... (2)}$$

Where: EC_i is irrigation water electrical conductivity, dS/m.

EC_d is drainage water electrical conductivity, dS/m.

The net crop water requirements and the irrigation interval (II) are calculated as cited by FAO (1979) and Israelson and Hansen (1962) as follows:

$$WHC = (FC - PWP)\,p_b \bullet d \bullet 10\,mm \qquad \text{..... (3)}$$

$$MaxCR = \frac{MAD \bullet WHC}{100}\,mm \qquad \text{..... (4)}$$

$$Max.CR = \frac{Max.g.w.r}{\eta}\,mm \qquad \text{..... (5)}$$

$$II = \frac{Max.CR}{Etcrop}\,day \qquad \text{..... (6)}$$

$$Et = Et_0 \times k_c \text{ mm/day} \qquad \text{..... (7)}$$

Where: *WHC* is soil water holding capacity, mm.

FC is soil field capacity, %.

PWP is soil permanent wilting point, %.

ρb is soil bulk density, g/cm3.

D is effective root zone depth, m.

MAD is management allowable deficit, mm/m.

Max.g.w.r is maximum gross water requirements, mm.

Et is net crop water requirements, mm.

Et_0 is potential evapotranspiration, mm/day.

K_c is crop factor.

Et_0 was calculated according to the data recorded by Kafr Saad weather station, Domitta Governorate, Egypt which is affiliated to the Central Laboratory for Agricultural Climate, Agricultural Center Res., Ministry of Agriculture and Land Reclamation, Egypt.

According to James (1988), the irrigation water amount is determined using a rectangular shape crested weir as follows:

$$Q = k.c_d A\sqrt{H} \text{ L/s .} \qquad \text{..... (8)}$$

Where: *Q* is orifice discharge, L/s

k is discharge coefficient.

cd is constant unit.

A is orifice area, m^2.

H is effective water head over the orifice centre, m.

Land levelling accuracy:

According to Mc Clung et al. (1985), at harvest, land levelling accuracy is determined including the following items:

a. Soil topography:

It is studied in terms of surveying grid and standard deviation.

b. Land levelling index (p.l.i.):

$$p.l.i. = \frac{\sum C + \sum F}{N}\,cm \qquad \text{..... (9)}$$

Where: *C* is cut required at grid point, cm.

F is fill required at grid point, cm.

N is number of points.

Faba bean seed yield:

At harvest, for each experimental unit, an area of 1 m^2 was taken randomly to determine the faba bean seed yield. Then, it was calculated on basis of 14% moisture content (d.b.).

Water use efficiency (WUE):

$$WUE = \frac{grain\ yield,\ kg/fed.}{appllied\ irrigation\ water\ amount,\ m^3/fed.}\,kg/m^3 \qquad \text{..... (10)}$$

Economic Analysis:

Due to using rice straw as an organic fertilizer for faba bean, the economic analysis is employed by applying the general formula of sequence cropping systems with respect to the crop intensification according to El-Hawary (2014). The formula is applied using web application at www.elhawary.net as follows:

$$EYAR_5 = \frac{NR/day\ sequence\ 'a'}{NR/day\ sequence\ 'b'}\ or\ \frac{sequence\ 'a'}{sequence\ 'b'} \qquad \text{..... (11)}$$

Where:

$$sequence\ 'a' = \frac{\left(\sum_{L=1}^{m}\left(\sum_{k=1}^{mL}(Y_{aLk}\,\Pr_{aLk}) - Co_{aL}\right)\right) + \left(\sum_{i=1}^{n}\left(\sum_{j=1}^{ni} Y_{aij}\,\Pr_{aij}\right) - \sum_{i=1}^{n} Co_{ai}\right)}{D_a}$$

$$sequence\ 'b' = \frac{\left(\sum_{L=1}^{m}\left(\sum_{k=1}^{mL}(Y_{bLk}\,\Pr_{bLk}) - Co_{bL}\right)\right) + \left(\sum_{i=1}^{n}\left(\sum_{j=1}^{ni} Y_{bij}\,\Pr_{bij}\right) - \sum_{i=1}^{n} Co_{bi}\right)}{D_b}$$

$EYAR_5$ is value as percentage = *($EYAR_5$ value - 1) × 100.*

m is number of monoculture crops pertaining to crop sequence.

mL is the total number of main and by-products together of the monoculture crop available for every *L* (where *L* is monoculture crop).

n is number of simultaneous or relay intercropping crops pertaining crop sequence.

ni is total number of main and by-products together of the intensive crop available for every *i* (where: *i* is intensive crop).

Y_{aLk}, Pr_{aLk} and Co_{aLk} are yield, price and production cost (main and by-products) of each crop of monoculture crops of sequence "a", respectively.

Y_{aij}, Pr_{aij} and Co_{aij} are yield, price and production cost (main and by-products) of each crop of crop sequence "a", respectively.

Y_{bLk}, Pr_{bLk} and Co_{bLk} are yield, price and production cost (main and by-products) of each crop of monoculture crops of sequence "b", respectively.

Y_{bij}, Pr_{bij} and Co_{bij} are yield, price and production cost (main and by-products) of each crop of intensive sequence "b", respectively.

ΣCo_{ni} is total cost of intensive sequence.

D_a and D_b are duration of sequences "a" and "b", respectively, day.

In this study, sequence 'a' was rice followed by faba bean, while, sequence 'b' was the traditional farmer sequence i.e. rice followed by sugar beet.

Statistical Analysis:

SAS computer software package version 9.10 is used to employ the analysis of variance and the LSD tests for faba bean seed yield data.

Regression and Correlation Analysis:

Microsoft Excel 2013 computer software is used to carry out the simple regression and correlation analysis to represent the relation between faba bean seed yield and precision land levelling slope under different of rotary ploughing treatment levels.

Resalts and Discussion

Soil Characteristics:

Through **Figures 2** to *7*, data show that the rotary plough after chisel plough 1 pass followed by 0.02% precision land levelling slope achieved the moderate soil mean weight diameter of 25 mm, the lower soil bulk density value of 1.28 g/m^3, the lower soil infiltration rate value of 20 mm/h and the higher concentration of soil macronutrients values of 24, 17 and 311 ppm for N, P and K, respectively. This result could be explained that the chisel plough 1 pass disturbs the soil, achieving the crumbled clods that tend to be loose and free to move with the beating action of the rotary plough blades, resulting in moderate size of soil particles. Whilst, the 2nd pass of the chisel plough increases the disturbed soil, minimizing the beating action of the rotary plough, creating larger soil particles. Whilst, using the rotary plough as a minimum tillage achieved the lower values of soil mean weight diameter. It could be illustrated that the untilled soil is objected to the subsequent beating action of the blades, leading to higher kinetic energy charged to the crumbled clods, causing higher impact action between the clods together, resulting in finer soil particles.

The figures declare that the precision land levelling achieved the soil particles of smaller mean weight diameter, lower values of soil bulk density, lower values of soil infiltration rate and more amount of the available soil macronutrients con-

Fig. 2 Effect of rotary plough on soil mean weight diameter (MWD) under different precision land levelling slope levels

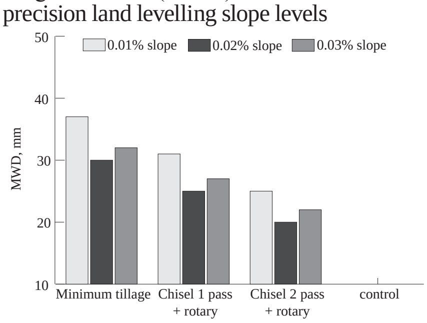

Fig. 3 Effect of rotary plough on soil bulk density under different precision land levelling slope levels

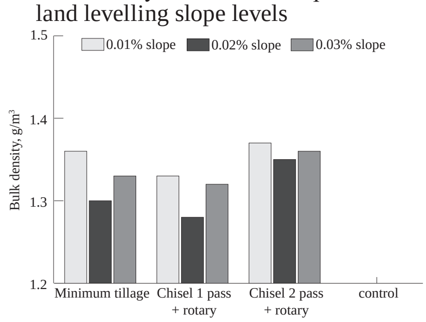

Fig. 4 Effect of rotary plough on soil infiltration rate under different precision land levelling slope levels

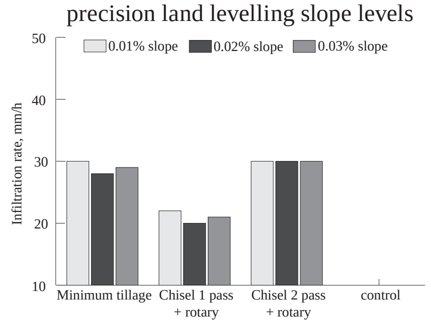

Fig. 5 Effect of rotary plough on available soil N concentration under different precision land levelling slope levels

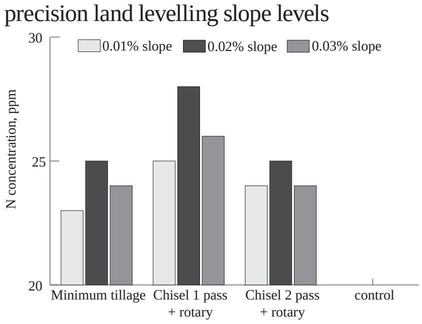

Fig. 6 Effect of rotary plough on available soil P concentration under different precision land levelling slope levels

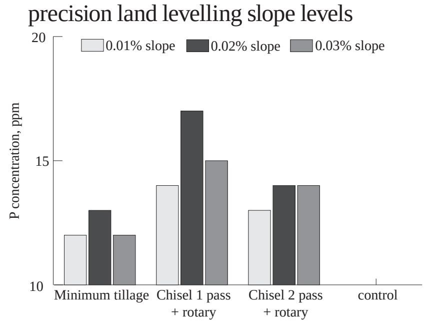

Fig. 7 Effect of rotary plough on available soil K concentration under different precision land levelling slope levels

centration than that were obtained using the traditional levelling by 25, 4, 11 and 105, 121 and 109%, respectively. This finding could be explained that the precision land levelling accomplished fine soil particles, which having a negligible electromagnetic charge, increasing the soil free pore spaces per unit volume, resulting in lower soil bulk density. Consequently, the irrigation water streams, detaches soil particles from the surface and pushes fine particles into surface pores, creating smaller pores that offer greater resistance to gravity, where they can impede the infiltration process. Meanwhile, the finer soil particles of greater specific surface area may release more amounts of the available soil macronutrients.

The figures reveal that rice straw application improved the soil characteristics, comparing with the bereaved of rice straw application. It is due to decomposition of the retained rice straw in the voids between soil particles, sticking one to another, increasing the free pore spaces per soil volume unit.

Applied Irrigation Water Amount:

Figure 8 transposes that the rotary plough after chisel plough 1 pass followed by 0.02% precision land levelling slope required the lower irrigation water amounts of 3369.05 m^3/ha during the growing season i.e. 1392.86, 1107.14 and 869.05 m^3/ha during flowering, bud setting and maturity growth stages, respectively. The rotary plough as minimum tillage, after chisel plough 1 pass and after chisel plough 2 passes saved the total irrigation water amount by 12, 18 and 15%, comparing with that required using the traditional practice. It may be explained that the rotary plough creates fine soil particles that impede the infiltration process. Also, the precision land levelling of 0.01 0.02 and 0.03% slope saved the total irrigation water amount by 28, 36 and 32% from that was required using the traditional land levelling. It is due to the high accuracy of precision land levelling which decreases the water irrigation losses by deep-percolation, evaporation and runoff. Rice straw application saved the total irrigation water amount by about 8% from that was required in case of the bereaved of rice straw application. This finding is illustrated that rice straw incorporation increases the soil moisture accumulation, resulting in the increase of soil water holding capacity, soil hydraulic conductivity and water retention.

Land Levelling Accuracy:

Figure 9 reveals that using rotary plough after chisel plough 1 pass followed by the precision land levelling of 0.01, 0.02 and 0.03% slope recorded the lower values of the difference between the highest and the lowest spots of 0.20, 0.20 and 0.40 m, with an average level for the total spot readings of 3.04, 3.15 and 3.45 m and a standard deviation of ± 0.2386, ± 0.1285 and ± 0.2646, respectively. While, using rotary plough after chisel plough 2 passes followed by the precision land levelling of 0.01, 0.02 and 0.03% slope accomplished the higher values of the difference between the highest and the lowest spots of 1.10, 0.80 and 1.80 m, with an average level for the total spot readings of 3.42, 3.40 and 3.47 m and a standard deviation of ± 0.3470, ± 0.2796 and ± 0.3351, respectively. While, the traditional levelling recorded the difference between the highest and the lowest spots value of 1.50 m, with an average level for the total spot readings of 3.45 m and a standard deviation of ± 4.3526.

This finding could be explained that the rotary plough after chisel plough 1 pass creates a proper disturbed surface which lowers the soil curette. In addition, this proper seed bed facilitates both the application and removal of soil water for irrigation and drainage. These practices can result in high efficiency of irrigation water application, uniform distribution of irrigation water and elimination of tail water. The irrigation water penetrated more rapidly in this proper seedbed than in other cases. When application of water continued; the soil water content become greater than other cases. The higher infiltration of water to depth appeared to be mainly due to the greater continuity of channels in soil which are not disturbed by either the intensive tillage or minimum tillage.

Due to the significant effect of the precision land levelling on the soil topography conservation.

Fig. 8 Effect of rotary plough on applied irrigation water amount under different precision land levelling slope levels

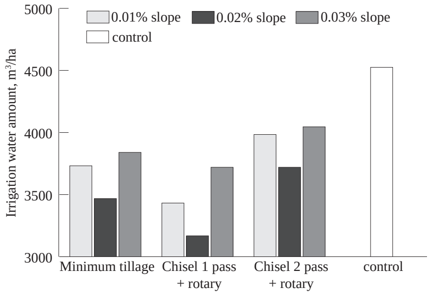

Fig. 9 Schematic diagram of the experimental field grid survey at harvest

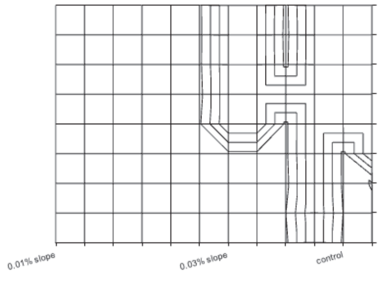

Faba Bean Seed Yield:

Figure 10 demonstrates that the higher faba bean seed yield of 3.33 t/ha was obtained using rotary plough after chisel plough 1 pass followed by precision land levelling of 0.02% slope. It is shown that using the rotary plough as minimum tillage, after chisel plough 1 pass and after chisel plough 2 passes increased faba bean seed yield by 105, 108 and 103% from that was obtained using the traditional practise, respectively. While, the precision land levelling of 0.01, 0.02 and 0.03% slope, increased faba bean seed yield by 119, 125 and 122% from that was recorded using the traditional levelling, respectively. This finding means that, faba bean seed yield was affected significantly by both the rotary plough and the precision land levelling which improves the soil conditions, resulting in the release of more available soil nutrients to uptake by faba bean plants. Meanwhile, rice straw application increased faba bean seed yield by about 109% from that was yielded using the bereaved of rice straw application. This result is explained that rice straw decomposition leads to the increase of nutrients solubility and nutrient availability to the plants that enhance plant growth and development.

The analysis of variance test indicates that there is a highly significant difference in faba bean seed yield due to the rotary plough and the precision land levelling. The L.S.D. test at 0.05 level shows that the rotary plough after chisel plough 1 pass followed by the precision land levelling slope of 0.02% achieved the highest faba bean seed yield among the other treatments. The regression and correlation analysis reveals that faba bean seed yield (y) correlated positively with the precision land leveling slope (x) as follows:

Minimum tillage: $y = 0.02\ x^2 + 0.08\ x + 1.28$ ($R^2 = 1$)

Rotary plough after chisel plough 1 pass: $y = 0.02\ x^2 + 0.06\ x + 1.32$ ($R^2 = 1$)

Rotary plough after chisel plough 2 passes: $y = 0.01\ x^2 + 0.02\ x + 1.33$ ($R^2 = 1$)

Water Use Efficiency:

Figure 11 reveals that the higher water use efficiency value of 098 kg/m3 was obtained using rotary plough after chisel plough 1 pass followed by 0.02% precision land leveling slope. Using rotary plough as a minimum tillage, after chisel plough 1 pass and after chisel plough 2 passes increased the water use efficiency by 123, 144 and 135% from that was recorded using the traditional practice, respectively. Also, the precision land levelling of 0.01, 0.02 and 0.03% slope, increased the water use efficiency by 164, 200 and 198% from that was obtained using the traditional levelling, respectively. While rice straw application increased the water use efficiency by 130% comparing with the bereaved of rice straw application.

Economic Analysis:

Figure 12 demonstrates that the higher net return value of 1302.98 $/ha was recorded using rotary plough after chisel plough 1 pass followed by precision land levelling of 0.02% slope. It achieved higher net return than that recorded using the control practice and sequence ‘b’ by 117.27 and 117.31%, respectively. While, rotary plough after chisel plough 2 passes followed by precision land levelling of 0.03% slope achieved the lower net return value of 1220.34 $/ha.

Conclusions

The rotary plough after chisel plough 1 pass followed by 0.02% precision land levelling slope under rice straw application improved the soil characteristics. It saved the total applied irrigation water amount by 18% from that required using the traditional practice. It conserved significantly the soil topography. It produced higher faba bean seed yield by 108% than that obtained using the traditional practice. It achieved higher net returns than that recorded using the control practice by 117.27%. Finally, It is recommended to apply the rotary and the precision land levelling under rice straw application due to the desirable soil conditions, the higher faba bean grain yield and the higher net returns, comparing with the traditional practice.

REFERENCES

Abd El-Aziz, F. I. 2008. Effect of biological and mineral fertilization on yield and quality of faba bean (Vicia faba L.) in Northern state. M.Sc. (Envir.) Thesis, (Council of Bio Sci, Advanced Tech. andEnvi-

Fig. 10 Effect of rotary plough on faba bean seed yield under different precision land levelling slope levels

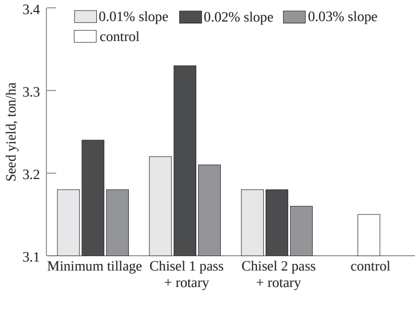

Fig. 11 Effect of rotary plough on faba bean water use efficiency under different precision land levelling slope levels

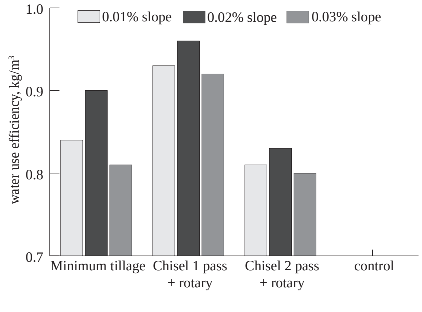

Fig. 12 Effect of rotary plough on net return under different precision land levelling slope levels

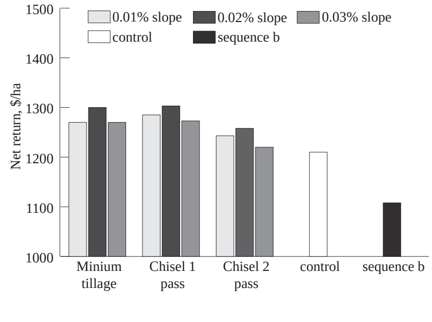

ronment. Academy of Sci. Sudan.
Abd El-Hameed, M. T., T. Horiuchi and O. Shiya. 2004. Composting of rice straw with oilseed rape cake and poultry manure and its effects on faba bean (Vicia faba L.)growth and soil properties. Bioresource Tech., 93(2): 189-193.
Abd El-Galil, H. S. 2007. Effect of using rotary plow on soil physical properties and barley yield under rainfall conditions. Misr J. Agric. Eng., 24 (4): 666-687.
AbouAmer, A. I., A. F. Hassan and M. A. Abd El Wahab. 2014. Effect of mineral fertilization and plant density on faba bean (Vicia faba) production in Siwa Oasis. Alex. J. Agric. Res. 59 (1): 19-26.
Ali, Laila K. 2011. Astudy of some methods of waste management of rice through its impact on soil physical properties, N, P and K contents in maize yield and water use efficiency under different tillage systems. Australian J. of Basic and Applied Sci., 5 (5): 1017-1034.
ASAE standard: S296.4 1992. Cubes, Pellet, and crumbles-definitions and methods for determining density, durability and moisture content: 384.
Bahnas, O. T. and M. Y. Bondok. 2010. Effect of precision land leveling on faba bean response to compost application.Misr J. Agric. Eng., 27 (2): 465-481.
Bescansa, P., M. J. Imaz, I. Virto, A. Enrique and W. B. Hoogmoed. 2006. Soil water retention as affected by tillage and residue management in semi-arid Spain. Soil and Tillage Res. 87: 19-27.
Doorenbos, J. and W. O. Prutt. 1977. Guidline of predicting crop water requirements. Irrigation and drainage paperno 24.FAO.
El-Gendy, A. M., M. A. El-Adl, H. N. Abd El-Maheed and E. M. Moohamed. 2001. Management of pressurized irrigated faba bean in sandy soils. Misr J. Agric. Eng., 18 (1): 29-44.
El-Gendy, A. M., M. A. Baiomy, M. M. Abdelhamed and Sahar A. Mosa. 2009. Design and fabrication of a simplified mechanical handling system of rice straw baling operation to reduce environment pollution. Misr J. Agric. Eng., 26 (2): 676-685.
El-Hawary, N. A. 2014. Formula for economic evaluation of crop sequence systems. The general formula for economic evaluation from the perspective of crop intensification. Book. Pub: LAMPERT Academic Publishing, Germany, 160 pp. ISBN 978-3-659-52049-5.
El-Khatib, S. I., N. M. El-Bialee, Ilham I. El-Khatib and A. M. El-Bialee. 2014. Effect of laser leveling, water quantities and rhizobium inoculation on fixing N2 efficiency with faba bean. Agriculture and Biology J. of North America, 5 (2): 87-96.
El-Serafy, Z. M. and A. M. El-Ghamry. 2006. Methods of soil and water analysis (Practices), Soils Dept., Faculty of Agric., Mansoura Univ., 253 pp.
FAO. 1979. Irrigation and drainge. Paper No. 33. Rome. Italy.
Garcia, I. 1978. Soil-Water Engineering.Laboratory Manual.Dept. of Agric. and Chemical Eng., Colorado State Univ., 4th Collins, Colorado, USA.
Hegab, A. S. A., M. T. B. Fayed, Maha M. A. Hamada and M. A. A. Abdrabbo. 2014. Irrigation requirements of faba bean in North Delta of Egypt in relation to planting dates. Annals of Agric. Sci., 59 (2): 185-193.
Israelson, O. W. and V. E. Hansen. 1962. Irrigation Principles and Practices.3rd Ed. John Willey and Sons. Inc., New York, 265 pp.
James, L. G. 1988. Principles of farm irrigation system design. John Willey&sons.Inc.,WashingMg State Univ., 73: 152-153 and 350-351.
Ji, X. H., J. M. Wu, H. Peng, L. H. Shi, Z. H. Zhang, Z. B. Liu, F. X. Tian, L. J. Huo and J. Zhu. 2012. The effect of rice straw incorporation into paddy soil on carbon sequestration and emissions in the double cropping rice system. J. Sci. Food Agric., 92: 1038-1045.
Kepner, R. A., R. Beiner and E. L. Barger. 1982. Principles of farm machinery. 3rd Ed., The AVI Pup. Com. Inc. 527 pp.
Khider, M. O. 2004. Development of a combined unit with a combine for utilization in field waste. M.Sc. thesis Agric. Mech. Dept. Faculty of Agric. Mansoura Univ.
Lentz, R. D. and D. L. Bjorneberg. 2003. Polyacrylamide and straw residue effects on irrigation furrow erosion and infiltration. J. Soil Water Conserv., 58: 312-319.
Mc Clung, J. A., S. Shepley, M. Ismail and M. N. Seif El-Yazal. 1985. Mechanical and economical study of land leveling in Middle Egypt.Ag. Mech. Proj. Paper work No. 21. Ministry of Agricultural and Land Reclamation.
Ministry of Agriculture and Land Reclamation. 2005. Faba bean planting. Central Administration for Agric. Extension, Egypt, Pamphlet No. 929 (In Arabic).
Ministry of Agricultural and Land Reclamation. 2013. Economic affairs sector. Bulletin of The Agric. Statistics. Part (1). Winter crops, Egypt, 2011-2012: 27-29. (In Arabic)
Rusu, T., P. I. Moraru, I. Bogdan, A. I. Pop and M. L. Sopterean. 2011. Effect of soil tillage system upon the soil properties, weed control, quality and quantity yield in some arable crops. World Academy of Sci., Eng. and Tech. 59.
Samiha, A. Ouda, M. A. Shreif and R. Abou El-Enin. 2010. Increasing water productivity of faba bean grown under deficit irrigation at Middle Egypt. 14th Int. Water Tech. Conf., Cairo, Egypt: 345-355.
Savci, S. 2012. Investigation of effect of chemical fertilizers on environment. APCBEE Procedia, 1: 287-292.

■■

Physico-Mechanical Properties of Cassava Stem as Related to Cutting

by
Sahapat Chalachai
Agricultural Systems and Engineering,
Asian Institute of Technology, Pathumthani 12120
Agricultural Engineering and Technology,
Rajamangala University of Technology Tawan-ok,
Chonburi 20110
THAILAND

Peeyush Soni *
Dept. of Agricultural and Food Engineering,
Indian Institute of Technology Kharagpur,
Kharagpur - 721302, West Bengal,
INDIA
* Corresponding author: soni@iitkgp.ac.in

Abstract

Shear, compression and bending properties of cassava stem (Huy-Bong, Rayong-81) were determined. Experiments were conducted at four-levels of loading rate (20-100 mm min^{-1}) with four-levels of knife bevel angle (15-60 degree) for both varieties. The maximum shear strength increased from 4.99 to 7.36 MPa for Huy-Bong and 2.80 to 3.68 MPa for Rayong-81, when the knife bevel angle was increased from 15 to 60 degrees at 20 mm min^{-1} loading rate. As the loading rate was increased from 20 to 100 mm min^{-1} at 30 degree knife bevel angle, the maximum shear strength decreased from 5.51 to 4.57 MPa for Huy-Bong and 3.06 to 2.68 MPa for Rayong-81. The specific cutting energy increased from 46.10 to 103.40 mJ mm^{-2} for Huy-Bong and 31.28 to 68.96 mJ mm^{-2} for Rayong-81 when the bevel angle was increased from 15 to 60 degrees at 20 mm.min^{-1} rate of loading. As the loading rate was increased from 20 to 100 mm min^{-1} with 30 degree knife bevel angle the specific cutting energy decreased from 62.25 to 39.18 mJ mm^{-2} for Huy-Bong and 37.08 to 30.46 mJ mm^{-2} for Rayong-81. For Huy-Bong, the highest compression strength and specific compressing energy at a 20mm min^{-1} loading rate were 8.06 MPa and 91.47 mJ mm^{-2}. The compression strength and specific compressing energy varied from 7.54 to 4.33 MPa and 101.47 to 56.24 mJ mm^{-2} for Huy-Bong and 6.02 to 4.79 MPa and 60.62 to 36.22 mJ mm^{-2} for Rayong-81 when loading rate was increased from 20 to 60 mm min^{-1}. But on the contrary the bending strength and specific bending energy for Huy-Bong decreased from 4.10 to 3.72 MPa and 98.46 to 85.67 mJ.mm^{-2} for Huy-Bong, and 2.95 to 1.72 MPa and 54.56 to 45.33 mJ mm^{-2} for Rayong-81 respectively.

Keywords: Cassava stems, Physico-mechanical properties, Shear strength, Compression, Bending energy, Cutting energy.

1. Introduction

Cassava (Manihot esculenta), which is also referred to as manioc or yucca, is an important staple food crop for Africa, Asia and Latin America. Around 500 million farmers worldwide are estimated to cultivate cassava. At the end of the 18th century and early 19th century, cassava become known to most parts of Asia, and was subsequently introduced to Southern Thailand from Malaysia, and later on distributed throughout the country within a few years. In some countries, cassava is also grown for its leaves, which contain up to 25% protein on a dry weight basis (FAO, 1997). Both leaves and roots can be fed to farm animals (Apata & Babalola, 2012), while stems can be used as firewood and a substrate for growing mushrooms. However, the cassava stem needs to be converted into forage before fed to animals. For this purpose, appropriate mechanical means are sought for effectively cutting cassava stem into forage. As the first step in designing such a machine, design values of relevant factors are required. This research determines, through direct measurements, key physical and mechanical properties of cut cassava stem, for popular varieties in the study area.

Many studies have been conducted to determine the mechanical properties of plants. Koniger (1953) and Persson (1987) studied the principles of cutting plant material and stated that mechanical separation occurs at a predetermined and well-defined location in the material, in contrast to crushing, where several failure planes usually develop randomly. The cutting process, in all cases, is initiated when edge of the knife first makes contact with the material. During the continued motion of the knife, the contact forces and stresses increase and a stress pattern is built up inside the stalk until failure conditions are reached, either over the entire section at the same time, or gradually beginning in one point of the section and continuing until complete separation has been achieved. As a consequence, the cutting process leading to the final separation can be considered as a sequence of elementary cutting and deformation processes or modes of failure, each governed by different principles. Chancellor (1988) stated that the biological materials, commonly subjected to cutting, can be classified into two general categories:

a) non-fibrous materials having uniform properties in all directions at the time of cutting, the cells of these materials usually being turgid with liquid cell materials; and
b) fibrous materials with high tensile strength fibres oriented in a common direction and with comparatively low strength materials bonding the fibres together.

Chancellor (1988) and Ince et al. (2005) believed that with the second category of materials, which comprise thick-stemmed crops such as sorghum and maize, the concentrated compressive stress applied by the cutting tool to the cell wall causes cell pressure to increase and produces a tensile failure in the cell wall at the point of contact with the cutting tool. The point of contact is subjected to

a) accentuated tensile stresses due to the addition of bending stresses at the point of indentation to the hydrostatic stresses;
b) a uniquely high shear stress because of the applied compression stresses in one direction and the hydrostatic tensile stresses in an orthogonal direction; and
c) movement of the tool in a direction parallel to its edge and perpendicular to the direction of the compressive force applied which can further add to the shear stress applied to the cell wall at the point of contact.

However, most studies on the mechanical and physical properties of plants have been carried out during their growth using failure criteria such as force, stress and energy or their Young's modulus and the modulus of rigidity. For example, Anoussamy et al. (2000) and Skubisz et al. (2007) studied plant anatomy, lodging processes, harvest optimization, animal nutrition, industrial applications and the decomposition of wheat straw in soil. Yiljep and Mohammed (2005), and Shaw and Tabil (2007) studied the physical properties of the cellular material that are important for cutting, tension, bending, density and friction by using laboratory methods and procedures.

The key mechanical properties of forage material in context of cutting are strength in tension, shear and bending, density, and friction. These properties depend on species, variety, age of the plant, moisture content and the cellular structure. The values of these properties are different at different diameters and different locations of the plant stem. Many studies have been conducted to determine the mechanical properties of forage plants. Halyk and Hurlbut (1968), and Choi and Erbach (1986) studied the mechanical properties of alfalfa stems and showed that the maximum shearing stress changed between 0.4-18.0 MPa depending on moisture content. Similar results were reported by Prasad and Gupta (1975) who studied the mechanical properties of maize stalk in relation to cutting under quasi-static deformation. The study showed that for maize stalks at moisture content of 74% (w.b.), with increasing approach rate from 200-1000 mm min^{-1}, the shear strength decreased from 3.63 to 2.10 MPa. Ahlgrimm (1977) showed a small effect of moisture content on shear strength, with values ranging from 49 to 79 MPa based on dry matter cross-sectional area of the stem. McRandal and McNulty (1980) conducted shearing experiments on field grasses and reported that the shearing stress was 16 MPa and the shearing energy was 12.0 mJ mm^{-2}. Chattopadhay and Panday (1998) investigated mechanical properties of sorghum stalk in relation to quasi-static deformation, and showed that the shear strength decreased from 3.74 to 1.94 MPa at the forage state when the cutting rate was increased from 10-100 mm/min at 30º knife bevel angle. Khazaei et al. (2002) showed that by increasing cutting rate from 20 to 200 mm min^{-1}, the shear strength of the pyrethrum stalk decreased. Chen et al. (2004) showed that the average values of the maximum force and the total cutting energy for hemp were 243 N and 2.1 J respectively. Ince et al. (2005) concluded that the maximum shear stress and specific cutting energy of sunflower stalk were 1.07 MPa and 10.08 mJ mm^{-2}. Natthapong et al. (2008) studied the shear strength characteristic of bio-fuel (Eucalyptus) by using Universal Testing Machine (UTM) and showed that the maximum cutting force, maximum

Fig. 1 LLOYD Universal Test Machine

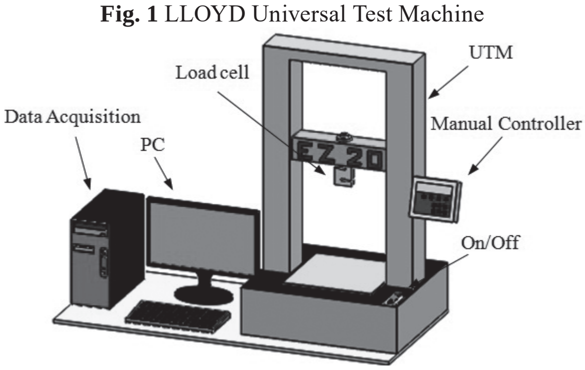

shear strength and specific energy with 30º knife bevel angle were less than that with 45º knife bevel angle. Adel et al. (2012) studied the influence of knife bevel angle, rate of loading and stalk section on major engineering parameters of lilium stalk, and showed that the shear strength and specific cutting energy increased when the knife bevel angle was increased. The highest compression strength and specific compressing energy were 6.86 MPa and 21.34 mJ mm^{-2}.

Other studies have been conducted on the bending characteristics of fibrous plants. Curtis and Hendrick (1969) determined that the section modulus in bending varied with the third power of the diameter for cotton stalks of diameters ranging from 7 to 16 mm; the modulus of elasticity varied from 600 to 3500 MPa. Prince et al. (1969) studied the modulus of rigidity of green lucerne and oven-dried specimens, finding mean values of 0.225 and 1.45 GPa respectively. Sakharov et al. (1984) reported that the required force to cut the stretched stalks was 50% less than that of unbent stalks. Chattopadhay and Panday (1998) determined the bending stress for sorghum stalk was 45.65 MPa at the forage stage. Ince et al. (2005) studied bending stress and modulus of elasticity of sunflower stalk, and showed that the bending stress decreased as the moisture content was increased. The average bending stress value varied between 37.77-62.09 MPa. The modulus of elasticity in bending also decreased as the moisture content and diameter of stalks increased.

Considering the importance of crop-specific characteristics, and the paucity of dedicated research on cassava, this study attempts to investigate some key mechanical and physical properties of cassava stalk. Keeping in mind the design and fabrication of a cassava stem cutting machine that is suitable for Thailand, this research determines shearing strength, compression strength, bending strength, specific shearing energy, specific compressing energy, and specific bending energy of cassava stems as a function of various stem regions, different rates of loading and different knife bevel angles.

2. Material and Methods

2.1 Research plan

The cassava stems were harvested randomly from a cassava farm in Buriram province of Thailand, from 10 months old healthy plants using a sharp knife, at a height of 100 mm above the soil surface. Harvested stems were securely wrapped and transported to the laboratory. All samples were kept under the shade in a normal environment. A test specimen was taken from same location i.e. near the root internodes (250 mm from the soil surface). Testing was completed as rapidly as possible in order to reduce the effect of drying. A UTM (LLOYD EZ20, United Kingdom) equipped with 50 N load cells with an accuracy of ±0.001 N was used to measure the shearing, compression and bending forces of the cassava stems (**Fig. 1**). The plan of the experimentation is given in **Tables 1** and **2**. A venire caliper (Mitutoyo, Japan, 0.02 mm) was used in measuring the stem diameters. Weights of the stems were recorded using a standard weight balance with an accuracy of 0.01 g (Mettler Toledo, USA).

Moisture content was determined by using the oven drying method (ASAE, 1983). The oven temperature was set at 105±3 ºC for 24 h and the **Eqn. 1** was used:

$$W_{wb} = \frac{W_w}{W_w + W_s} \times 100 \quad .....(1)$$

Where W_w is the weight of water (moisture) present in cassava stems (g), Ws is the weight of cassava stems solids (g), and W_{wb} is moisture content (%) on wet basis.

The mass per unit length of the specimen (Mohsenin, 1986) can be expressed by the **Eqn. 2**:

$$M = \frac{md}{t} \quad .....(2)$$

Where M is the mass per unit

Table 1 Research plan to study the effect of knife bevel angle

Independent variables	
Crop	Cassava (Huy-Bong and Rayong-81 varieties)
Crop maturity	Forage
Knife bevel angle, deg	15, 30, 45 and 60
Rate of loading, mm/min	20
Mode of deformation	Shear
Dependent variables	
Force	
Energy	

Table 2 Research plan to study the effect of rate of loading

Independent variables	
Mode of deformation	Shear
Crop	Cassava (Huy-Bong and Rayong-81 varieties)
Crop maturity	Forage
Knife bevel angle, deg	30
Rate of loading, mm/min	20, 40, 60 and 100
Mode of deformation	Compression and Bending
Crop	Cassava (Huy-Bong and Rayong-81 varieties)
Crop maturity	Forage
Loading plate (probe), diameter	30 mm
Rate of loading, mm/min	20, 40 and 60
Dependent variables	
Force	
Energy	

length, m is mass of cassava stems, d is diameter of cassava stems, and l is the length of cassava stems.

In this study, tests were conducted under quasi-static condition, using the UTM to determine shear, compression and bending resistance of cassava stems at the forage stage for different knife bevel angles (15-60º) and rate of loading (20-100 mm min^{-1}). A small fixture was used to hold the cassava stem samples at the base of the test machine.

2.2 Shear Test

The specially fabricated fixture (fixed clamp) was fixed rigidly on the base platform of the test machine under the crosshead (movable clamp). A flat knife of 6 mm thickness, 50 mm width, 125 mm length, and 0.05 mm of edge radius was fitted on the crosshead of UTM, perpendicular to the length of the cassava stem specimen (**Fig. 2**). The flat knife was fabricated out of high carbon steel and had 15, 30, 45 and 60 degree bevel angle. The cassava stem specimens were held onto fixture with the help of plate supports of the fixed clamp (U-type clamps) at both ends of the sample. During downward movement of the crosshead, the knife cut the sample by shear and passed through the slots provided in the fixture below the specimen (Adel et al., 2012). The force required for shearing the cassava stems at the crosshead speed of 20, 40, 60 and 100 mm min^{-1} was recorded against time on the UTM chart recorder.

During the shearing tests, the shearing force on the load cell with respect to knife penetration for different loading rates and knife bevel angles was recorded. The maximum shear strength (σs) in MPa and specific cutting energy (Ess) in mJ mm^{-2} were calculated by using **Eqns 3** and **4** (Chattopadhyay and Pandey, 1998; Adel et al., 2012),

$$\sigma_s = \frac{F_{max}}{A} \quad .....(3)$$

Where F_{max} is the maximum cutting force and A is the cross-sectional area of cassava stems at the plane of shear.

The specific shearing energy was calculated by integrating the curves of shear force and displacement.

$$E_{ss} = \frac{1}{A}\int F_s dx = nx\frac{f}{A} \quad .....(4)$$

Where F_s is the shearing force, x is the knife displacement, n is the number of units under force-displacement curve on the UTM chart, and f is the scale factor of unit area.

2.3 Compression Test

A parallel plate apparatus with both plate surfaces larger than the major dimension of the stalk specimen were used. For this study, cassava stem samples were placed between flat steel plates in the following manner: a specimen plate, 100 mm square upon which the sample is placed, and a loading plate 30 mm in diameter for applying the force. The cassava stem specimen

Fig. 2 Setup for measurement of Shear strength: (a)schematic of apparatus, (b) fixed clamp and (c) movable clamp

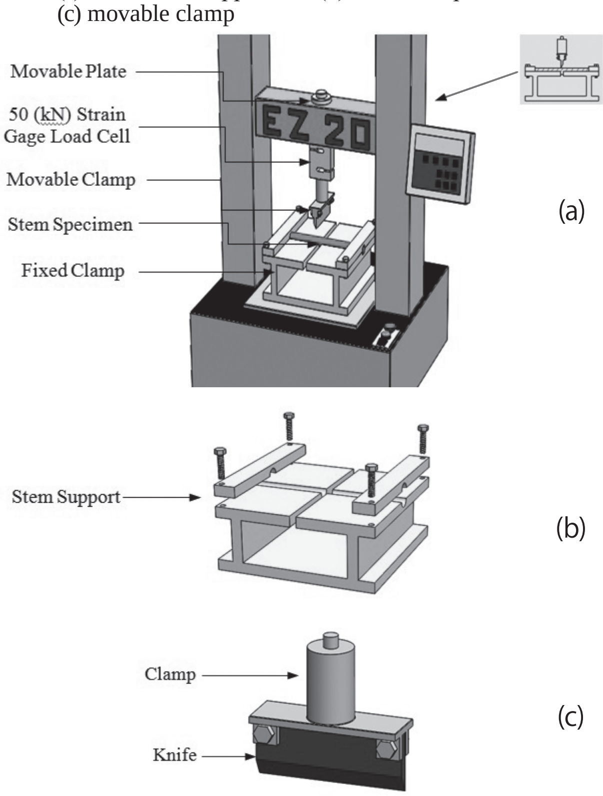

Fig. 3 Schematic of compression test of cassava stems

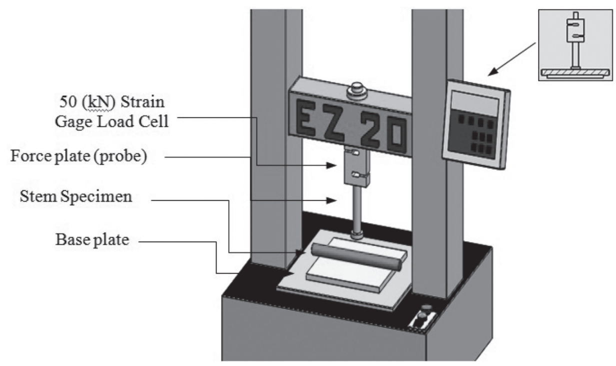

Fig. 4 Schematic of bending test of cassava stems

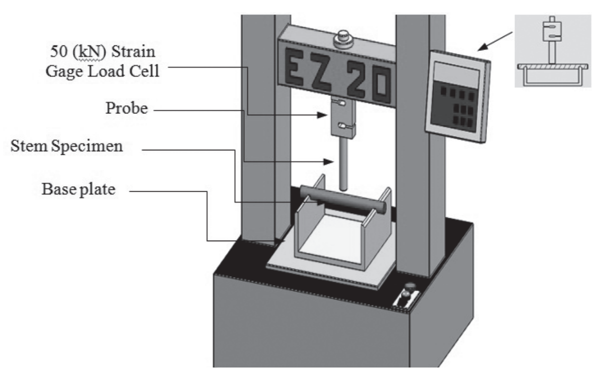

of 100 mm length was placed on the base platform (**Fig. 3**). The arrangement allowed a more concentrated load application to the center of the sample. The compressive force on the cassava stem specimen was applied by a force plate (probe) at the deformation rates of 20, 40 and 60 mm min^{-1}. Force-displacement curve was recorded on the chart recorder.

The force displacement curve was recorded on the chart recorder. The linear portion of the force displacement curve was used to compute the modulus of elasticity in compression was calculated by using **Eqn 5** (Chattopadhyay & Pandey, 1998; Adel et al., 2012),

$$\sigma_c = \frac{F_c d}{A \Delta L} \quad .....(5)$$

Where σ_c is the modulus of elasticity in compression, F_c is the compressive force, ΔL is the transverse deformation due to compressive force, and d is the diameter of the Cassava stems at the point of the compression.

The specific compressing energy was calculated by determining the area under the linear portion of the compressing force and displacement curve. Here, the compressive energy (E_{sc}) was calculated using **Eqn. 6** (Chattopadhyay & Pandey, 1998; Adel et al., 2012).

$$E_{sc} = \frac{1}{A} \int F_c \, dx = n \times \frac{f}{A} \quad .....(6)$$

Where F_c is the compressing force, x is the knife displacement, n is the number of units under force-displacement curve on the UTM chart, and f is the scale factor of unit area.

2.4 Bending Test

Specimen was placed at the three-point loading apparatus under the probe and the force was applied to the cassava stems (**Fig. 4**). The movable plate was moved at the rates of 20, 40 and 60 mm min^{-1} and the force-displacement curve was recorded.

The bending energy (σ_b) in MPa and specific bending energy (E_{sb}) in mJ/mm^2 were calculated by using **Eqns. 7** and **8** (Chattopadhyay & Pandey, 1998; Annoussamy et al., 2000; Adel et al., 2012).

$$\sigma_b = \frac{My}{I} \text{ and } M = F_b \times L \quad .....(7)$$

Where M is the maximum bending moment at which the stem fails, y is the distance of outermost fibre from the neutral axis, I is the second moment of area of the stem cross-section, F_b is the maximum bending force at which the stem fails, and L is the level arm of the bending force.

The bending energy (E_b) was calculated using **Eqn 8**.

$$E_b = \frac{1}{A} \int F_b \, dx = n \times \frac{f}{A} \quad .....(8)$$

3. Results and Discussion

Variation in the strength of cassava stems in shear, compression and bending with different knife bevel angles and loading rates were determined during the cutting process. Physical properties of the two cassava varieties Rayong-81 (*R-81*) and Huy-Bong are summarized in **Table 3**. Samples were taken from the lower portion of plants as it had larger diameter and mass per unit length, and had smaller moisture content. Results of the analysis of variance (ANOVA) showed that the variety had a significant effect on all measured physical properties ($P < 0.01$). Grossman (1982) reported that the differences in the woody versus succulent nature of tissue depend on the physiological age of the stalk section.

3.1 Shearing Strength

The cassava has a fibrous stem with a tubular section. In the cutting process, shearing of the fibres is achieved by compression, which results these hollow tubes to collapse before shearing the fibres. Otherwise, it shows the properties of a solid cut after compression. A representative force-displacement curve is shown in **Fig. 5**. The curve shows three different sections: A, B and C. In section A, from the moment when knife contacts the stem, the force increases from zero until the collapse of the hollow core. Due to this failure in stem structure, the force decreases. Then in section B, the compression continues with

Fig. 5 Force-displacement curve for cutting of cassava stem; sections A, B and C show compression until collapsing of the hollow core; compression and cutting; and cutting, respectively

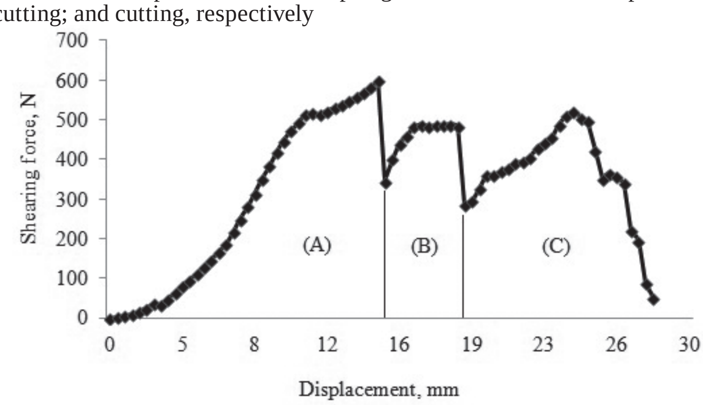

Table 3 Physical properties of cassava stems

	Mean		Std. Deviation	
	R-81	Huy-Bong	R-81	Huy-Bong
Moisture content, %	71.55**	68.40**	1.75	1.39
Diameter, mm	17.98**	18.67**	2.35	1.71
Mass per unit length, g/mm	2.41**	2.83**	0.61	0.67

** Significant at 1% level

cutting of the stalk. As the knife moves, cutting continues. In section C, the force reduces after the cutting is accomplished. Similar behavior was also reported by Ince et al. (2005) with sunflower stalks that is also is a fibrous material.

3.1.1 Effect of knife bevel angle on maximum shear strength

The maximum shear strength for cassava stems increased from 4.99 to 7.36 MPa for shearing of Huy-Bong variety, and from 2.80 to 3.68 MPa for Rayong-81 variety, as the knife bevel angle was increased from 15º to 60º at 20 mm min^{-1} quasi-static loading rate (**Fig 6**). This behavior was found to be statistically significant ($P < 0.01$). A similar increase in shear strength with respect to knife bevel angle for cutting forage was reported by Chancellor (1988). Prasad and Gupta (1975) found at moisture content of 73% (w.b.) the mean value of shear strength for maize was 8.02 MPa. Chattopadhyay and Pandey (1998) reported that the shear strength increased from 3.74 to 8.18 MPa for sorghum stalk at the forage stage as the knife bevel angle was increased from 30º to 70º at 10 mm min^{-1} rate of loading. Natthapong et al. (2008) on shear strength characteristics of biomass fuel showed that the maximum shear strength at 30^{a} knife bevel angle was less than that of at 45º knife bevel angle. Adel et al. (2012) reported that for Lilium stalk, the maximum shear strength increased from 0.76 to 1.31 MPa with knife bevel angle increasing from 30º to 60º.

3.1.2 Effect of loading rate on maximum shear strength

The maximum shear strength of cassava stems decreased with increase in loading rate (**Fig. 7**). When the rate of loading was increased from 20 to 100 mm min^{-1} with a 30° knife bevel angle, the maximum shear strength of Huy-Bong variety decreased from 5.51 to 4.57 MPa, and from 3.06 to 2.68 MPa for Rayong-81 variety at the forage stage. The decrease in maximum shear strength with respect to loading rate was significant ($P < 0.01$) for Huy-Bong variety but non-significant for Rayong-81 variety. Similar results were reported by Prasad and Gupta (1975) for maize, where the maximum shear strength decreased with the rate of loading from 20 to 100 cm min^{-1}. Chattopadhyay and Pandey (1998) showed that the shear strength decreased from 3.74 to 1.94 MPa for sorghum stalk at the forage stage with a 30º knife bevel angle, when the loading rate was increased from 10 to 100 mm min^{-1}. Adel et al. (2012) for lilium stalk, reported that the maximum shear strength decrease from 1.15 to 0.83 MPa with loading rate increasing from 30 to 50 mm min^{-1}.

Preston (1974) showed that a relatively high value of the maxi-

Fig. 6 Effect of the knife bevel angle on maximum shear strength for cutting Cassava stems at 20 mm/min loading rate; △, stems of Huy-Bong variety; □, stems of R-81 variety (Error bars represent ±SD, n=35).

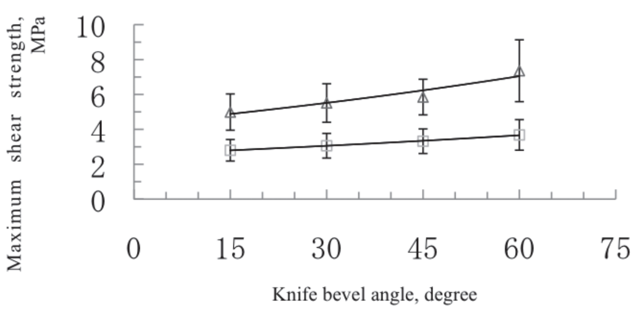

Fig. 7 Effect of the loading rate on maximum shear strength for cutting Cassava stems with a 30º knife bevel angle; △, stems of Huy-Bong variety; □, stems of R-81 variety (Error bars represent ±SD, n=35)

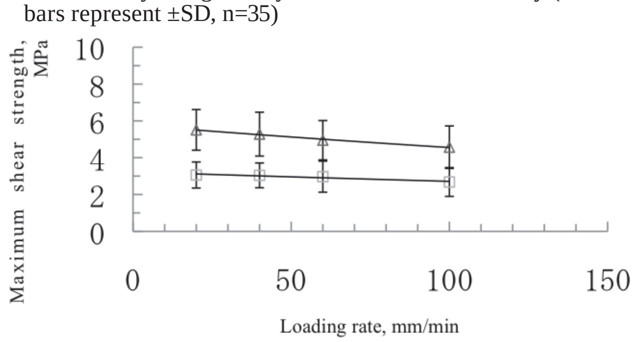

Fig. 8 Effect of the knife bevel angle on specific cutting energy for cutting cassava stems at 20 mm/min loading rate (quasi-static); △, stems of Huy-Bong variety; □, stems of R-81 variety (Error bars represent ±SD, n=35).

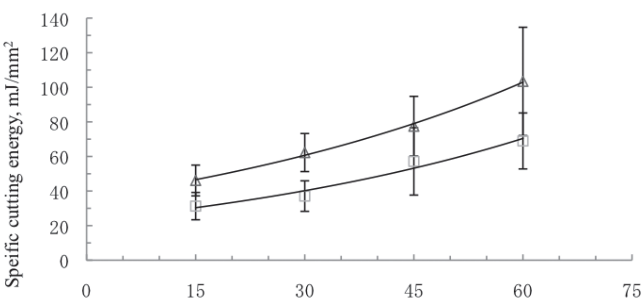

Fig. 9 Effect of the loading rate on specific cutting energy for cutting cassava stems with a 30º knife bevel angle; △, stems of Huy-Bong variety; □, stems of R-81 variety (Error bars represent ±SD, n=35)

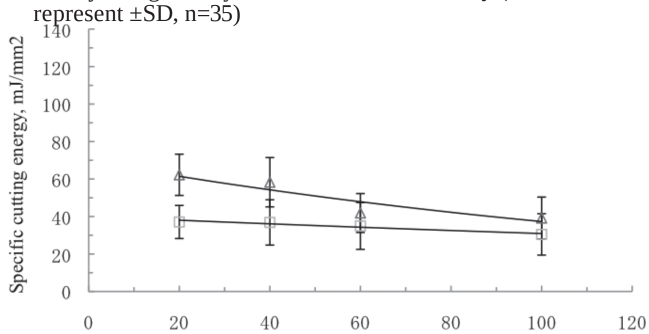

mum shear strength was due to the outer layer of the stem (stem wall). Strength of this layer increases with the age and diameter due to the gradual accumulation of lignin in the stem wall and reduction in moisture content which, in turn, enhances the stiffness of the stem wall. Chattopadhyay and Pandey (1998) explained this behavior on the basis of the fact that the plant stalk possesses visco-elastic material and therefore, the viscous resistance against cutting is higher at a slower rate of loading.

3.1.3 Effect of knife bevel angle on specific cutting energy

The specific cutting energy requirement increased exponentially as the knife bevel angle was increased from 15º to 60º at 20 mm min^{-1} rate of loading (**Fig. 8**). For Huy-Bong variety it increased from 46.10 to 103.40 mJ mm^{-2}, and for Rayong-81 variety it increased from 31.28 to 68.96 mJ mm^{-2}. The increase in specific cutting energy with respect to knife bevel angle was statistically significant ($P < 0.01$) for both varieties.

The specific cutting energy for Huy-Bong was higher than Rayong-81 variety because of the higher stem wall stiffness that increases with the stem diameter and decreases with stalk moisture content. Similarly Berentsen (1973), who used a die and punch method, and found the values of specific cutting energy in the range of 5.3 to 22.8 mJ mm^{-2} for grasses with a linear increase of energy consumption with a decrease in crop moisture. Another research from Chattopadhyay and Pandey (1998) showed that the specific cutting energy for sorghum stalks increased from 34.1 to 101.1 mJ mm^{-2}. Natthapong et al. (2008) studied the strength characteristics of biomass fuel and reported that with increase in diameter of crop, the specific cutting energy increased also. However, the greater energy required to cut the cassava stem at Huy-Bong variety was due to greater resistance offered by the stem wall at higher crop maturity as explained in section of effect of loading rate on maximum shear strength

3.1.4 Effect of loading rate on specific cutting energy

The specific cutting energy decreased with increasing loading rate for both varieties (**Fig. 9**). As the rate of loading was increased from 20 to 100 mm min^{-1} with a 30º knife bevel angle, the specific cutting energy decreased from 62.25 to 39.18 mJ mm^{-2} for Huy-Bong variety, and 37.08 to 30.46 mJ mm^{-2} for Rayong-81 variety; which is similar to the results observed by Prasad and Gupta (1975) with maize stalk. Another study from Ince et al. (2005) showed that the specific shearing energy increased towards lower from the upper regions. The values varied between 1.88 to 8.5, 1.7 to 10.7 and 2.4 to 11.0 mJ mm^{-2} for the upper, middle and lower regions respectively. It was greater in the lower regions because of the accumulation of more mature fibers in the stem.

The decrease in specific cutting energy requirement with respect to rate of loading in the range of 20 to 100 mm min^{-1} was statistically significant ($P < 0.01$). This type to behavior was observed due to higher viscous resistance against cutting the plant stalk at slower loading rate.

3.2 Compression Stress

The differences in the values of the compression strength and specific compression energy reduced as the loading rate increased for both varieties. Duncan's multiple range tests showed that with increasing loading rate from 20 to 60 mm min-1 the compression strength and specific compression energy decreased significantly ($P < 0.01$) in the ranges of 7.54 to 4.33 MPa and 101.47 to 56.24 mJ mm^{-2} for Huy-Bong variety, and 6.02 to 4.79 MPa and 60.62 to 36.22 mJ mm^{-2} for Rayong-81 variety respectively (**Table 4**).

Similar results were reported by Adel et al. (2012) for lilium stalk; with increasing loading rate from 30 to 50 mm/min the compression strength and specific compression energy decreased in the range of 5.49 to 4.33 MPa and 10.90 to 7.07 mJ mm^{-2} respectively. Another research from Simonton (1992) reported that the compression strength and specific compressing energy for geranium also varied with the stalk regions. When increasing the stem diameter, the compression strength and specific compression energy were increased. The mean values of the compression strength and specific compression energy for the upper sample were 3.73 MPa and 8.14 mJ mm^{-2} and 6.27 MPa and 9.90 mJ mm^{-2} for the lower sample, respectively.

3.3 Bending Stress

The bending strength was evaluated as a function of loading rate. As the loading rate of the cassava stem increases, the bending strength decreased, indicating a reduction in the brittleness of the stem. Duncan's multiple range tests showed that with increasing loading rate from 20 to 60 mm min^{-1} the bending strength and specific bending energy decreased significantly (P

Table 4 Effect of loading rate on the compression strength and specific compressing energy

Loading rate (mm/min)	Compression strength (MPa)		Specific compressing energy, (mJ mm^{-2})	
	Huy-Bong	R-81	Huy-Bong	R-81
20	$7.54^{a}\pm0.54$	$6.02^{a}\pm0.25$	$101.47^{a}\pm4.92$	$60.62^{a}\pm3.25$
40	$5.19^{ab}\pm0.40$	$5.33^{ab}\pm0.25$	$93.71^{b}\pm5.59$	$57.71^{b}\pm5.73$
60	$4.33^{c}\pm0.42$	$4.79^{c}\pm0.31$	$56.24^{c}\pm2.77$	$36.22^{c}\pm3.42$

Common letter in a column means that these are non-significant ($P < 0.01$) by Duncan's test (Mean± standard deviation, n = 35)

< 0.01) in the ranges of 4.10 to 3.72 MPa and 98.46 to 85.67 mJ mm^{-2} for Huy-Bong variety, and 2.95 to 1.72 MPa and 54.56 to 45.33 mJ mm^{-2} for Rayong-81 variety respectively (**Table 5**). Results reveal that the bending strength and specific bending energy values are statistically different from each other.

Similar results were also reported by Annoussamy et al. (2000), Nazari et al. (2008) and Adel et al. (2012). Bending strength was lower towards the upper regions of stalk. The variation range of bending strength and specific bending energy for near the growth tip specimens were 0.26 to 1.45 MPa and 0.76 to 3.72 mJ mm^{-2} and 0.97 to 1.66 MPa and 4.43 to 6.28 mJ mm^{-2} for near the root internode specimen, respectively.

4. Conclusions

The shear strength and energy consumption in cutting of cassava stem were significantly affected by the interactions of the knife bevel angle and loading rate of cutting. It was found that, the shear strength and cutting energy were directly correlated with knife bevel angles but inversely correlated with loading rate of cutting. The mechanical strength and energy consumption in shear, compression and bending of the Huy-Bong variety were almost twice as that of Rarong-81 variety because of the larger diameter of Huy-Bong. Moreover, the compression and bending stress did not vary significantly with the rate of loading and knife bevel angle.

In the cutting blade design, the shear, compression and bending strength should be more than 7.36, 7.54 and 4.10 MPa respectively. Furthermore, the specific cutting energy, specific compressing energy and specific bending energy should be higher than 103.40, 101.47 and 98.46 mJ mm^{-2} respectively. However, the results of this study can provide theoretical references for the design of mechanical cassava stem cutting device, achieving the purpose of appropriately designing cassava stem cutting unit and cassava stem chopping for forage.

Acknowledgments

The authors wish to gratefully acknowledge the kind support received from the AIT, and RMUTTO.

REFERENCES

Adel, H., H. Gholamreza, H. K. Mohammad, R. H. Seyed and K. Javad. 2012. Influnce of knife bevel angle, rate of loading and stalk section on some engineering parameters of lilium stalk. Iranica Journal of Energy & Environment, 3(4), 333-340.

Ahlgrimm, H. J. 1977. Effect of physiological and morphological factors on the strength of plant stems, especially timothy. Landbauforschung Volkenrode, Diss., Sondesheft 37, Techn. Univ. Carolo-Wilhelmina, Braunschweig.

Annoussamy, M., G. Richard, S. Recous and J. Guerif. 2000. Change in mechanical properties of wheat straw due to decomposition and moisture. Applied Engineering in Agriculture, 16(6), 657-664.

Apata, D. F. and T. O. Babalola. 2012. The use of cassava, sweetp and cocoyam, and their by-products by Non-Ruminants. International Journal of Food Science and Nutrition Engineering, 2(4), 54-62.

ASAE. 1983. Moisture measurement. In ASAE Standard S 410. Agricultural Engineers Handbook (pp. 329-330).

Berentsen, O. J. 1973. Energy requirements for grass chopping. Norway Institute of Agricultural Research Report, 22.

Chancellor, W. J. 1958. Cutting of biological material. In Handbook of Engineering in Agriculture, Vol. 1, (pp. 35-63).

Chattopadhyay, P. S. and K. P. Pandey. 1998. Mechanical Properties of sorghum stalk in relation to quasi-static deformation. Journal of Agricultural Engineering Research, 73, 199-206.

Chen, Y., J. L. Gratton and J. Liu. 2004. Power requirement of hemp cutting and conditioning. Biosystems Engineering, 87(4), 417-424.

Choi, C. H. and D. C. Erbac. 1986. Corn stalk residue shearing by rolling coulters. Transactions of the ASAE, 29(6), 1530-1535.

Curtis, L. M. and J. G. Hendrick. 1969. A study of bending strength properties of cotton stalk. Transaction of the ASAE, 12(1), 39-45.

FAO. 1997. Food and Agriculture Organization of the United Nation. In. http://www.fao.org (Accessed In July, 2014).

Grossman, H. H. 1982. Anatomy and Morphology. In Geraniums Mastalerz and Holcomb, (pp: 331-340).

Halyk, R. M. and I. Hurlbut. 1968. Tensile and shear strength characteristics of alfalfa stems. Transactions of the ASAE, 11(2), 256-257.

Ince, A., S. Ugurluay and M. T. Ozcan. 2005. Bending and Shearing Characteristics of Sunflower Stalk Residue. Biosystems Engineering, 92(20), 175-181.

Table 5 Effect of loading rate on the bending strength and specific bending energy

Loading rate (mm/min)	Bending strength (MPa)		Specific bending energy (mJ mm^{-2})	
	Huy-Bong	R-81	Huy-Bong	R-81
20	4.10^{a}±0.28	2.95^{a}±0.19	98.46^{a}±2.02	54.56^{a}±2.19
40	3.75^{b}±0.15	2.54^{a}±0.07	91.66^{b}±1.41	50.31^{b}±2.43
60	3.72^{b}±0.08	1.72^{b}±0.09	85.67^{c}±1.31	45.33^{c}±1.47

Common letter in a column means that these are non-significant (P < 0.01) by Duncan's test (Mean± standard deviation, n = 35)

Khazaei, J., H. Rabani, A. Ebadi and F. Golbabaei. 2002. Determining the shear strength and picking force of phyrethrum flower. Iranian Journal of Agricultural Science, 33(3), 433-444.
Koniger, R. 1953. Tentative theory for the cutting of plant stems. Grundlagen der Landtechnik, (5), 96-97.
McRandal, D. M. and P. B. McNulty. 1980. Mechanical and physical properties of grasses. Transactions of the ASAE, 23(4), 816-821.
Mohsenin, N. N. 1986. Physical Properties of Plant and Animal Material. Gordon and Branch. New York, USA.
Natthapong, P. and A. Weerachai. 2008. Study of shear strength characteristics of biomass fuel. Journal of Thai Society of Agricultural Engineering Research, the 9th TSAE national conference 31 January to 1 February, 2008.
Nazari, G. M., A. Jafari, S. S. Mohtasebi, A. Tabatabaeefar, A. Sharifi, M. J. O'Dogherty, S. Rafiee and G. Richard. 2008. Effects of moisture content and level in the crop on the engineering properties of alfalfa stalks. Biosystems Engineering, 101, 199-208.
Prasad, J. and C. P. Gupta. 1975. Mechanical properties of maize stalks as related to harvesting. Journal of Agricultural Engineering Research, 20(1), 79-87.
Persson, S. 1987. Mechanics of Cutting Plant Material. ASAE Monograph No.7. St. Joseph, Michigan.
Preston, J. 1974. The Physical Biology of Plant Cell Walls. Chapman & Hall, London, 491 p.p.
Prince, R. P., T. W. Bartok and D. M. Bradway. 1969. Shear stress and modulus of elasticity of selected forages. Transactions of the ASAE, 12(3), 426-429.
Sakharov, V. V., G. G. Rakmanberdiev and G. G. Guagev. 1984. An investigation into the severing of pre-tensed mulberry stems by a screw-type cutter. Mekhanizatsiya i Elekfikikatsiya Sel' Skaogo Khozyaistva, 3, 61-62.
Shaw, M. D. and L. G. Tabil. 2007. Compression, relaxation and adhesion properties of selected biomass grinds. Agricultural Engineering International, the CIGR Ejournal, Manuscript FP, 07-006, Vol 9.
Simonton, W. 1992. Physical properties of zonal geranium cutting. Transaction of the ASAE, 35(6), 1899-1904.
Skubisz, G., T. I. Kravtsova and L. P. Velikanov. 2007. Analysis of the strength properties of pea stalks. International Agrophysics, 21, 189-197.
Yiljep, Y. D. and U. S. Mohammed. 2005. Effect of knife velocity on cutting energy and efficiency during impact cutting energy and efficiency during impact cutting of sorghum stalk. Agricultural Engineering International, the CIGR Journal, Manuscript PM, 05-004, Vol. 7.

■■

Development of a Watermelon (*Citrlluslanatus*) Seed Extractor

by

Shrinivas Deshpande
PM.Tech (Ag. Engg) Scholar
University of Agricultural Sciences,
GKVK, Bengaluru, INDIA
shrihd9@gmail.com

G. Senthil Kumaran
Principal Scientist & Head
Section of Agricultural Engineering,
Indian Institute of Horticultural Research,
Bengaluru, INDIA
senthil@iihr.ernet.in

A. Carolin Rathinakumari
Senior Scientist
Section of Agricultural Engineering,
Indian Institute of Horticultural Research,
Bengaluru, INDIA
carolin@iihr.ernet.in

Abstract

Engineering properties such as physical and textural properties of the matured watermelon (*Citrulluslanatus*) fruit and its seeds were measured in order to design and develop the watermelon seed extractor. The developed seed extractor consisted of following systems for (i) watermelon cutting, (ii) watermelon seed extraction, (iii) seed separation and (iv) power transmission. The extractor was evaluated with three types of scrapers namely stainless steel, wooden and nylon; two cutting planes viz., transverse and longitudinal planes and three rotational speeds viz., 50, 100 and 150 rpm. The best combination was observed to be for transverse cutting with nylon scraper at a speed of 100 rpm. The best performance for capacity, extraction efficiency, seed loss, seed damage, germination percentage and vigour index were found to be 1.98 kg of seeds/h, 99.49 %, 0.19 %, 0.26 %, 97.04 % and 3,284, respectively.

Keywords: Watermelon, watermelon seed, seed extractor

Introduction

Watermelon (*Citrulluslanatus*) is one of the important vegetable crops, which belongs to the family Cucurbitaceae is a vine-like flowering plant originally from Southern Africa. It is a special kind of fruit referred by botanists as a "pepo", a berry which has a thick rind (exocarp) and fleshy center (mesocarp and endocarp). The skin is smooth, with dark green rind or sometimes pale green stripes that turn yellowish green when ripe. Watermelon is an important summer season crop whose peak season of harvest falls on the hot summer days and is highly relished due to its cool and thirst quenching property. The pulp is juicy and sweet, with an attractive red colour that attracts consumers (Shankara et al., 2012).

Coming to the seed extraction process, most of the government and private agencies are extracting the watermelon seeds manually. This manual method of extracting melon seeds involves manual cracking of the fruits with wooden clubs or cutting off the head or tail then boring the fruits with a knife. The fruit so treated is left about 1-2 days to decompose, and then the seeds are removed by washing in clean water. Thus the manual process is both time and effort-consuming process (Amir, 2004). Once the seed extraction is performed, the whole fruit is being wasting or it is only used fed animal as feed.

In India, watermelon is cultivated in an area of 74,640 hectare with a total production of 1809.83 million tonne with a productivity of 24.2 t/ha. Similarly in the state of Karnataka the watermelon cultivated area is about 9,500 ha with the total production of 317.3 million tonne and productivity of 33.4 t/ha during the year 2013-14 (Anonymous, 2014).

In India, the recommended seed rate for cultivation of watermelon is 0.3 kg/ha and 1 kg/ha for hybrids and varieties respectively. So the estimated seed requirement to cultivate 9,500 and 74,640 ha of land is about 9 and 72 tonnes, respectively for Karnataka and India. This traditional method requires a lot of time, labour and tedious. By traditional method of extraction process the demand of seeds is difficult to meet economically due time and energy constraints.

By considering all these points, there is a need to develop a machine to extract good quality or high vigour watermelon seeds from the fruit to meet out seed requirement as well as to extract good quality watermelon juice for further value addition. Hence a watermelon seed extractor is proposed to be developed.

Materials and Methods

Development of a Watermelon Seed Extractor

The machine was fabricated and developed for the extraction of seeds as well as quality juice from the whole watermelon fruit. The watermelon seed extractor was designed developed and fabricated in the Section of Agricultural Engineering, Indian Institute of Horticultural Research, Hessaraghatta, Bengaluru. The various physical and textural properties of matured watermelon fruit as well as its seeds were measured in order to design various systems of the seed extractor and were as follows (**Fig. 1**);

i. Watermelon cutting system
ii. Watermelon seed extracting system
iii. Seed separation system
iv. Power transmission system

Watermelon Cutting System

The watermelon cutting system consisted of a fruit holding trolley, circular cutting blade, a hopper and main frame. A stainless steel circular serrated blade of 400 mm diameter and 2 mm thick was mounted above the frame with necessary shaft, bush and fasteners.

The top surface of trolley frame was covered with 1 mm thick stainless steel sheet. A stainless steel flat of 25 × 3 mm was bent into semicircular form and fitted on the frame to hold the fruit while cutting. Four wheels were provided at four corners of the frame so that the frame could be moved forward and backward. Handle was provided to move the fruit holding trolley in forward and backward movement while cutting the fruit.

The hopper of the cutting system has 620 mm length, 450 mm width with the hopper bottom of 50 mm diameter, which was fabricated using 1 mm stainless steel sheet in order to collect the juice and seeds while cutting.

Watermelon Seed Extracting System

The watermelon seed extracting system consisted of a scraper fitted to stainless steel shaft, and power transmission system. A scraper shaft of 725 mm length, 20 mm diameter made up of stainless steel was mounted on a main frame with the help of pillow bearing blocks. The scrapers with different materials were fabricated such as stainless steel, wooden and nylon. The scraper was fixed on the scraper shaft with the help of nut and bolt. The scraper shaft was driven by chain and sprocket arrangement with necessary speed reduction ratio.

Seed Separation System

The seed separation system consisted of (i) concentric cylindrical drums viz. perforated cylindrical drum and solid cylindrical drum, (ii) pulp beaters and (iii) drive transmission system. The cylindrical drums were fabricated out of stainless steel (SS 304 grade) of 1 mm thickness stainless steel material had diameters of 220 mm and 300 mm respectively for perforated and solid drum, respectively. Two types of perforated drums having 3 mm and 5 mm diameter perforations were fabricated to conduct the preliminary studies on juice separation system.

Beater holders which were fabricated out of 85 mm, 60 mm and 5 mm stainless steel flats. The beaters were fitted to the beater holder and fabricated in 'T' shape. These beaters were mounted on a shaft of 25 mm diameter at an interval of 60 mm at spiral arrangement in order to push and move forward material. The shaft was driven by necessary belt and pulley from the main power source.

Fig. 1 Developed watermelon seed extractor

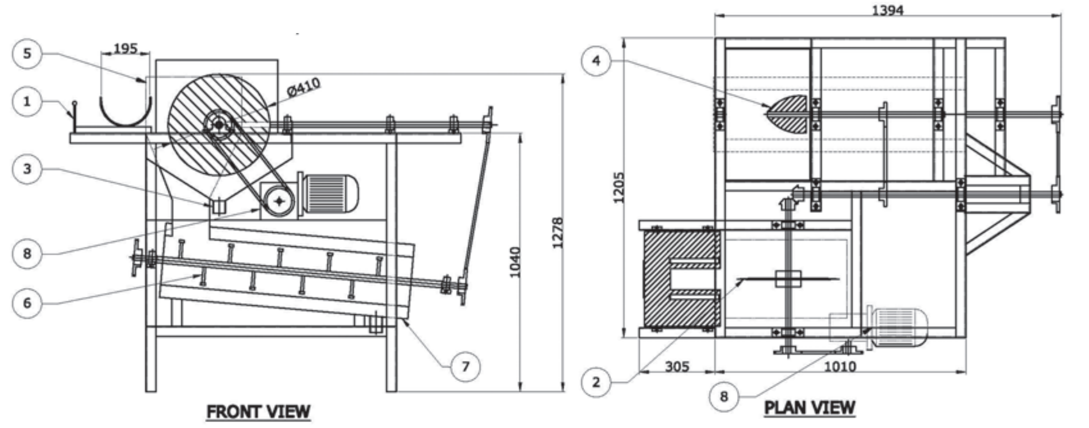

1. Moving trolley
2. Cutting blade
3. Drain
4.Pulp breaker
5. Hopper
6. Juicer
7. Seed separation drun
8. Drum - Geared motor

Power Transmission System

The extraction unit was fitted with a three phase 50 rpm, 1 hp (0.75 kW) geared motor. Provision was made at the base point to move the motor to and fro to provide required belt tension. The cutting system is driven by the geared motor with the help of 'V' belt and pulley. Further the power at the end of the cutting system shaft was transmitted to the load shaft with the help of bevel gears. From this load shaft, scraper shaft got the power through chain drive and crushing shaft got the power from the load shaft through crossed 'V' belt and pulley to rotate the beater shaft in clock wise direction.

Performance Evaluation of the Watermelon Seed Extractor

The developed seed extractor was tested as per the standard procedure for combinations of various treatments as given below (**Table 1**). The watermelon fruit was fed through fruit cutting unit where it cut the fruit into two halves. After the cutting one half of fruit was fed to scraper manually. The pulp, juice along with seeds was scraped out from fruit and collected in the seed separation unit. In seed separation unit, juice was collected through juice outlet and the uncrushed pulp along with the seeds was collected from the seed outlet. The collected pulp along with the seeds from seed outlet was kept for fermentation for a duration of 24 h (**Fig. 2**). Once the fermentation period was completed, the seeds were separated by washing the fermented pulp with the help of clean water and were dried under shade. The same procedures were followed for all the trials and were carried out with 3 replications to overcome the experimental errors. After recording all the observations various dependent parameters like Capacity, Seed extraction efficiency, Percentage seed damage, Percentage Seed loss and Seed vigour index were measured by using the following formulae whereas germination study was carried out in the walk in germinator chamber which was maintaining 20 ± 1 ºC temperature and 90 % relative humidity.

Extraction capacity (kg/h) = *Weight of seeds extracted (kg) / Time taken (h)*

Extraction efficiency (%) = *(Total weight of the seed collected at seed outlet (g)) / (Total weight of the seed collected at all outlets (g)) × 100*

Percentage seed losses = $(M_o / M_t) \times 100$

Percentage of damege seeds = $(M_d / M_t) \times 100$

Seed vigour index (VI) = *[Whole seedling length (mm) × Germination (%)]*

Where, M_o = Total weight of seeds expelled out of the machine with peel and washed water (g)

M_t = Total weight of the seeds contained in the fruit sample (g)

M_d = Total weight of damaged seeds collected from all outlets (g)

Statistical Analysis

The results of the machine performance for different treatments of watermelon seed extraction were analyzed using Factorial Completely Randomized Design (FCRD) with three replications by using AGRES software (Fisher and Yates, 1963).

Experimental Results

Performance Evaluation of Watermelon Seed Extractor

The prototype watermelon seed extractor was tested for its performance with three different scrapers, two cutting planes and three operating speed with three replications. For each trial one fruit was fed and various observations were recorded. The performance parameters namely capacity of the seed extractor, seed extraction efficiency, percentage seed loss, percentage seed damage, germination percentage and seed vigour index for three scrapers, two cutting planes and three operating speed were tested and results were tabulated in **Table 2**.

Capacity of the Seed Extractor

The results of the extractor ca-

Table 1 Experimental design

Independent parameters	Levels	Dependent parameters	Replications
Scraper type	Sc_1 (Stainless steel) Sc_2 (Wooden) Sc_3 (Nylon)	1. Capacity of the extractor 2. Seed extraction efficiency 3. Percentage seed damage 4. Seed loss 5. Germination percentage 6. Seed vigour index	3
Cutting plane	Cp_1 (Transverse) Cp_2 (Longitudinal)		
Peripheral speed	S_1 (50 rpm) S_2 (100 rpm) S_3 (150 rpm)		

Fig. 2 Performance evaluation of developed watermelon seed extractor

pacity revealed that, the capacity of developed seed extractor was increased with increase in the speed for stainless steel and wooden scraper whereas the capacity of the extractor was decreased with increase in speed for nylon scraper. The data presented in the **Table 2** observed that different scrapers, cutting planes and operating speeds had higher significant effect over the capacity of the extractor. The nylon scraper with transverse cutting plane at 50 rpm operating speed showed the highest capacity of 1.98 kg seeds/h whereas lowest capacity was found for wooden scraper (0.40 kg seeds/h) with transverse cut at an operating speed of 50 rpm. Because in this combination enough time was available to the seeds to get separated from the fruit as well as sufficient area of contact between the scraper and fruit. The similar findings were obtained for extraction watermelon seeds machine by Eliwa and Elfatih (2012).

Seed Extraction Efficiency

The results of the extraction efficiency indicate that, the extraction efficiency of developed seed extractor was increased with increase in the speed for all scrapers in both cutting planes. The data presented in the **Table 2** observed that different scrapers, cutting planes and operating speeds had higher significant effect over the extraction efficiency of the extractor. The nylon scraper with transverse cutting plane operated at a higher speed of 150 rpm showed the highest extraction efficiency of 99.49 % compared to all combinations. Because, of the shape and material factor, serrations provided on the nylon scraper and sharp edge provided at the front which improves the penetration into the fruit. The extractor had shown the highest extraction efficiency at higher speed of 150 rpm because at higher speed almost all the pulp and seed were removed by the scraper irrespective of juice conversion. This resulted in higher extraction efficiency at higher speed. The results of Eliwa and Elfatih (2012) showed that higher extraction efficiency was found at higher speed with transverse cutting plane.

Table 2 Pattern of different dependent parameters observed in the performance evaluation of seed extractor

Scraper	Cutting Plane	Speed	Capacity (kg of seeds/h)	Efficiency, %	Seed loss, %	Seed damage, %	Germination, %	Vigour index
Sc_1	Cp_1	S_1	0.61	93.95	0.77	5.28	72.00	1,134
		S_2	1.06	97.93	0.19	1.87	80.00	1,374
		S_3	0.95	95.01	0.83	4.16	82.00	1,540
	Cp_2	S_1	0.49	94.04	0.72	5.24	86.57	2,069
		S_2	0.66	94.87	0.37	4.76	84.00	1,554
		S_3	1.21	95.92	0.58	3.51	88.00	2,544
Sc_2	Cp_1	S_1	0.40	89.46	3.67	6.87	84.00	1,571
		S_2	1.27	95.54	1.83	2.63	70.00	1,044
		S_3	0.66	92.35	2.49	5.16	72.00	1,158
	Cp_2	S_1	0.46	90.24	3.12	6.64	68.00	1,078
		S_2	1.13	94.83	2.20	2.97	94.00	2,645
		S_3	0.46	91.55	3.44	5.00	92.61	2,472
Sc_3	Cp_1	S_1	1.98	98.88	0.38	0.74	92.00	2,933
		S_2	0.89	97.39	1.15	1.46	70.00	1,325
		S_3	1.39	99.49	0.19	0.32	86.00	2,039
	Cp_2	S_1	1.00	97.65	0.95	1.41	72.48	1,238
		S_2	1.53	99.48	0.26	0.26	97.04	3,284
		S_3	1.23	98.92	0.53	0.55	96.64	2,904

Where,
Sc_1 – Stainless steel scraper; Sc_2 – Wooden scraper; Sc_3 – Nylon scraper
Cp_1 – Transverse plane; Cp_2 – Longitudinal plane
S_1 – 50 rpm; S_2 – 100 rpm; S_3 – 150 rpm

Percentage Seed Loss

The results of the percentage seed loss showed that, the seed loss of developed seed extractor was decreased with increase in the speed for stainless steel and nylon scraper, whereas increase in seed loss with increase in speed was observed for wooden scraper in both cutting planes. The data presented in the Table 2 observed that different scrapers, cutting planes and operating speeds had higher significant effect over the percentage seed loss of the developed extractor. The minimum percentage seed loss was observed for both nylon and stainless steel scraper (0.19 %) with a transverse cutting operated at 150 and 100 rpm speed for nylon and stainless steel, respectively followed by the nylon scraper (0.26 %) with longitudinal cutting operating at a speed of 100 rpm. The lesser seed loss is due to the shape and material factor as well as serrations provided on the nylon scraper. Due to this reason, the scooping action performed by scraper led to minimum seed loss compared to wooden scraper.

According to Eliwa and Elfatih (2012) it was observed that increasing cutting speed tends to increase seed losses due to increasing vibration and instability of the fruit over pulp scraping unit. But in case of developed seed extractor decrease in seed losses were observed with increase in speed. Because at higher speed, there was less resident time was given to pulp and seeds and it reached the outlet in lesser time compared to lower speed.

Percentage Seed Damage

The results of the percentage seed damage revealed that, the seed damage of developed seed extractor was decreased with increase in the speed for all the scrapers in both cutting planes. The data presented in the **Table 2** observed that different scrapers, cutting planes and operating speeds had higher significant effect over the percentage seed damage of the developed extractor. The nylon scraper with longitudinal cut operating at a speed of100 rpm showed the minimum (0.26 %) percentage of seed damage followed by nylon scraper (0.32 %) with longitudinal cut at an operating speed of 150 rpm. The maximum percentage of seed damage (6.87 %) was observed in the wooden scraper with transverse cut operating at a speed of 50 rpm.

According to Eliwa and Elfatih (2012) most of seeds were damaged during cutting the fruits into two halves and during separation of pulp and seeds from its rind. Due to the impact and shearing force seeds were damaged in any of the section as explained. It was observed that increase in cutting speed tends to decreased seed damage because of the less resident time took in the seed separation system as well as extraction system.

Germination Percentage

The results of the germination study revealed that, the germination percentage of the watermelon seeds extracted from the developed seed extractor was increased with increase in the speed for all the scrapers in both cutting planes. The data presented in the **Table 2** observed that different scrapers, cutting planes and operating speeds had higher significant effect over the germination percentage of watermelon seeds extracted from the developed seed extractor. The nylon scraper with longitudinal cut operating at a speed of 100 rpm gave the maximum germination percentage of 97.04 %. The least germination percentage was observed in wooden and nylon scraper with transverse cutting operating at a speed of 100 rpm. According to Kushwaha et al. (2005) at higher peripheral speed there was increased deformation of seed and may be the possible cause of the lower germination and constant speed in crushing chamber. But in developed seed extractor, germination percentage was increasing as the speed increased because; same speed was maintained in all system. Thus at 100 rpm speed, higher germination percentage was observed.

Seed Vigour Index

The results of the Seed vigour index indicated that, the vigour of the watermelon seeds extracted from the developed seed extractor was increased with increase in the speed for all the scrapers in both cutting planes. The data presented in the **Table 2** observed that different scrapers, cutting planes and operating speeds had higher significant effect over the vigour index of watermelon seeds extracted from the developed seed extractor. The highest seed vigour index (3,284) was observed in nylon scraper with longitudinal cut operating at a speed of 100 rpm whereas the least seed vigour index (1,044) was observed in wooden scraper with transverse cut operating at a speed of 100 rpm. According to Kushwaha et al. (2005) at higher peripheral speed there was increased deformation of seed and may be the possible cause of the lower germination. This lesser germination percentage results in lower vigour values. Thus at 100 rpm speed higher Seed vigour index was observed with longitudinal cutting plane.

Conclusions

By considering the performance of the each treatment, capacity of the extractor(kg/h), extraction efficiency (%), percentage seed loss (%), percentage seed damage (%),germination percentage (%) vigour index and physical performance during the operation were observed to optimize the design and operational parameters. By analyzing the overall machine extraction process, the nylon scraper with transverse cutting plane at 100 rpm operating speed was recommended as the best combination for watermelon seed extractor based to extract high vigour seeds as well as good quality juice for further value addition.

Acknowledgement

It gives me an immense pleasure to acknowledge The Institution of Engineers (India) for giving the financial assistance in the form IE(I) R & D Grant-in-aid to carry out the proposed work.

REFERENCES

Shankara Swamy, J. and Pawan Kumarand Rajeev Kumar. 2012. Processing and quality evaluation of watermelon squash. IOSR J. Scientific and Applied Research. 3(1): 79-85.

Amir, I. F. S. 2004. Construction and performance of machine for separating watermelon seeds.Unpublished P.hd. Thesis, Mansoura University, Egypt.

Anonymous. 2014. Indian Horticulture Database.National Horticulture Board, Ministry of Agriculture, Government of India.

Fisher, R. A. and F. Yates. 1963. Statistical table for biological, agricultural and medicinal research. Oliver and Boyel, Edinburg.

Eliwa, A. A. and A. Elfatih. 2012. Developing a local extraction watermelon seeds machine. J. Appl. Sci. Res. 8(1): 474-482.

Kushwaha, H. L., A. P. Srivastava and Harpal Singh. 2005. Development and performance evaluation of an okra seed extractor. Agricultural Engg. Int.: The CIGR Ejournal. 1-13.

■■

Predicting Wheat Harvest Time Using Satellite Images and Regression Models

by
Sepideh Taghizade
Department Biosystems Engineering,
University of Tabriz,
Tabriz
IRAN

Hossain Navid *
Department of Photogrammetry
and Remote Sensing,
K.N. Toosi University of Technology,
Tehran, IRAN
* Corresponding author: navid@tabrizu.ac.ir

Yasser Maghsodi
Department Biosystems Engineering,
University of Tabriz,
Tabriz
IRAN

Mohammad Moghadam Vahed
Department Biosystems Engineering,
University of Tabriz,
Tabriz
IRAN

Reza Fellegarii
Department Biosystems Engineering,
University of Tabriz,
Tabriz
IRAN

Abstract

Cereals have an important role in human food security. Therefore, accurate estimation of harvesting time is necessary to minimize the loss in wheat farming. The objective of this study was to determine wheat harvest time using satellite images accurately. Field data was sampled from the farms in Meiham region of Kordestan province in west of Iran. Also, satellite remote sensing technique was applied during wheat growing season in 2016 using Landsat 8 images. The vegetation indexes were used as input in prediction model in this study. The results illustrated that satellite imaging has enough potential to predict the harvesting time of wheat accurately. R-squared and RMSE values of the best structured stepwise regression model in this study were 0.785 as well, and 1.13 respectively. This method can beneficially be employed by farm managers to have an accurate estimation of the most appropriate harvesting time and be able to manage the process which is an important challenge for them.

Keywords: Harvesting time; Satellite imagery; Stepwise regression model; Wheat farming.

Introduction

Agriculture and crop production is an intrinsic accountability in securing the survival of the human species. Cereals have the most important role in the human food supply. Among the cereals, wheat has an essential role in food security for countries located in Middle East. In Iran, wheat provides more than 40 percent of the calories and 50 percent of protein required in the people diet and so it is a necessary product (Kamali et al., 2012). This makes wheat, one of the most important agricultural productions. Sustainable production of wheat requires understanding the growth stages of wheat (such as maturity and harvest time) and also providing suitable machinery (cultivators, planters and harvesters) at these times (anonymous, 2014). Therefore, there are some researches to estimate the growth stages of wheat (Van Ittersum et al., 2003; Yin and Van Laar, 2005).

Wheat maturity stage is one of the most significant stages of wheat growth. In general, wheat maturity can be divided into two categories: morphological and technological maturity. At the technological maturity stage, the product is suitable for harvesting (Mares, 1987; Philips, 1974). The technological maturity stage is actually the harvest time and the quality and yield of wheat is the maximum amount at this stage. Evers et al. (2010), presented a simulation model of wheat development integrating above-ground plant structure, organ-level microclimate, photosynthesis, assimilate distribution within the plant structure, and organ growth and development. They used an empirical sigmoid relationship between leaf mass and leaf length for plant organ development calculation. The results showed that more efforts were needed to model mechanistically other major physiological processes such as nitrogen uptake and distribution, and tiller and leaf senescence. Other researchers (Jones et al., 2000; Dalghandi et al., 2015) used some parameters such as weather temperature, soil moisture, etc. to predict wheat growth stages. The disadvantage of these models is the unavailability of the above parameters for all farms. Therefore, it is needed to have an alternative or complementary method for these models. Harvest time (technological maturity) is an important factor in farm management. For example, harvest time effects on the performance of the plants rotation because, delay in harvesting time could reduce the yield of second crop in the plants rotation. Sun et al. (2007) studied the effect of harvesting time in the rotation of winter wheat - maize. Results showed that each day of delay in wheat harvesting (the first cultivated crop in the rotation) leaded to 0.6% maize yield decrease (second cultivated crop).

Remote sensing is fairly a new technique which could help researchers to get more information of plants, periodically. The remote sensing, which focuses on the examination of images of the earth's surface, has rapidly evolved since the discovery of the infrared spectrum and photography in the early 1800s (Campbell, 2002). The application of remotely sensed images leads to collect of reliable and timely data from crop performance (Lyle et al., 2013). Most vegetation indexes (VIs) incorporate reflectance in a few wavebands which could be collected mainly by satellite broadband sensors. VIs have been used to determine plant stage of development (Baghzouz et al., 2010; Eklundh et al., 2011; Hmimina et al., 2013; Huete, 2012; Soudani et al., 2012). In the last decade, remote sensing has been very effective in farm management decisions such as cultivation, fertilization and yield determination (Bausch et al., 2008; Bao et al., 2008; Wang et al., 2007). Jongschaap and Schouten (2005) showed that using remote sensing, wheat area could be appraised with more than 80% accuracy. They also reported good fitting; i.e. model-based estimations of regional wheat production were in accord with agricultural statistics. Ren et al. (2008) estimated winter wheat yield using MODIS-NDVI (Normalized Difference Vegetation Index) data in Shandong, China. They reported that the relative errors of the predicted yield were in range of 4.62 - 5.40% and that whole RMSE was 214.16 kg/ha. Song et al. (2016) evaluated the performance of time series of Landsat 8 images to wheat yield prediction. They used NDVI. Their results showed that there was good fitting (R^2 = 0.87) between this vegetation index and the yield of wheat.

Although satellite images were used in some agricultural applications, no research has yet been conducted on harvesting time prediction using Landsat 8. Therefore, the main objective of this study was to evaluate the performance of Landsat 8 satellite images to determine wheat harvest time. Furthermore, developing a regression model for estimating wheat harvest time is another purpose of this study.

Material and Methods

Field Data Collecting Method

The study was done in the Meiham region in the Kordestan (35°09´N, 47°91´E) province in the west of Iran (**Fig. 1**). During field surveys before harvest season, 30 wheat farms were selected from study area. The locations of farms were recorded using GPS (Garmin 62s). The required descriptive information of farms and the crop density of each farm were also recorded. The yield samplings were done (from the middle of June till harvesting day) using a 1m × 1m quadrate in the randomly selected points in each farm. The yield samplings were carried out by five random throws of the quadrate and choosing three crops in each throw. At each sampling, fifteen crops were sampled for each farm. As the plant densities were consistent in one farm, fifteen crops were sufficient for

Fig. 1 The map of the study area

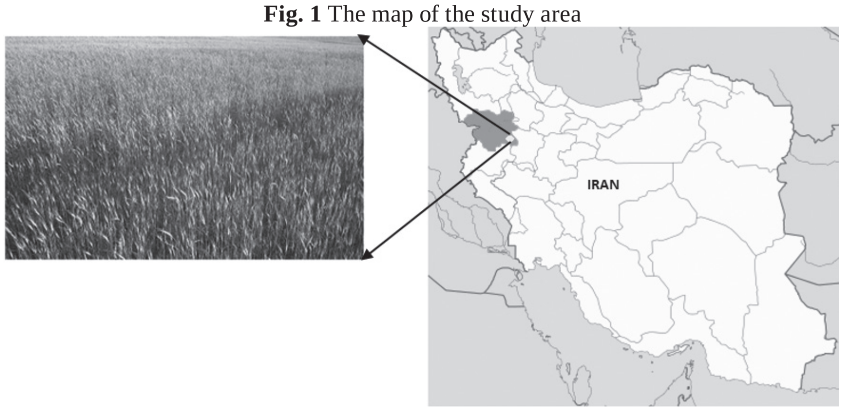

sampling. By measuring the grain mean weight of sampled crops in each farm and knowing crop density, the yield for each farm was calculated until harvest day. Yield samplings were performed with two days intervals and the yield of other days were obtained by interpolating. For each farm, the day with maximum yield was the best harvesting time.

Landsat 8 Images and Spectral Vegetation Indexes

Landsat 8 includes two sensors and eleven bands summarized in **Table 1** (Irons et al., 2012). Landsat provides the spatial resolution and continuous record needed to capture time histories and it is very useful for agricultural applications. In this study, the Landsat images of study area were acquired according to wheat growing calendar. Seven cloud free images of wheat growing period were selected. **Table 2** shows all images of the study area, from the tillering to ripening (maturity) of wheat. FLAASH module/ENVI was used for atmospheric correction. In addition, geometric correction was done for images. Then, corrected images were used to calculate the VIs. These indexes have made a simple and suitable approach for obtaining information from remote sensing data. In this study four VIs were used as following:

1. Normalized Difference Vegetation Index (NDVI): NDVI is the most widely used index for remote sensing of vegetation in the past two decades. This index has been used in many applications, including estimation of crop yields and above-ground dry biomass (Rouse et al, 1974, Tucker et al. 1986, Ren et al. 2008). NDVI is calculated by following Eq. 1.

NDVI = (NIR - RED) / (NIR + RED). .....(1)

Where, NIR and RED are spectral reflectance of Near Infrared and red bands.

2. Soil Adjusted Vegetation Index (SAVI): SAVI attempt to reduce the influence of the soil by assuming that most soil spectra follow the same soil line (Huete, 1998). The formula of SAVI is demonstrated in Eq. 2.

SAVI = (1 + L) (NIR - RED) / (NIR + RED + L) ......(2)

Where, the constant L = 0.5 has been adjusted to account for first-order soil background variation.

3. Enhanced Vegetation Index (EVI): EVI is developed as a standard satellite vegetation product for the Terra and Aqua Moderate Resolution Imaging Spectro-radiometers (MODIS). EVI is a vegetation index designed to enhance the vegetation signal with improved sensitivity in high biomass regions and enhanced vegetation monitoring through minimizing soil and atmosphere influences (Huete et al., 1997). While the EVI is calculated similarly to NDVI, it is corrected for some distortions in the reflected light caused by the particles in the air as well as the ground cover below the vegetation. The formula of EVI is demonstrated in Eq. 3.

EVI = 2.5 (NIR - RED) / (NIR + 6 × RED - 7.5 × Blue + 1) ......(3)

where Blue is spectral reflectance of blue band.

4. Normalized Difference Water Index (NDWI): NDWI is sensitive to changes in liquid water content of vegetation canopies. NDWI is less sensitive to atmospheric effects than NDVI, (Gao, 1996). The formula of NDWI is demonstrated in Eq. 4.

NDWI = (NIR - SWIR) / (NIR + SWIR). .....(4)

where SWIR is spectral reflectance of short wave infrared band.

The above mentioned spectral indexes were calculated for farm pixels for all images from tillering to ripening stages.

Development of Regression Models for Wheat Harvest Time Estimation

The stepwise regression method was used to determine effected growth stages using SPSS 16 software. Seven stepwise regression models of harvest time vs. vegetation indexes were developed to find the relation between them for each wheat growth stage. The models inputs were spectral indexes and best harvest time was the output of models. Field observation data was divided into two categories: 70 % of data was used for model development and 30 % was used for validation of models.

Table 1 Description of Landsat 8 bands (Irons et al., 2012)

Band Specifications	Wavelength (μm)
Band 1 - aerosol (30 m)	0.43-0.45
Band 2 - blue (30 m)	0.45-0.51
Band 3 - green (30 m)	0.53-0.59
Band 4 - red (30 m)	0.64-0.67
Band 5 - near infrared (30 m)	0.85-0.88
Band 6 - shortwave infrared (30 m)	1.57-1.65
Band 7 - shortwave infrared (30 m)	2.11-2.29
Band 8 - panchromatic (15 m)	0.50-0.68
Band 9 - cirrus (30 m)	1.36-1.38
Band 10 - thermal Infrared (100 m)	10.60-11.19
Band 11 - thermal Infrared (100 m)	11.50-12.51

Table 2 Landsat 8 imagery list studied at this research in different growth stages of wheat

No.	Date of image acquiring	The growth stage of wheat
1	2016- 04- 06	Tillering
2	2016- 04- 22	Stem elongation
3	2016- 05- 01	Booting
4	2016- 05- 08	Awn emergence
5	2016- 05- 17	Flowering
6	2016- 06- 09	Dough development
7	2016- 06- 18	Ripening

Results

Developing Regression Models at Different Growth Stages of Wheat

As it could be seen in the Table 3, the stages after flowering have the stronger ability to predict harvesting time of wheat. Moreover, **Table 3** shows the image coincide provided the best regression model with dough stage (R^2 = 0.785; RMSE = 1.13). The spectral indexes were used in this model were NDVI and NDWI. NDVI is one of the most extremely used indexes. The range of NDVI values is between [-1, +1]. Based on phenology studies of the United States Geological Survey (USGS), the NDVI values are categorized as follows; the regions of sand or snow usually have very low NDVI values (e.g. 0.1 or less). Sparse vegetation like grasslands or senescing crops have moderate NDVI values (i.e. nearly 0.2 to 0.5). Dense vegetation such as tropical forests or crops at their peak growth stage may result high NDVI values (about 0.4 to 0.8) (Ali and Salman, 2015).

In this research, the NDVI is the only index which has entered in all models. Song et al. (2016) demonstrated that Landsat NDVI data could be used to predict the wheat yield. In their research, the booting stage of wheat was the best stage for yield prediction. Also, the results of Ren et al. (2008) research which used NDVI to estimate wheat regional yield showed that the best predicted yield data of winter wheat could be achieved nearly 40 days before harvest time (about booting stage). However, to predict wheat harvest time in Meiham region, we found that about 15-20 days ahead of harvest time (dough development stage) is the best time. The results of this research and mentioned researches showed that NDVI can be a good index for agricultural applications such as harvest time prediction and yield estimation. Additionally, it can be concluded that the best time for wheat harvest time prediction is after the best time for yield estimation.

Furthermore, NDWI is an index which is sensitive to changes in liquid water content of vegetation canopies. that interacted with the incoming solar radiation (Gao, 1996). NDWI is less sensitive to atmospheric effects than NDVI. Also, in various stages of wheat growth, the amount of liquid water content changes. Therefore, there is a relationship between harvest day of wheat and NDWI, and the most relationship was found at the dough development stage. Meng et al. (2011), just used NDWI index to estimate mature date of winter wheat. The results showed that NDWI could predict mature date with accuracy of 0.65.

Evaluation of the Developed Regression Model for Harvest Time Predicting

In order to assess the predictive performance of the developed models, we used three models which had the better estimations (the models of flowering, dough development and ripening stages). In this step, we used the 30% remained data for evaluating. **Figs. 2**, **3** and **4** illustrate the performance of these models, in a scatter plot between predicted and observed harvest days. The R^2 and RMSE values of developed model based on dough development stage were achieved 0.752 and 1.22, respectively. In addition, as it can be seen in **Fig. 2**, the image coincide with dough development stage had the best predictive performance.

The performance of developed models at flowering (R^2 = 0.502 and RMSE = 2.21) and ripening (R^2 = 0. 453 and RMSE = 2.42) stages were less than dough development stage. Therefore, it can be concluded that the suitable period for anticipated harvest time using satellite images for achieving highest yield is wheat dough development stage.

Conclusions

The objective of this study was to predict wheat harvest time to reduce yield gap (the difference between yield potential and the actual yield) using satellite images in Meiham region. The analyses of attained results showed Landsat satellite imagery is able to produce valuable information using spectral indexes. Regional estimation of harvest time has different important aspects including farm management, commercial politics and so on. Moreover, the knowledge of harvest time could help to crop harvest without decreasing of yield. The advantage of remote sensing technologies and spectral indexes is their abilities to continuous visit of crops. However, many environmental factors such as the amount of cloud and atmospheric conditions could affect the estimations. It should be noted that NDVI and NDWI are important indexes in crop and vegetation

Table 3 The developed models at different growing stages of wheat

No.	The growth the stage	The growth stage of wheat	R^2	RMSE
1	Tillering	Y= −2.461 NDWI + 1.658 EVI + 9.410 NDVI + 178.763	0.123	2.87
2	Stem elongation	Y= 3.312 NDWI − 18.415 SAVI + 48.818 NDVI +176.586	0.361	2.54
3	Booting	Y= −8.590 NDWI + 24.514 NDVI + 175.655	0.352	2.67
4	Awn emergence	Y= 25.758 NDWI − 0.618 SAVI − 3.277 NDVI + 178.756	0.420	2.71
5	Flowering	Y= 37.825 NDVI + 171.356	0.591	2.02
6	**Dough development**	**Y= 71.340 NDWI + 82.732 NDVI + 164.530**	**0.785**	**1.13**
7	Ripening	Y= 132.159 NDVI + 159.174	0.582	1.92

studies. The best model to predict wheat harvest time was extracted from indexes related to wheat dough development stage (R^2 = 0.785; RMSE = 1.13). Therefore, Landsat 8 images could be used for harvest time prediction. This paper only demonstrates a primary research of crop harvesting time prediction using satellite imagery. To further advance the use of satellite remote sensing to precision harvest, the following researches are suggested:

- The relationships between vegetation indexes and harvest time were affected by satellite image acquisition date, so the harvest time predicting models could be different when images on different dates are used. Therefore, a general model could be developed using several year's data, which can implement harvest time prediction with satellite images at different dates.
- integrating of crop models and satellite remote sensing based models could improve the predicting capability of these models. Therefore, combination of these two categories of models is suggested for future researches.

REFERENCES

Ali, S. M. and S. S. Salman. 2015. Estimating the Yield of Rice Farms in Southern Iraq using Landsat images. International Journal of Scientific & Engineering Research, 6(8), pp.1607-1614.

Anonymous. 2014. Technical instructions for wheat planting. Iran's Ministry of Agriculture.

Baghzouz, M., D. A. Devitt, L. F. Fenstermaker and M. H. Young. 2010. Monitoring vegetation phenological cycles in two different semi-arid environmental settings using a ground-based NDVI system: A potential approach to improve satellite data interpretation. Remote Sensing, 2(4), pp.990-1013.

Bao, Y., L. Liu and J. Wang. 2008. Estimating biophysical and biochemical parameters and yield of winter wheat based on LANDSAT TM images. In IGARSS 2008-2008 IEEE International Geoscience and Remote Sensing Symposium IEEE. 2: II-789).

Bausch, W. C., A. D. Halvorson and J. Cipra. 2008. Quickbird satellite and ground-based multispectral data correlations with agronomic parameters of irrigated maize grown in small plots. biosystems engineering, 101(3): 306-315.

Campbell, B. A. 2002. Radar remote sensing of planetary surfaces. Cambridge University Press.

Dalghandi, M., B. Andarzian, S. Borumand nasab, A. Masah bvani and A. Javaheri. 2015. Evaluation of CERES- Wheat, DSSAT 4.5 in the simulation of wheat yield and phenological stages in terms of allocation of agricultural water management. (Case study: Ahvaz city). Journal of Soil and Water (Agricultural Science and Technology). 28(1): 82-91.

Fig. 2 Scatter plot of predicted and observed harvest time for dough development stage (the boarder lines indicate confidence level of 0.01)

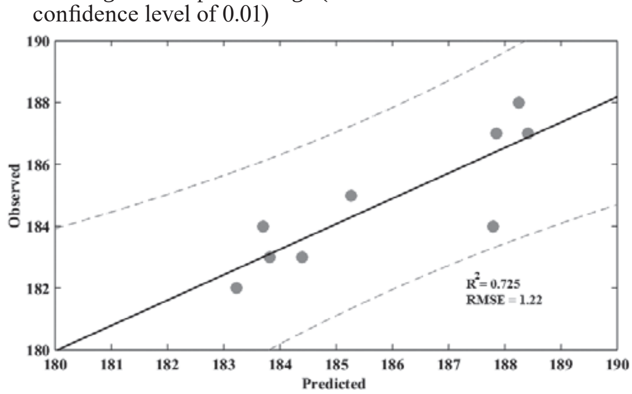

Fig. 3 Scatter plot of predicted and observed harvest time for flowering stage (the boarder lines indicate confidence level of 0.01)

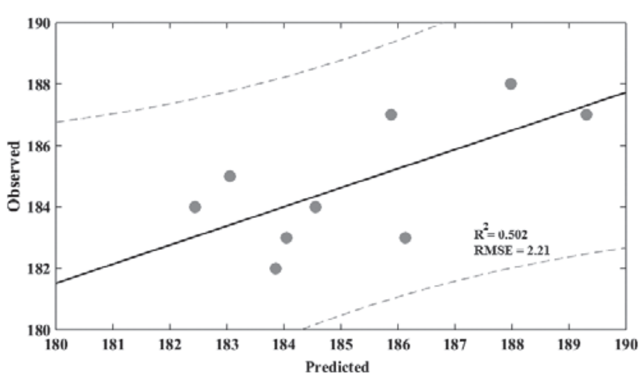

Fig. 4 Scatter plot of predicted and observed harvest time for ripening stage (the boarder lines indicate confidence level of 0.01)

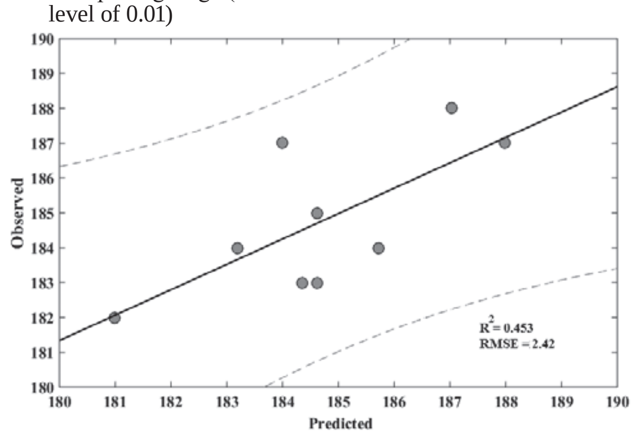

Eklundh, L., H. Jin, P. Schubert, R. Guzinski and M. Heliasz. 2011. An optical sensor network for vegetation phenology monitoring and satellite data calibration. Sensors, 11(8), pp.7678-7709.
Evers, J. B., J. Vos, X. Yin, P. Romero, P. E. L. Van Der Putten and P. C. Struik. 2010. Simulation of wheat growth and development based on organ-level photosynthesis and assimilate allocation. Journal of Experimental Botany, 46: 250-251.
Gao, B. C. 1996. NDWI- A normalized difference water index for remote sensing of vegetation liquid water from space. Remote sensing of environment, 58(3): 257-266.
Hmimina, G., E. Dufrêne, J. Y. Pontailler, N. Delpierre, M. Aubinet, B. Caquet, A. De Grandcourt, B. Burban, C. Flechard, A. Granier and P. Gross. 2013. Evaluation of the potential of MODIS satellite data to predict vegetation phenology in different biomes: An investigation using ground-based NDVI measurements. Remote Sensing of Environment, 132, pp.145-158.
Huete, A. R. 1988. A soil-adjusted vegetation index (SAVI). Remote sensing of environment, 25(3): 295-309.
Huete, A. R. 2012. Vegetation indices, remote sensing and forest monitoring. Geography Compass, 6(9), pp.513-532.
Huete, A. R., H. Q. Liu, K. V. Batchily and W. J. D. A. Van Leeuwen. 1997. A comparison of vegetation indices over a global set of TM images for EOS-MODIS. Remote sensing of environment, 59(3): 440-451.
Irons, J. R., J. L. Dwyer and J. A. Barsi. 2012. The next Landsat satellite: The Landsat Data Continuity Mission. Remote Sensing of Environment, 122, 11-21.
Jihua, M., W. Bingfan, D. Xin, D. Taifeng and N. Liming. 2011. Predicting mature date of winter wheat with HJ-1A/1B data. Transactions of the Chinese Society of Agricultural Engineering, 2011(3).
Jones, J. W., J. White, K. Boote, G. Hoogenboom and C. H. Porter. 2000. Phenology Module in DSSAT v4.0. Documentation and Source Code Listing. Agricultural and Biological Engineering Department, University of Florida, Gainesville, FL., USA.
Jongschaap, R. E. and L. S. Schouten. 2005. Predicting wheat production at regional scale by integration of remote sensing data with a simulation model. Agronomy for sustainable development, 25(4), pp.481-489.
Kamali, G., H. Momenzadeh and M. Vazife dust. Assessment of changes in biomass and yield in periods of drought and rain with the help of MODIS data in Isfahan. Ecology of Agriculture, 3(2): 181-190 (in Persian).
Lyle, G., M. Lewis and B. Ostendorf. 2013. Testing the temporal ability of Landsat imagery and precision agriculture technology to provide high resolution historical estimates of wheat yield at the farm scale. Remote Sensing, 5(4):1549-1567.
Mares, D. J. 1987. Pre-harvest sprouting tolerance in white grained wheat. Fourth International Symposium on pre-harvest sprouting in cereasls. Westview Press, Boulder, Colorado. 64-75.
Philips, P. R. and J. R. O'Callaghan. 1974. Cereal harvesting - a mathematical model. Journal of agricultural engineering research, 19(4): 415-433.
Ren, J., Z. Chen, Q. Zhou and H. Tang. 2008. Regional yield estimation for winter wheat with MODIS-NDVI data in Shandong, China. International Journal of Applied Earth Observation and Geoinformation, 10(4): 403-413.
Ren, J., Z. Chen, Q. Zhou and H. Tang. 2008. Regional yield estimation for winter wheat with MODIS-NDVI data in Shandong, China. International Journal of Applied Earth Observation and Geoinformation, 10(4), pp.403-413.
Rouse Jr, J. W. 1974. Monitoring the vernal advancement and retrogradation (green wave effect) of natural vegetation.
Song, R., T. Cheng, X. Yao, Y. Tian, Y. Zhu and W. Cao. 2016. Evaluation of Landsat 8 time series image stacks f r predicitng yield and yield components of winter wheat. In Geoscience and Remote Sensing Symposium (IGARSS), IEEE International, 6300-6303.
Soudani, K., G. Hmimina, N. Delpierre, J. Y. Pontailler, M. Aubinet, D. J. Bonfil, B. Caquet, A. De Grandcourt, B. Burban, C. Flechard, D. Guyon, A. Granier, P. Gross, B. Heinesh, B. Longdoz, D. Loustau, C. Moureaux, J. M. Ourcival, S. Rambal, L. Saint André and E. Dufrêne. 2012. Ground-based Network of NDVI measurements for tracking temporal dynamics of canopy structure and vegetation phenology in different biomes. Remote Sensing of Environment, 123, 234-245.
Sun, H., X. Zhang, S. Chen, D. Pei and C. Liu. 2007. Effects of harvest and sowing time on the performance of the rotation of winter wheat-summer maize in the North China Plain. Industrial Crops and Products, 25(3): 239-247.
Tucker, C. J., C. O. Justice and S. D. Prince. 1986. Monitoring the grasslands of the Sahel 1984-1985. International Journal of Remote Sensing, 7(11), pp.1571-1581.
Van Ittersum M. K., P. A. Leffelaar, H. Van Keulen, M. J. Kropff, L. bBastiaans and J. Goudriaan. 2003. On approaches and applications of the Wageningen crop models. European Journal of Agronomy 18, 201-234.
Wang, L., J. J. Qu, S. Zhang, X. Hao and S. Dasgupta. 2007. Soil moisture estimation using MODIS and ground measurements in eastern China. International Journal of Remote Sensing, 28(6): 1413-1418.
Yin, X. and H. H. Van Laar. 2005. Crop systems dynamics: an ecophysiological simulation model for genotype-by-environment interactions. Wageningen: Wageningen Academic Publishers.

■■

Design, Development, and Evaluation of a Fuzzy-based Automatic Guidance System for JD955 Combine Harvester

by

Alireza Mahdavian

Saeid Minaei*

Ahmad Banakar

Biosystems Engineering Department,
Faculty of Agriculture, Tarbiat Modares University,
P.O. Box 14115-111, Tehran 14114, IRAN
*Corresponding author: minaee@modares.ac.ir

Abstract

An automatic steering system based on fuzzy logic was developed aiming at navigating a JD955 combine harvester. This system included electro-hydraulic components to steer the harvester using electrical signals, a machine vision system to determine the lateral and angular deviations of the harvester, a fuzzy control system to generate correction signals and a safety system for the steering circuit. Results of evaluation showed that the image processing system was able to detect a specific path accurately in 98% of the cases. Root Mean Square (RMS) of deviations from the path was used to evaluate the system performance. Evaluation of the system was performed on straight-line and curved paths at travel speeds of 1 and 2 m/s and path negotiation modes of manual or automatic steering. Results showed that travel speed increase in the automatic mode caused the error RMS to increase from 6.7 to 11.6 cm. Also, it was found that the automatic steering system was successful in navigating the harvester on a straight path with more accuracy compared to human operators (RMS of 6.7 compared to 9.2 for manual steering). However, on the curvilinear path, deviation from the path in the manual mode was significantly smaller than that in the automatic steering mode i.e. the drivers had higher performance in steering the combine on a curvilinear path.

Keywords: Grain combine harvester, Auto guidance, Control system, Machine vision, Hydraulic system

Introduction

A basic component of automation in agriculture is autonomous navigation. Efforts to develop automatic steering systems for farm machinery started about 50 years ago. A number of aims and motivations are pursued in agricultural automation: controlled-traffic farming (CTF), headland turning and driving ergonomics are fields could be involved with automatic steering (Chamen et al., 2003; Holpp et al., 2013; Sabelhaus et al., 2013)

In recent years, researchers worked hard to optimize different agricultural machines (Ortiz-Laurel and Roessel-Kipping, 2014; Vatsa and Singh, 2014; Kate et al., 2015; Shirwal et al., 2015; Jethva and Varshney, 2016) but the first studies on autonomous navigation date back to the 1920s (Willrordt, 1924), prototype guidance systems based on machine vision techniques have been actively developed since the 1980s, while the first GPS-based systems were designed in the 1990s. An overview of these developments can be found in literature (Wilson, 2000; Li et al., 2009; Kraus et al., 2013). Most navigation systems in the agriculture sector use a camera as sensor and are based on computer vision methodology (Reid and Searcy, 1987). They are popular in agricultural robotics due to their low-priced cameras and more availability than GPS- and Laser-based systems. There is, however, extensive research carried out using other approaches due to certain issues such as light condition sensitivity and atmospheric effects (Stoll and Kutzbach, 2000; Heidman et al., 2002; Slaughter et al., 2008) developed a method for navigating through a cabbage field in which the crop was planted in a grid pattern. They used the knowledge of the environment to build a grid-based model of the local environment in the camera view to obtain the guidance information. There are also stereo-based methods which try to extract in-depth information for robust navigation (Kise et al., 2005). The present study focuses on evaluating a fuzzy controller developed for simulating a human driver behavior, employed in an automatic steering system by testing its vision-based path detector.

Although there is a plethora of research on infield automatic steering for small farm machinery, the concept of introducing field robots should be also considered (Johnson, Naffin, Puhalla, Sanchez, and Wellington; 2009). According to this concept, large teams of smaller autonomous machines are to replace smaller groups of heavier machines as a way to build collective behavioral systems that are more economical, more scalable and less susceptible to overall malfunction (Blackmore et al., 2008; Bochtis et al., 2010; Sørensen and Bochtis, 2010). Literature, however, includes numerous proposals regarding control laws for tractor-trailer systems; most studies have concern about reverse motion because forward motion seems to be stable by nature. these control laws are not well-adopted for an agricultural context due to delays and nonlinearities in actuators and wide variations in soil conditions (Siew et al., 2009; Cariou et al., 2010). Cariou et al. (2010) studied headland maneuvers with a trailer and objective of the research was to maintain a constant angle between the tractor and trailer. Model Predictive Control method was used to anticipate speed variations and limit significant overshoots in a longitudinal motion similar to Cariou et al. (2010). However, the trailer was again ignored both in the forward and backward motions. As mentioned, most research has been done on the small and front wheel steering farm machines thus this research was conducted in the area of the heavy and rear-wheel steered farm vehicles.

The type of control system used for automatic guidance affects vehicle performance (Barawid et al., 2007). Studies conducted in this area have benefited from various steering controllers such as open loop, PID, FPID, and adaptive controllers (Benson et al., 1998; Stombaugh et al., 1998; Wu et al., 1998; Perez-Ruiz et al., 2012). Each of these systems has their advantages, but it should be noted that the aim of an automatic guidance system is simulation of human driver behavior and controllers based on fuzzy logic are best suited to handle this job.

On the one hand, automatic steering reduces manual effort, allowing drivers to spend all their time on controlling and adjusting the system. On the other hand, it makes the job more accurate. Agricultural implements are designed for different purposes and they often work in inappropriate conditions at variable speeds. The long work hours and its tedious nature cause driver exhaustion, reduction of accuracy and loss of safety in machine navigation.

What is meant by a navigated vehicle in agriculture is an automatic machine capable of detecting the crop rows, crop edges or a predetermined path and following it. Undoubtedly, accurate and automatic steering of agricultural machinery in all farm operations such as tillage, planting, and harvesting etc.

Fig. 1 The automation hydraulic circuit designed to complement the manual steering system

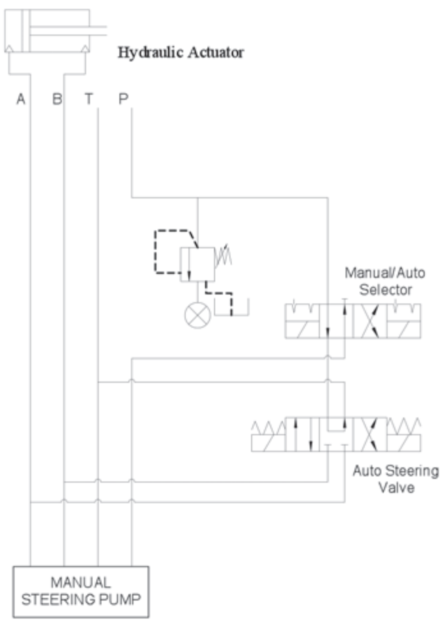

Fig. 2 Electro-hydraulic valves installed beneath the harvester cab

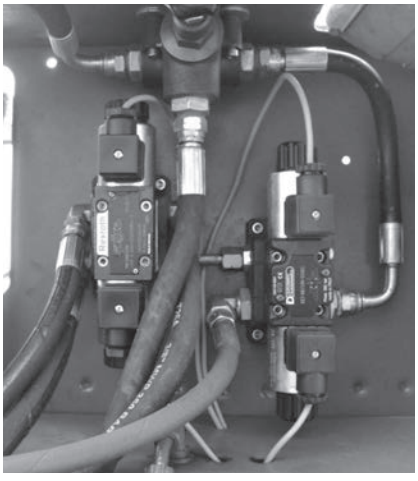

Fig. 3 Video camera installed in front of the combine harvester for imaging the path

is valuable especially for combine harvesters where the operator's failure to continuously monitor the machine adversely affects its efficiency and performance. Combine harvesters are heavy, rear-wheel-steered vehicles with considerable research interest and importance. In such a machine, the automatic steering system can help the driver in many aspects since it allows the driver to focus his attention more on monitoring different parts of the harvester. This, in turn, increases work efficiency and decreases crop losses. A JD955 combine harvester was used as the test platform in this research.

Materials and Methods

The process of developing the automatic steering system includes design and construction of the hydraulic steering circuit, machine vision system, fuzzy control system and steering circuit safety system as described below.

Hydraulic Steering Circuit

In order to steer the harvester using the electrical signals from the control system, in addition to the existing hydraulic system, a complementary hydraulic circuit should be designed satisfying two conditions: first, the new circuit should not interfere with the performance of the existing hydraulic system, and second, each should have the ability to steer the combine harvester individually.

Design of the complementary hydraulic system is shown in **Fig. 1** which includes two main 4 × 2 and 4 × 3 hydraulic valves. The former valve serves as a selection switch between manual and automatic circuits, while the latter acts as the main valve for steering left and right in the auto-steering mode. Considering the system working pressure and the oil flow rate in the hydraulic actuator, 1/4 inches valves were selected for the system.

The valves were installed beneath the driver cab (**Fig. 2**), and the manual activation buttons were placed on the left side of the driver seat.

Design of the Machine Vision System

In this research, a machine vision system was utilized as a sensor for the automatic steering system to detect the path and determine the harvester deviation from the determined path.

An Eye Vision EVE-717SN camera equipped with a 0.33-inch CCD sensor was used (**Fig. 3**). This camera was able to capture images with a 520 TVL resolution. The output signal of the camera was analog which required a mediator to digitize the signal for subsequent image processing. The camera was installed on its special stand 40 degrees below the horizon in front of the combine harvester at the cabin floor height aiming at capturing the appropriate field of view. Since the camera was not perpendicular to the ground surface, captured images covered a the trapezoidal ground area with a minor base of 210 cm, height of 210 cm and major base of 280 cm.

The efficient Hough Transform was used for image processing purposes and determining harvester deviation from the path. The algorithm was responsible for extracting the line or the path coordinates from images, therefore, it measured the desired factors (i.e. lateral and angular deviation of the harvester from the path).

A scale difference occurs in imaging when the camera is positioned at a non-vertical angle relative to the surface of the captured image. As mentioned above, the camera was installed at a 40 degree angle with respect to the horizon. A sample image captured by the installed camera is shown in **Fig. 4**. Image rectification, the process of correcting angular and distance distortions of images captured at an angle, was applied to the image. The raster points were marked 30 cm spacing

Fig. 4 Actual dimensions of the captured image used for calibration and angle corrections

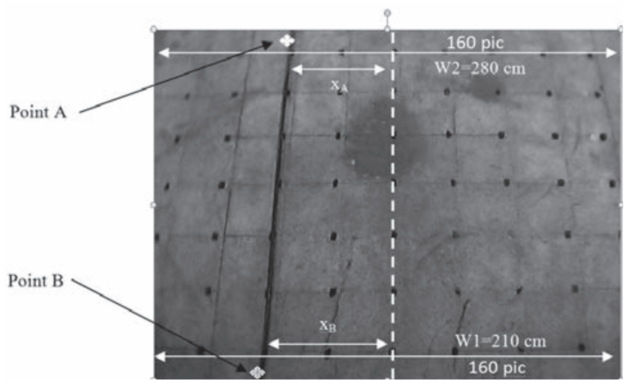

Fig. 5 Block diagram of the automatic steering system designed in this study

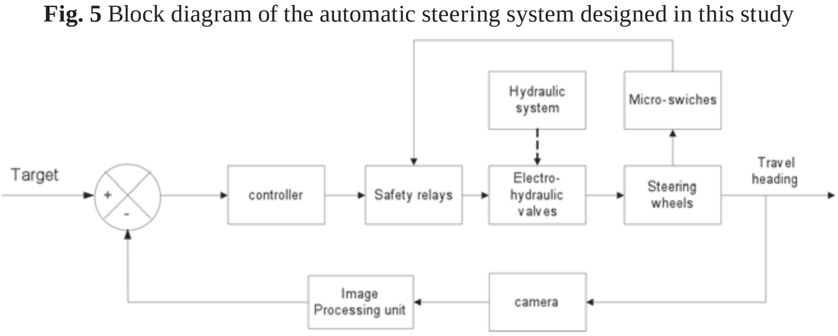

on the ground. It is obvious from the marked points that the black-colored line in the image is parallel to the white dashed line (reference path). In fact, its angular deviation is equal to zero although it has deviated 60cm to the left. The algorithm identified the angle of this line as 5 degrees (which is equal to the angle between the line and the reference path).

In order to correct this shortcoming, the line angle was calculated using trigonometric relationships and corrected distances of the line end points (point A, point B). According to **Fig. 4**, the modified lateral distance of point A from the reference line is 1.3 times larger than its lateral distance in the image (correction factor of 1.3 resulted from dividing 280 to 210).

$$T = tan^{-1}\left(\frac{(x_A \times 1.3) - x_B}{y_A - y_B}\right) \quad .....(1)$$

3.3. The Control System

This system is responsible for making decisions and sending appropriate commands so as to modify vehicle heading and position states. Having determined the lateral and angular deviation of the combine harvester from the path using the process algorithm, the control system took the responsibility of transmitting the appropriate command signals to the steering actuator for modifying harvester heading considering its deviation from the path. Sending an appropriate command is important in the time to reach steady-state condition and also in navigating precision. Guidance of vehicles with rear wheel steering, as the combine harvester, is generally more difficult than that of a front wheel steering system. The steering of such vehicles is heavily dependent on the driver skills and alertness with experience playing a crucial role. In fact, the steering of such vehicles is similar to driving front steering vehicles in reverse gear. Such driving requires more experience and the skill to predict the vehicle heading in response to a given command. In doing so, the control system should take advantage of a control model featuring a database of expert rules. Thus, a fuzzy control system was designed in this experiment to perform the task. The control system flow chart is illustrated in **Fig. 5**.

As mentioned earlier, two factors were considered as the inputs of the system: lateral deviation (D) and angular deviation (T) from the travel path.

The output parameters were the wheel angle and "holding time" signals. The former is the wheel angle with respect to the forward direction and the latter is the time that wheels remain at a specific angle. These two factors were selected in order to precisely model the driver behavior in various driving conditions and different path curvatures. Different combinations of these two factors practically cover all steering conditions. For instance, when faced with an obstacle along the straight path, the vehicle requires larger wheel angles and shorter hold times. This implies that the driver should turn the steering wheel sharply and return it to its initial position. When making a mild long turn (large curvature), the vehicle requires low wheel angle and long hold time; i.e., the driver should slightly turn the steering wheel and hold it until the turn is complete.

Fig. 6 and **7** show the system outputs for different inputs. These diagrams are the results of the input membership functions, fuzzy rules and output membership functions. **Fig. 6** is the diagram of the first output command (wheel angle) for inputs D and T, while **Fig. 7** depicts the second output of the system command (hold time) for different inputs.

The fuzzy inference engine used in this research was the widely-used Mamdani's Minimum Model.

Fig. 6 Wheel angle as a function of lateral and angular deviations resulting from the fuzzy rule base

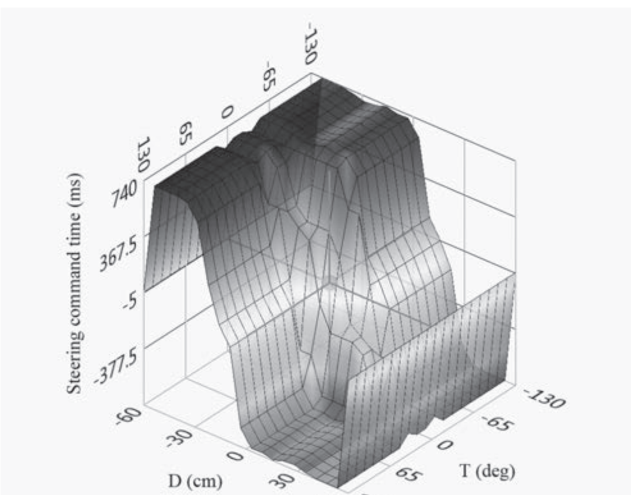

Fig. 7 Wheel hold time as a function of lateral and angular deviations based on the fuzzy rule

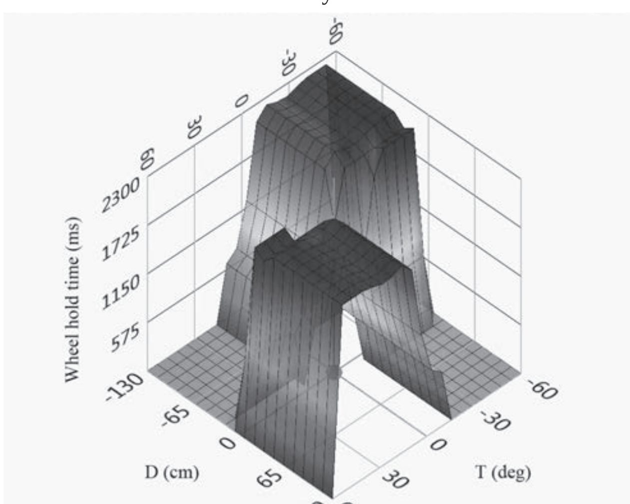

Table 1 Results of ANOVA indicating the effect of lateral deviation on the error in measuring deviationt

Mean Square Error.	Sum of Squares	DOF	Source of Error
0.904^{ns}	5.42	6	Lateral deviation
0.068	2.45	32	error
	7.78	42	summation

^{ns} - None Significant

Table 2 Results of ANOVA indicating the effect of path position in the captured image on angle measurement accuracy

Mean Square	Sum of Squares	DOF	Source
9.64**	57.78	6	D
2.91**	17.49	6	T
4.64**	167.07	36	D × T
0.23	22.67	98	error

** - Significant on the 1% probability level

In this method, output of each rule is calculated by a minimal logic operator, and then a summation operator (max) is used to deduce the results so as to produce the final output. Hence, the control system determined the two numerical outputs, i.e. wheel angle and hold time, through making the necessary calculations based on its inputs which are the outputs of the image processing system.

The image processing system outputs, i.e. lateral and angular deviations, from the inputs of the fuzzy decision-making section and the outputs of the fuzzy system, i.e. wheel angle and hold time, are sent to the actuator for heading correction. The automatic steering system needs mediator hardware to be able to communicate effectively with the processing unit and the actuators. The interface should receive the control signals, and be able to enhance and convert them into electrical signals suitable for driving the actuator. In doing so, a model 4716 interface card made by Advantech was used.

It should be noted that in every control system there is always a possibility if generating erroneous signals and sending inappropriate commands. Therefore, countermeasures are required to protect the system from any damage. The circuit can be safeguarded by placing two micro-switches on both sides of the steering actuator and by installing two protrusions as end-of-the-stroke indicators that can trigger the micro-switches (**Fig. 8**).

Once the piston reaches the end of its stroke, the protrusions activate the micro-switches and open the electrical circuit, thus the process of sending the commands to the steering actuator is terminated. In this situation even if a signal is sent to a solenoid (due to faults in the electrical circuit or incorrect settings), it passes through the relay creating no risk for the system.

Results and Discussion

Accuracy of the Algorithm in Detecting Angular and Lateral Deviations

Accuracy of the algorithm in determining the combine harvester deviations from the path (**Fig. 9**) was evaluated through comparing the results of the algorithm with manual measurements of the lateral and angular deviations.

This algorithm can measure lateral deviations in the [-110, 110] cm range. In order to determine the accuracy of lateral deviation measurement throughout the image width, this factor was evaluated in 7 treatments (30 cm intervals i.e. 90, 60, 30, 0, -30, -60, -90 cm) in terms of the lateral distance and in 7 replications. Analysis of variance of the data was performed and the results are shown in **Table 1**.

It is obvious from the table that the effect of lateral distance on D measurement accuracy is non-significant. In other words, the differences in measurement accuracy of lateral deviations at different points of the image were stochastic, and the algorithm was able to identify the target line with equal accuracy throughout the image width. The mean error of total measurements was 0.9 cm, and the coefficient of variation of the experiment was 26.

Fig. 8 Attachments installed to the steering axel of the harvester for axel mid-and-end point detection

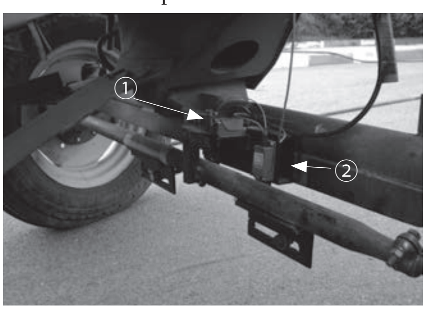

1: Mid-course finder, 2: End of course Micro switch

Fig. 9 Lateral deviation (D) and angular deviation (T) parameters, considered as navigation error parameters

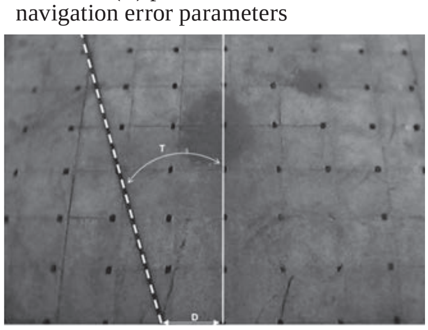

Fig. 10 Lateral and angular deviation levels for testing of algorithm accuracy in determining the deviations

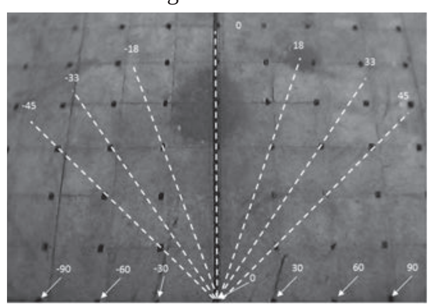

Table 3 A summary of the parameters measured in the tests

Max E (cm).	S.D (cm)	Ave (cm)	RMS (cm)	Speed (m/s)	Steering	Path type
16	6.4	2.0	6.7	1	Automatic	Straight
18	9.1	2.0	9.2		Manual	
24	10.4	5.3	11.6	2	Automatic	
29	6.6	5.0	15.3		Manual	
38	11.5	16.2	19.8	1	Automatic	Curvilinear
31	11.0	11.0	16.1		Manual	
39	18.1	17.0	24.7	2	Automatic	
31	12.0	16.5	18.5		Manual	

In order to study the algorithm accuracy in measuring the angular deviation (T) in terms of the lateral distance and angular deviation, this factor was evaluated by testing 7 levels of transverse distance and 7 angles in 3 replications. The numerical values of distance and angle levels are shown in **Fig. 10**.

As shown in **Fig. 11**, the means of all treatments show less than 2 degrees of error in measuring the angular deviation for treatments of 0, +18 and -18 degrees at all lateral deviation levels. It should be noted that, at ± 33 and ± 45 degree levels where the mean errors of 4 degrees were also observed, increasing the lateral deviation, in + treatments, to the right of the image increases the error. That is while in the − treatments, this increased error occurs by increasing the deviation to the left. Since the angular deviation is normally lower than 20 degrees in navigating the combine harvester, the algorithm error in measuring the lateral deviation is lower than 2 cm.

System Accuracy in Steering the Combine Machine

In previous studies, the average lateral deviation error (Ave) has been used as an index for evaluating steering accuracy. In this research, in addition to the average index, root mean square (RMS) of the deviations from the course was also used which efficiently describes the traversed course error relative to the reference course. The standard deviation (SD) and maximum error (Max E) indexes were also calculated and reported to study the accuracy of the automatic steering system.

The system was tested under 8 different conditions in terms of path types (straight and curvilinear), travel speed (1 and 2 m/s) and steering mode (automatic and manual). **Table 3** summarizes the mean values of the measured indexes in these conditions.

Evaluating the System on a Straight-line Path

Regarding the harvester working conditions which usually follows a straight path, the performance of the steering system on a straight-line course was first studied. Treatments of travel speed (1 and 2 m/s) and steering mode (at 4 levels of, driver 1, driver 2, deriver 3 ,and automatic control) in three replications were considered to evaluate the system. Results of statistical analysis of deviation data are given in **Table 4**.

In the straight path, average of RMS values and the coefficient of variation were 11.6 cm and 5%, respectively.

It can be concluded from the results that the effects of travel speed and steering mode on navigation accuracy are significant. Comparisons of the means for different steering levels using the LSD test are shown in **Fig. 14** while the path tracking samples in various steering modes on two paths at various speeds are shown in **Figs. 12**, **13**, **15**, **16**, **18** and **19**.

Based on the comparison of the means, there is no significant difference among the human drivers while the differences in the accuracy of steering by the automatic system and the human drivers are significant. The auto-steering system was able to navigate the combine harvester more accurately along the straight path than all the human drivers. However, increasing forward speed decreased accuracy of the automatic system (**Fig. 14**).

Evaluating the System on a Curvilinear Course

Sometimes agronomic consider-

Fig. 11 Accuracy of angle measuring when the harvester is located in different lateral (D) and angular (T) deviations

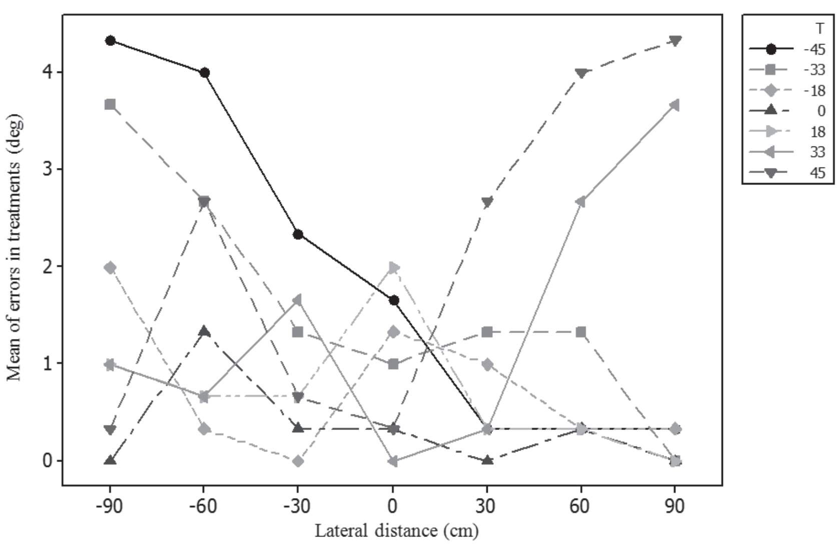

Table 4 Results of ANOVA indicating the effect of travel speed and steering mode on navigation accuracy (RMS) following a straight-line path

Mean Square	Sum of Squares	DOF	Source of Error
210.04**	210.04	1	Speed
8.07**	24.17	3	Steering mode
0.09ns	0.28	3	Speed × Steering mode
0.37	5.89	16	Error

**: Significant at the 1% probability level; ns : Non-significant

Table 5 Results of ANOVA indicating the effect of travel speed and steering on navigating accuracy (RMS) in curvilinear course

Mean Square	Sum of Squares	DOF	Source of Error
37.10**	37.10	1	Speed
8.07**	44.46	1	Steering
0.04ns	0.04	1	Speed × Steering
0.99	7.97	8	Error

**: Significant at the 1% probability level; ns : Non-significant

ations require planting in curved rows, therefore, the harvester should follow the same path when harvesting these crops. The effects of travel speed (1 and 2 m/s) and steering (automatic and manual) on steering accuracy were studied in three replications (**Table 5**). The curvilinear path was selected as shown in Fig. 17 based on the conventional planting patterns.

In the curvilinear path tests, average of the RMS values and the coefficient of variation were calculated as 19.77 cm and 5%, respectively.

Analysis of variance (**Table 5**) revealed that the effects of travel speed and steering mode were highly significant. It can also be concluded that these two factors have no interaction with each other. Hence, the increased travel speed resulted in a decrease in navigating accuracy (**Table 1**). Unlike the observations in the straight path, human drivers performed more accurately in steering the harvester than the automatic steering system on the curvilinear path. A few points should be noted when analyzing the results of this part of the experiment:

1. Human drivers were in good posture and physical status and focused mostly on accurate steering of the combine harvester throughout these experiments. In real conditions, exhaustion deviate the driver from the normal condition after a few hours, and he should also use his strength and power to pay more attention to monitoring the status of other parts of the combine harvester.
2. The minimum radius of curvature (25 m) which corresponds with maximum curvature was selected for this experiment. The curvilinear paths on fields have larger ra-

Fig. 12 A sample of the harvester path tracking sample in automatic steering mode on a straight-line course at 1 m/s

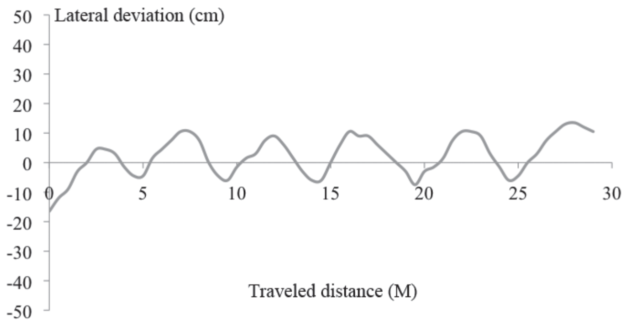

Fig. 13 A sample of the harvester path tracking sample in manual steering mode on straight-line course at 1 m/s

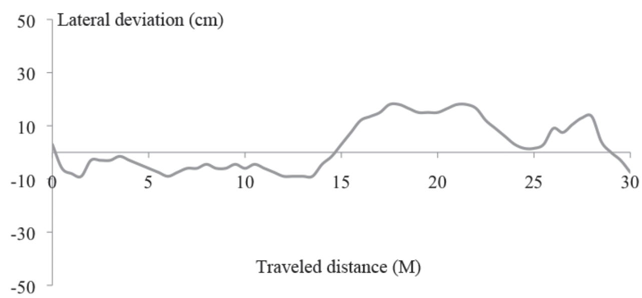

Fig. 14 Comparison of the means for steering treatments on a straight-line course

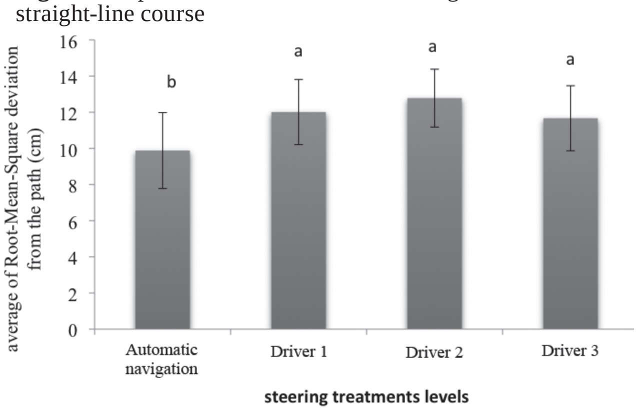

Fig. 15 A sample of the harvester path tracking sample in manual steering mode on straight-line course at 1 m/s

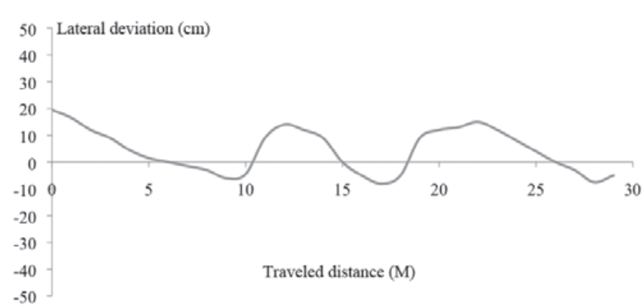

dii depending on the row planting patterns and the curvilinear paths occur with milder curvatures in real-life farming conditions.

3. The system and fuzzy control section in this study were designed aiming at detecting and following a straight path. Increased errors along curvilinear paths were expected when compared to straight-path and manual steering situations (as shown in **Table 1**).

REFERENCES

Barawid, O. C., A. Mizushima, K. Ishii and N. Noguchi. 2007. Development of an autonomous navigation system using a two-dimensional laser scanner in an orchard application. Biosyst Eng 96: 139-149

Benson, E. R., T. S. Stombaugh, N. Noguchi, J. D. Will and J. F. Reid. 1998. An evaluation of a geomagnetic direction sensor for vehicle guidance in precision agriculture applications. ASAE Pap. 983203:

Blackmore, B. S., S. Fountas, T. A. Gemtos and H. W. Griepentrog. 2008. A specification for an autonomous crop production mechanization system. Int. Symp. Appl. Precis. Agric. Fruits Veg. 824. pp 201-216

Bochtis, D. D., C. G. Sørensen and S. G. Vougioukas. 2010. Path planning for in-field navigation-aiding of service units. Comput Electron Agric 74: 80-90

Cariou, C., R. Lenain, B. Thuilot and P. Martinet. 2010. Autonomous maneuver of a farm vehicle with a trailed implement: motion planner and lateral-longitudinal controllers. Robot. Autom. (ICRA), 2010 IEEE Int. Conf. IEEE, pp 3819-3824

Chamen, T., L. Alakukku, S. Pires, C. Sommer, G. Spoor, F. Tijink and P. Weisskopf. 2003. Prevention strategies for field traffic-induced subsoil compaction: a review: Part 2. Equipment and field practices. Soil tillage Res 73: 161-174

Heidman, B. C., A. Abidine, S. Upadhyaya, D. Hills and P. Robert. 2002. Application of RTK GPS based auto-guidance system in agricultural production. 6th Int. Conf. Precis. Agric. pp 1125-1134

Holpp, M., M. Kroulik, Z. Kviz, T. Anken, M. Sauter and O. Hensel. 2013. Large-scale field evaluation of driving performance and ergonomic effects of satellite-based guidance systems. Biosyst Eng 116: 190-197

Jethva, K. R. and A. K. Varshney. 2016. Design and Development of Reciprocating Type Cumin Cleaner Cum Grader. Agric Mech ASIA, AFRICA, Lat Am 47: 8

Kate, A. E., N. C. Shahi, U. C. Lohani and J. P. Pandey. 2015. Development and Testing of Pedal Operated Wild Apricot Pit Grader. AMA- Agricultural Mech ASIA AFRICA Lat Am 46: 48-52

Kise, M., Q. Zhang and F. R. Más. 2005. A stereovision-based crop row detection method for tractor-automated guidance. Biosyst Eng 90: 357-367

Kraus, T., H. J. Ferreau, E. Kayacan,

Fig. 16 A sample of the harvester path tracking sample in automatic steering mode on a straight-line course at 1 m/s

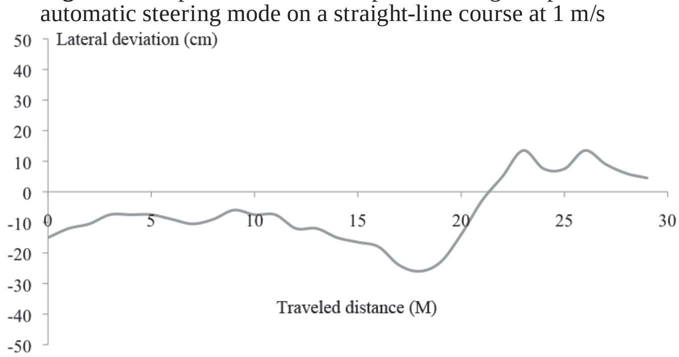

Fig. 17 Angular coordinates of the curvilinear course

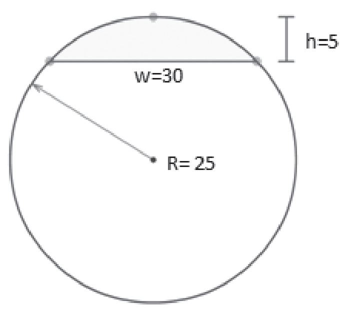

Fig. 18 A sample of the harvester path tracking sample in automatic steering mode on a curvilinear course at 1 m/s

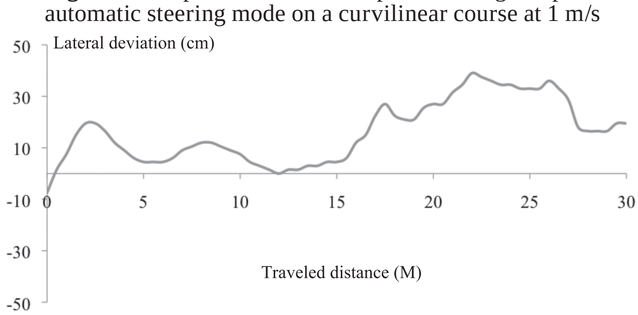

Fig. 19 A sample of the harvester path tracking sample in manual steering mode on a curvilinear course at 1 m/s

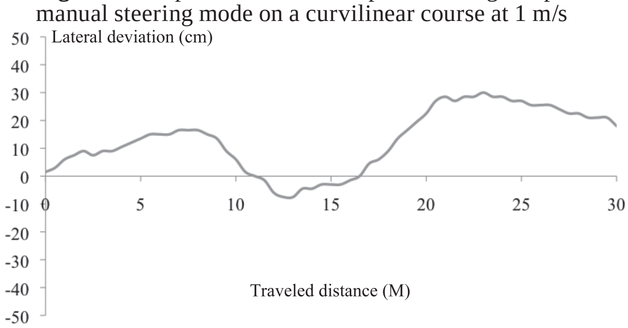

H. Ramon, J. De Baerdemaeker, M. Diehl and W. Saeys. 2013. Moving horizon estimation and nonlinear model predictive control for autonomous agricultural vehicles. Comput Electron Agric 98: 25-33
Li, M., K. Imou, K. Wakabayashi and S. Yokoyama. 2009. Review of research on agricultural vehicle autonomous guidance. Int J Agric Biol Eng 2: 1-16
Ortiz-Laurel, H. and D. Roessel-Kipping. 2014. Development of a mechanical harvesting aid for prickly pear cactus fruit.
Perez-Ruiz, M., D. C. Slaughter, C. Gliever and S. K. Upadhyaya. 2012. Tractor-based Real-time Kinematic-Global Positioning System (RTK-GPS) guidance system for geospatial mapping of row crop transplant. Biosyst Eng 111: 64-71
Reid, J. and S. Searcy. 1987. Vision-based guidance of an agriculture tractor. IEEE Control Syst Mag 7: 39-43
Sabelhaus, D., F. Röben, L. P. M. zu Helligen and P. S. Lammers. 2013. Using continuous-curvature paths to generate feasible headland turn manoeuvres. Biosyst Eng 116: 399-409
Shirwal, S., I. Mani, N. P. S. Sirohi and A. Kumar. 2015. Development and Evaluation of Carrot Harvester. AMA- Agricultural Mech ASIA AFRICA Lat Am 46: 28-34
Siew, K. W. , J. Katupitiya, R. Eaton and H. Pota. 2009. Simulation of an articulated tractor-implement-trailer model under the influence of lateral disturbances. Adv. Intell. Mechatronics, 2009. AIM 2009. IEEE/ASME Int. Conf. IEEE, pp 951-956
Slaughter, D. C., D. K. Giles and D. Downey. 2008. Autonomous robotic weed control systems: A review. Comput Electron Agric 61: 63-78
Sørensen, C. G. and D. D. Bochtis. 2010. Conceptual model of fleet management in agriculture. Biosyst Eng 105: 41-50
Stoll, A. and H. Dieter Kutzbach. 2000. Guidance of a forage harvester with GPS. Precis Agric 2: 281-291
Stombaugh, T. S., E. R. Benson and J. W. Hummel. 1998. Automatic guidance of agricultural vehicles at high field speeds. ASAE Pap. 983110:
Vatsa, D. K. and S. Singh. 2014. Development and Evaluation of Power Tiller Operated Zero Till-Drill for Mechanizing Wheat Sowing in Hills. Agric Mech ASIA, AFRICA, Lat Am 45: 86
Wilson, J. N. 2000. Guidance of agricultural vehicles -a historical perspective. Comput Electron Agric 25: 3-9
Wu, D., Q. Zhang, J. F. Reid, H. Qiu and E. R. Benson. 1998. Model recognition and simulation of an E/H steering controller on off-road equipment. Urbana 51: 61801

■■

Seed Drill Discharge Rate Variation Due to Varietal Differences Using an Automated Calibration Test Rig

by
Daanvir Karan Dhir *
Research Assistant
CSIR-CMERI CoEFM
Gill Road, Ludhiana, Punjab 141 006
INDIA
* Corresponding Author
karandhir198@gmail.com

Pradeep Rajan
Principal Scientist
CSIR-CMERI CoEFM
Gill Road, Ludhiana, Punjab 141 006
INDIA

S. R. Verma
Ex. Dean, CoAE & T,
Punjab Agricultural University,
Ludhiana, Punjab 141 00
INDIA

Abstract

India occupies about 12.40% of the total world wheat area, whereas it contributes 11.77 % in the total wheat production globally. The seed cum fertilizer drills are majorly used for sowing wheat crop in India and other parts of Asia. Farm equipment calibration is an important aspect to reduce seed wastage and implement precision farming practices. An automated seed drill calibration test rig was designed and developed to study the inter-varietal differences in the seed rate with respect to different operating speeds of the seed drill and active lengths of the fluted roller. The developed test rig is capable of measuring the seed rate variation at meter level accuracy. The inter-varietal variations, due to bulk density of seeds, can account up to a variation of 17% or 23.9 kg/ha under similar operating conditions. Also, the operating speed is having significant effect on seed rate variation only with other pertinent variables like variety and active length. The study highlights the seed rate variation through the seed rate distribution with respect to the mean seed rate using jitter plots and recommend variety specific calibration process before each sowing season to have precision in seed sowing.

1. Introduction

Agriculture remains the principal source of livelihood for more than 58% of the Indian population and employs about 52% of total work force (National Academy of Agricultural Sciences, 2016). The world would require around 840 million tonnes of wheat by 2050 from its current production level of 642 million tonnes. To meet this demand, developing countries have to increase their wheat production by 77% and more than 80% of demand should come from vertical expansion (Sharma et al., 2015).

India stands first in area and second in production next to China in the world. India occupies about 12.40% of the total world wheat area, whereas it contributes 11.77% in the total wheat production globally. There is not much scope for area expansion under wheat. Increasing the wheat productivity by adopting improved cultivation practices would be the main emphasis (Indian Council of Agricultural Research, 2013). Wheat production in India during the crop year 2012-13 at 93.51 million tonnes from an area of 30.0 million hectares was less than the record production of 94.88 million tonnes from 29.55 million hectares during the preceding year 2011-12 (Directorate of Wheat Research, 2014).

The high cost of production and low productivity, despite significant increase in food grain production, might throw the Indian farmers out of economic competition arena of free market. As per studies, the farm production and productivity could be increased by 10-15% by adopting the appropriate mechanization technologies (National Academy of Agricultural Sciences, 2016).

Precision farming, though in many cases a proven technology, is still mostly restricted to developed

(American and European) countries. Except for a few, there is not much literature to show the scope and its implementation in India. Precision farming is only a concept in many developing countries and strategic support from the public and private sectors is essential to promote its rapid adoption. There is a scope of implementing precision farming for major food-grain crops such as rice, wheat, especially in the states of Punjab and Haryana. (Shanwad et al., 2004).

Calibration of farm equipment is often overlooked as a means of improving machine performance and controlling input costs. Calibration is more important than ever and requires more attention from farmers. Calibration of the grain drill metering system can help eliminate uneven stands and control input costs (seeds) by achieving targeted seeding rates (Hawkins and Ess, 2006). Seed metering systems, especially the fluted roller mechanism, are based on volume displacement. Seed size varies between varieties and the size of seeds of the same variety may vary from year after year. Therefore, if one lot of seed varies in size and weight from another, two different amounts or number of seeds will be metered if the drill setting is not changed accordingly (Hofman, 1998).

Two wheat varieties, namely WH-1105 and HD-3086 have been among the twelve new varieties released by the Central Sub-Committee of Directorate of Wheat Research on Crops Standards, Notification and Release of Varieties for Agricultural Crops (CVRC) for different production conditions of the country (Directorate of Wheat Research, 2014) and the same was selected for the current study.

Various Indian Standards and Regional Network for Agricultural Machinery (RNAM) codes are followed during manufacturing and calibration of seed drills. These standards have been established long back without any major addition/revision in the quality parameters or the test methods to determine the performance and precision. Since precision farming is gaining acceptance in India, relevant standards should be formulated for the accurate calibration of these metering mechanism. Although IS:6316 (1993) & IS: 6813 (2000) mention the permissible variation in seed rate due to change in speed, level of seeds in hopper and distance travelled by seed drill; no particular standard has been framed to calibrate the seed drill on the basis of different seed varieties at a particular seed rate setting used for sowing. In view of the above, this study was conducted to assess the variation in seed rate by the fluted roller seed metering mechanism for two different seed varieties with meter level accuracy.

2. Materials and Methods

The manufacturing and testing of farm equipment is India is governed by the specifications prescribed in the Bureau of Indian Standards (BIS) or RNAM codes. The laboratory tests were conducted to examine the seed discharge rate variation due to varietal differences in a commercially available seed drill and suggest the development of necessary standards with new testing methods to foster precision farming practices in India and Asia.

2.1 Theoretical Calculations of Seed Rate

The physical properties of both the varieties of wheat seeds are tabulated in **Table 1** along with the theoretical seed rates. To ascertain the theoretical seed rate at different active lengths, equation proposed by Bernaki et.al. (1972) was utilized, since this equation takes into account the flow of seed above the static layer over the bottom plate. The theoretical seed rate values calculated using this formula always tend to be higher than the actual seed rate values. The expression to determine the seed rate per hectare is:

$$Q = \frac{2800\gamma p(1-\alpha)\beta l n D^2}{Z a k^2} \quad .....(1)$$

Where,

Q - Seed rate per hectare, kg/ha
γ - Bulk Density, kg/m^3
α - Constant
β - Coeff. of material feed reduction
l - Active length of fluted roller, cm
n - Reduction ratio
D - Outer dia. of fluted roller, cm
Z - Number of furrow openers
a - Distance between furrow openers, m
k - Coeff. Based on the width of slot

The coefficients for the calculation

Table 1 Physical properties of WH-1105 & HD-3086 and theoretical seed rate calculations

	WH-1105	HD-3086		WH-1105	HD-3086
A. Physical properties					
Length, mm ± SD	5.98 ± 0.78	6.15 ± 0.87	Sphericity	0.62	0.61
Width, mm ± SD	3.11 ± 0.32	3.21 ± 0.30	True Density, kg/m^3	1.25	1.21
Thickness, mm ± SD	2.56 ± 0.29	2.75 ± 0.28	Bulk Density (γ), kg/m^3	0.80	0.79
Equivalent diameter, mm	3.62	3.79	Moisture content, %	11	12
B. Parameters					
Furrow Openers (Z) × Spacing (a), m		11 × 0.2	Dia. of ground wheel (Dg), m		0.38
Number of flutes (N)		10	Dia. of flute (d & D), cm		1.01 & 4.62

of the theoretical seed rate is taken from Bernaki et.al. (1972) and other values were measures as shown in **Table 1**. The theoretical seed rate for the two varieties, WH-1105 and HD-3086, at three different La (6.3, 13.3, 20.9 mm) are, 136.4, 288.0, 452.2 and 134.0, 283.0, 444.6 kg/ha respectively.

2.2 Experimental Setup

The automated calibration test rig comprises two major assemblies, a) seed drill assembly, and b) dynamic weighing assembly as illustrated in **Figure 1** and **Figure 2**. A commercially available fluted roller seed metering mechanism was used to complete the seed drill assembly so that the experimental setup resembles a commercial grade seed drill. The seed drill assembly consists of a seed hopper, fluted roller seed meter, seed rate setting mechanism and drive unit. The test apparatus was likewise prepared with a rate setting lever to change the active/dynamic length of the fluted roller. Different working speeds of the stepper motor [Nema23, BH57SH100-3004A, Bholanath make], simulating field operating speed of seed drill, were controlled utilizing Pulse Width Modulation (PWM) strategy.

The dynamic weighing assembly consists of: a) digital load cell [single point bellow type load cell, RSL910, Pulse Electronic make] b) digital weight transmitter [RS201, Rudra make], and c) National Instruments DAQ system [cRIO 9035]. The acquired data set was sampled so that it can reflect five values within a travel distance of 100 m. These sampled data was further analysed to determine the variation in seed rate among the selected varieties.

Full factorial experiment with three independent variables, namely a) variety (2 levels - WH-1105 and HD-3086), b) seed drill operating speed (3 levels - 3, 5 and 7 km/h), and c) active length of the fluted roller (3 levels - 6.3 mm (30% exposure), 13.3 mm (60% exposure) and 20.9 mm (100% exposure)) was conducted for measuring the seed drill discharge rate variation. Full factorial design was selected so that effect of each factor along with interactions between factors can be analyzed.

3. Results and Discussions

The experimental data was investigated to determine the variations in seed drill discharge rate due to varietal difference at different operating speeds and active lengths. Jitter plots were used to represent the sampled data with the bold lines representing the mean seed rate, not the set seed rate. The data was then statistically analyzed to determine the effect of variety and operating speed on seed discharge rate with respect to active length of the fluted roller.

3.1 Variation of Seed Rate From Mean Seed Rate

Figure 3(a) shows the seed discharge rate distribution for two varieties at an active length of 6.3 mm with the bold line representing the mean seed rate. The general trend observed in this jitter plot is that mean seed rate for WH-1105 at three operating speeds is 76 kg/ha, which is higher than HD-3086 being

Fig. 2 Automated calibration test rig (experimental setup)

Fig. 1 Schematic diagram of automated calibration test rig

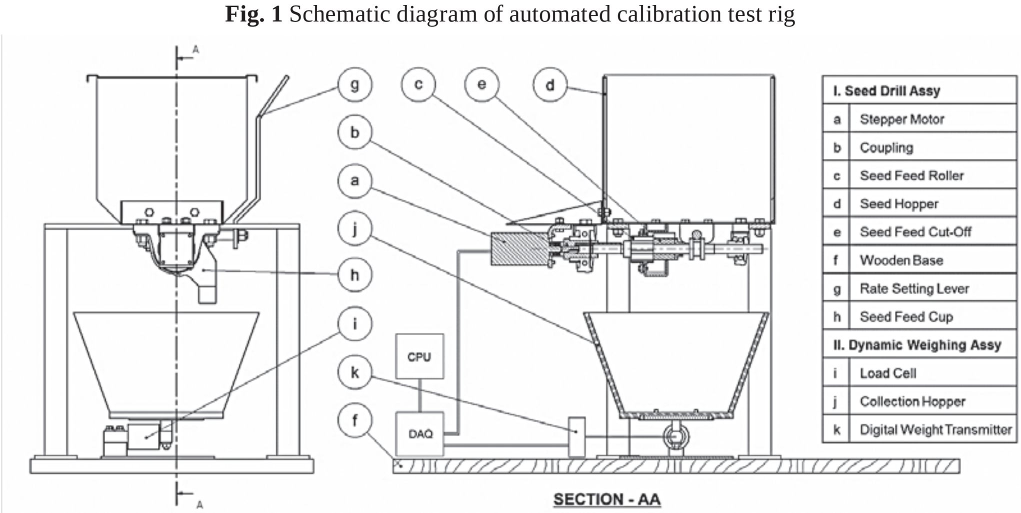

Table 2 Overall ANOVA Table

Source	DF	Sum of Squares	Mean Square	F Value	P Value
Variety	1	274.35	274.35	38.39	0*
Active length	2	75531.7	37765.85	5283.99	0*
Speed	2	20.17	10.08	1.41	0.25
Variety*Active length	2	20073.47	10036.74	1404.28	0*
Variety*Speed	2	69.33	34.66	4.85	0.009*
Active length*Speed	4	38644.58	9661.14	1351.73	0*
Variety*Active length*Speed	4	36057.66	9014.41	1261.25	0*

* shows the values that are significantly different at the 0.01 level

65 kg/ha at the theoretical seed rate of 136.4 / 134.0 kg/ha respectively. Further, the inter-speed variation for the two varieties is almost negligible at the speeds of 3 and 7 km/h while a 1.2% variation exists at 5 km/h.

Similarly, the mean seed rate values (bold lines) in **Figure 3(b)** for WH-1105 is higher than HD-3086 at all the three operating speeds. The maximum and minimum variation in the mean seed rates of the two varieties is 6.1% and 2.7% at 3 and 5 km/h respectively. The variation decreases with the operating speed because maximum difference occurs at low operating speed since low speeds are critical to higher deviations.

At 20.9 mm active length, the mean seed rate values for the two varieties is almost equal at 3 km/h and the mean seed for WH-1105 is only 1.8% higher than HD-3086 at 5 km/h operating speed. The seed rate values obtained at this active length are closely distributed near the mean seed rate values in comparison to the other two active lengths of 6.3 and 13.3 mm where the values are much more scattered and dispersed away from the mean.

3.2 Difference Between Mean Seed Rate

At 6.3 mm active length, the variation in the seed rate values for WH-1105 is approximately 17% higher than HD-3086 and this difference is almost constant for all the three operating speeds. This difference is not much significant at 13.3 mm active length where the mean seed rate for WH-1105 is higher at 3 km/h than 5 and 7 km/h resulting in maximum variation at this speed while the mean seed rate for HD-3086 is almost equal at all the operating speeds. At 20.9 mm active length, the mean seed rate values are almost the same for the two varieties at 3 km/h. The mean seed rate values tend to increase with the increase in operating speed for WH-1105 and vice versa for HD-3086. A prominent rise and fall in the seed rate values for WH-1105 and HD-3086 respectively at 7 km/h with respect to the other operating speeds results in a variation of 7.8% between the two mean seed rate values involved.

The results depict that a maximum of 17% variation could exist for two different commercially used wheat varieties. This suggests a major design flaw in the fluted roller mechanism, since a variation of only 1.7% between the bulk densities of the two varieties could result in a 10 times amplified percentage variation in seed rare. This also necessities a need for the development of standard variation values similar to those stated in the IS: 6316 (1993) & IS: 6813 (2000), so that the design and fabrication of the present fluted roller design may be altered accordingly to offer a variety specific calibration. Furthermore, it is required on the part of seed drill manufacturers to provide such calibration data and guidelines to the farmers for an easily conducive calibration.

Fig. 3 Jitter plot of seed rate distribution at different active lengths of fluted roller for WH-1105 and HD-3086 at, (a) 6.3 mm active length. (b) 13.3 mm active length

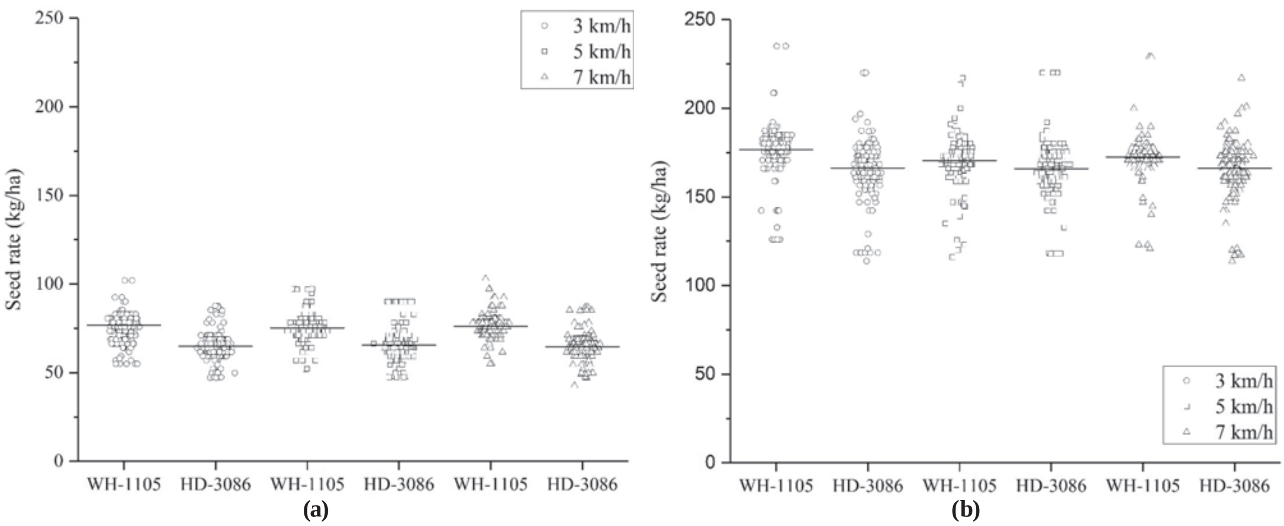

3.3 Analysis of Variance (ANOVA)

Statistical analysis of the experimental data was carried out using the three factor full factorial design, which compares means across the selected factors and the results are presented in **Table 2**. The analysis of variance indicates that both variety and active length of fluted roller had a significant influence on the seed rate values, its distribution and variation from the mean at 1% confidence level. However, operating speed doesn't have a direct significant effect on the seed rate. It may be due to the fact that the laboratory experiments were conducted at negligible slip and absence of any vibrations which is very common in field conditions.

The interaction between the factors, i.e. variety, operating speed and active length had a significant influence on the seed rate and its variation from the mean value. Therefore, operating speed assumes importance while deciding the optimum operational conditions for a seed drill and the chosen variety.

4. Conclusions

The performance of a commercially available fluted roller seed metering mechanism, used in a seed drill, was analysed with the developed automated seed drill calibration test rig, to determine the variation in seed discharge rate for different varieties under same operational conditions. The results revealed that the maximum variation between the two varieties could result in a difference of 23.9 kg/ha under the same operational settings. Low operating speeds are critical to seed rate variations and the seed rate is more uniform at higher speed of operation. New automated testing methods, like the developed automated seed drill calibration test rig, has to be developed and incorporated in the standard test codes of seed drills and seed-cum-fertilizer drills so that a quick and accurate calibration of the seed drill can be undertaken before each sowing season. The study shown that design changes in the present fluted roller mechanism is very much essential and development of standards / calibration charts for varietal differences to foster precision farming practices.

Acknowledgement

The authors gratefully acknowledge the financial and technical support received from Department of Science & Technology (DST) and Council for Scientific & Industrial Research (CSIR) under the Network Program - "Centre for Precision & Conservation Farming Machinery (CPCFM)".

REFERENCES:

Directorate of Wheat Research. 2014. DSR Annual Report 2013-14. Indian Council of Agricultural Research. Retrieved from: http://www.dwr.res.in.

Bernaki, H., J. Haman and Cz. Kanafajski. 1972. Agricultural Machines, Theory and Construction, Vol. I., Department of Agriculture and the National Science Foundation, Washington D.C, US.

Hawkins, S. E. and D. R. Ess. 2006. Grain Drill Metering Systems and the Need for Calibration. Purdue Extension. Department of Agricultural and Biological Engineering. Purdue University. ABE-126-W.

Hofman, V. 1998. Calibrating Drill Seed Meters. Extension Agricultural and Bio systems engineering. North Dakota State University. AE-1144.

Indian Council of Agricultural Research. 2013. Wheat: The crop for ensuring Indian food security. In DWR Perspective Plan Vision 2025. India. Retrieved from: www.farmers.gov.in .

National Academy of Agricultural Sciences. 2016. Practical and Affordable Approaches for Precision in Farm Equipment and Machinery. Policy Paper 84. India.

Shanwad, U. K., V. C. Patil and H. H. Gowda. 2014. Precision Farming: Dreams and Realities for Indian Agriculture. Map India 2004 Proceedings. India.

Sharma, I., B. S. Tyagi, G. Singh, K. Venkatesh and O. P. Gupta. 2015. Enhancing wheat production - A global perspective. Indian Journal of Agricultural Sciences. 85 (1): 3-13.

■■

Optimization of Combine Crop Parameters for Paddy Harvesting by Head Feed Combine

by
Ingole Omprakash Avdhut
M. Tech student

Anil Kumar
Assistant Professor

Vijaya Rani
Assoc. Professor and Head

by
S. Mukesh
Assistant Professor

Nitin Kadwasra
M. Tech student

Kanishk Verma
M. Tech student

Department of Farm Machinery and Power Engineering,
CCS Haryana Agricultural University, Hisar - 125004, Haryana, INDIA

Abstract

A head feed combine was evaluated for optimization of combine parameters viz., cylinder speed (14.42, 15.53 and 16.64 m s^{-1}), forward speed (3.5, 4.0 and 4.5 km h^{-1}) and crop parameter viz., grain moisture content (18.1 to 22.4%) in relation to threshing efficiency, cleaning efficiency and total grain losses for scented and non-scented paddy varieties. Moisture content of 18.1%, cylinder speed of 15.53 m s^{-1} and forward speed of 4.0 km h^{-1} was found optimum for harvesting of scented paddy variety Pusa - 1121, whereas moisture content of 18.1%, cylinder speed of 16.64 m s^{-1} and forward speed of 4.5 km h^{-1} was found optimum for harvesting of non-scented paddy variety HKR - 127.

Key words: Cleaning efficiency, Combine, Grain losses, Threshing efficiency

Introduction

Paddy is one of the most important crop for food security in India, contributing significantly towards providing food and livelihood for 130 million peoples. The area under paddy cultivation in India is around 44 million ha, which is largest in the world against total area of 160 million ha. The total rice production of the world was 742 million tones out of which 105 million tones were produced in India in 2014 (Anonymous, 2015a). The small states of Punjab and Haryana, often referred to as the "Food Bowl" of the country, produces 50% of the national rice production (Dhillon et al., 2010). In Haryana, rice was grown over an area of around 1.3 million ha with total production of 40 million tones with productivity of 3077 kg ha^{-1} during 2014-15 (Anonymous, 2015b).

In paddy cultivation, harvesting and threshing operations are laborious involving human drudgery and require about 150-200 man-h ha^{-1} for harvesting of paddy alone (Veerangouda et al.,2010). Traditionally, paddy is harvested by manual labour using sickles/reaper followed by threshing manually or by stationary power thresher. Due to the non-availability of labours, crop harvesting is often delayed which exposes the crop to vagaries of nature. Timely harvesting is utmost important, as delayed harvesting leads to a considerable loss of grain and straw owing to over maturity resulting in loss of grains by shattering and also hampers the seed bed preparation and sowing operations for the next crop. The paucity of labour force is forcing the farmers to go for crops, which are more remunerative and less labour intensive, thus affecting the paddy cultivation. Therefore, an efficient method of harvesting is the immediate need of the farmers. At such stage, when timeliness of harvesting and threshing operations is the main criterion, the use of combine harvesters would be the most appropriate.

Combine harvester mostly have rasp-bar or spike tooth type longitudinal drum and straw walker. The conventional tangential threshing unit mostly works by impact and due to higher moisture content of paddy the percentage of broken grains increases. To overcome this problem axial flow combines were introduced. In axial flow combine, crop advances through the threshing mechanism in a direction parallel to the axis of rotor resulting in less grain damage. Another development in axial flow combines are the introduction of head feed combines. In head feed combine only the head parts of the crop comes in contact with the threshing drum. The head feed combine also overcomes the problem of straw. It can process paddy straw in different ways viz., windrow them in an orderly manner or in bundles or cut them in even length and spread them uniformly on ground which will work as a mulch for succeeding crop.

It is estimated that more than 50 % area under rice is combine harvested and it is increasing continuously due to shortage of farm labour. The majority of left over rice straw is burnt in the field which results in huge loss of plant nutrients, organic matter and degradation of soil properties due to wastage of residue. Straw burning results in almost complete loss of nitrogen while about 25, 20 and 60 % loss of phosphorous, potassium and sulphur, respectively. In addition to these, burning causes severe air pollution which badly affects the human and animal health. It has been estimated that one ton of straw on burning release 3 kg particulate matter, 60 kg CO, 1460 kg CO_2, 199 kg ash and 2 kg SO_2 (Gupta et al.2004). This can affect regional environment which also has linkage with global climate change. The head feed combine cuts the crop from very near to the ground and spread the straw uniformly in the field in small pieces which can be easily handled either by retaining the straw as mulch on the ground or incorporating it in the soil, which will improve soil health. Another benefit of using the head feed combine is that it can drop the straw in windrow or in bundles, which can be easily collected by manual labour or by the straw balers.

The performance of combines

Table 2 Range of independent parameters

Parameters	Range of independents parameters selected for the study
Moisture content, M1 – M2 – M3 (%)	22.3 – 22.4 × 20.3 – 20.4 × 18.1
Forward speed, F1 – F2 – F3 (km h^{-1})	3.5 × 4.0 × 4.5
Cylinder speed, C1 – C2 – C3 (m s^{-1})	14.42 × 15.53 × 16.64

Table 1 Technical specification of head feed combine harvester

Dimension, mm	L × W × H × W	4445 × 1910 × 2635 × 3130
Engine	Model	E4DE-T
	Engine type	Water-cooled, 4-cylinder, DI turbo
	Total displacement (CC)	2955
	Power/Revolutions (hp/rpm)	71/2700
Engine crawler	Fuel tank capacity (L)	67
	center distance (mm)	1030
	width × ground contact (mm)	450 × 1580
	contact pressure (kgf/cm^2)	0.22
Driving system	Transmission type	HST servo control
	Range	3-stage
	The type of turn	Brake soft spin turn
	Number of reaped crops	4
	Reaping interval (mm)	1450-1500
Reaping unit	Width of reaping cutting blade (mm)	1450
	Type of reaping cutting blade	Two blades sliding cutting
	Type of speed	Speed-synchronized + elevator (3)
Threshing unit	Threshing type	Half feeding, single trash drum
	Threshing cylinder	Loop type
	Threshing cylinder, Diameter x width (mm)	424 × 900
	Processing cylinder (1), Diameter x width (mm)	140 × 725
	Processing cylinder (2), Diameter x width (mm)	140 × 100
	Sieve case, width x diameter (mm)	665 × 1550
Grain discharging system	Tank capacity (kg)	1400
	Turning radius (degree) – turning type	270 - Electric motor

depends critically on straw throughput and grain losses. The threshing effectiveness and losses of combine harvester are greatly influenced by machine parameters viz. cylinder type, cylinder speed, number of crop rotation, feed rate, method of feeding and forward speed of operation. Crop parameters viz. moisture content of grain and straw, green matter present as impurity, grain-straw ratio and environmental factors viz. temperature, humidity etc. also influence the performance of combine harvester. Thus, there was a need to evaluate and optimize the combine parameters for efficient harvesting of crop.

Materials and Methods

The head feed combine (DSM 72) having loop type threshing mechanism whose specifications are presented in **Table 1**, was evaluated for optimization of combine parameters viz., cylinder speed, forward speed and crop parameter viz., grain moisture content in relation to threshing efficiency, cleaning efficiency and total grain losses for scented paddy variety Pusa - 1121 and non-scented paddy variety HKR - 127. The experimental variables are presented in **Table 2**. This study was conducted in Himmatpura village of Tohana in Fatehabad, Haryana during November 21st - 28th, 2014. The test was conducted broadly as per ISI test codes (IS: 8122-2 (2000) Part - II). The quantitative data was quantified according to standards laid down and tabulated to draw meaningful inferences. The data for threshing efficiency, cleaning efficiency and grain losses were analyzed using a Randomized Block Design (RBD). ANOVA was calculated and the influence of each variables and their interaction were tested at 5 percent level of significance in OPSTAT programme prepared by Dr. O.P. Sheoran of CCS HAU, Hisar.

Results and Discussion

The effect of machine parameters viz., cylinder speed, forward speed and crop parameter viz., grain moisture content were studied in relation to threshing efficiency, cleaning efficiency and total grain losses for scented and non-scented paddy varieties. Crop and field parameters of scented and non-scented paddy varieties are presented in **Table 3**.

Table 3 Crop and field parameters of scented and non-scented paddy varieties

Particulars	Scented paddy varieties	Non-scented paddy varieties
Variety	Pusa – 1121	HKR – 127
Soil moisture content, %	15.2	15.5
Bulk density of soil (w. b), g cm^{-3}	1.49	1.49
Grain moisture content (w. b), %	18.1-22.4	18.1-22.3
Straw moisture content (w. b), %	52.5	52.8
Plant height, cm	115	93
Length of panicle, cm	18	17.5
No. of grains per panicle, no.	76	84
Number of $hillm^{-2}$, no.	23	22
Straw grain ratio	1.26	1.21

Table 4 Effect of grain moisture, forward speed and cylinder speed on threshing efficiency in paddy variety Pusa - 1121

Grain moisture, (%)	22.4				20.3				18.1			
Forward speed, (km h^{-1})	3.5	4	4.5	Mean (clynder speed)	3.5	4	4.5	Mean (clynder speed)	3.5	4	4.5	Mean (clynder speed)
Cylinder speed (m s^{-1})												
14.42	97.674	97.445	97.176	97.432	98.515	98.456	98.417	98.463	99.577	99.548	99.518	99.548
15.53	97.874	97.545	97.346	97.588	98.715	98.641	98.637	98.664	99.757	99.738	99.718	99.738
16.64	97.974	97.785	97.576	97.778	99.045	98.976	98.877	98.966	99.807	99.808	99.808	99.808
Mean (Forward speed)	97.841	97.592	97.366		98.758	98.691	98.644		99.714	99.698	99.681	
Mean (Grain moisture)	97.599				98.698				99.698			
Mean (Forward speed)	(3.5 km h^{-1}) = 98.771				(4.0 km h^{-1}) = 98.660				(4.5 km h^{-1}) = 98.564			
Mean (Cylinder speed)	(14.42 m s^{-1}) = 98.481				(15.53 m s^{-1}) = 98.663				(16.64 m s^{-1}) = 98.851			
CD (P = 0.05)	MC = 0.049			FS = 0.049				CS = 0.049			MC × FS × CS = NS	

Table 5 Interaction between moisture content, forward speed and cylinder speed for threshing efficiency in paddy variety Pusa - 1121

Moisture content (%)	Forward speed,(km h^{-1})			Grain moisture (%)	Cylinder speed, (m s^{-1})			Forward speed (km h^{-1})	Cylinder speed,(m s^{-1})		
	3.5	4	4.5		14.42	15.53	16.64		14.42	15.53	16.64
22.4	97.841	97.592	97.366	22.4	97.432	97.588	97.778	3.5	98.589	98.782	98.942
20.3	98.758	98.691	98.644	20.3	98.463	98.664	98.966	4	98.483	98.641	98.856
18.1	99.714	99.698	99.681	18.1	99.548	99.738	99.808	4.5	98.37	98.567	98.754
Interaction	MC × FS = 0.085			MC × CS = 0.085				FS × CS = 0.085			

Effect of Independent Variables on Threshing Performance in Paddy Variety Pusa - 1121

The prediction equation for paddy variety Pusa - 1121 using multiple regression technique was:

T_E = 106.79 – 0.448 MC – 0.207 FS + 0.167 CS (R^2 = 0.99) .....(i)

C_E = 105.47 – 0.434 MC – 0.012 FS + 0.125 CS (R^2 = 0.98) .....(ii)

G_L = – 4.199 + 0.407 MC + 0.150 FS – 0.137 CS (R^2 = 0.97) .....(iii)

Where,

T_E = Threshing efficiency, (%),

C_E = Cleaning efficiency, (%)

G_L= Total grain losses, (%),

R^2 = Multiple coefficient of determination (Significant at $p = 0.05$)

Effect of Grain Moisture Content, Forward Speed and Cylinder Speed on Threshing Efficiency in Paddy Variety Pusa - 1121

The regression coefficient of grain moisture content and forward speed was negative in equation (i), which indicated that increase of these variables resulted in decrease in threshing efficiency. The positive value of regression coefficients of cylinder speed indicated that threshing efficiency increased with the increase in cylinder speed. The coefficient of determination indicated that these variables contributed 99% in total variation of threshing efficiency.

The effect of interactions of variables viz. grain moisture - forward speed, grain moisture - cylinder speed and cylinder speed - forward speed were significant but the interactions of grain moisture - forward speed - cylinder speed were non-significant (**Table 4** and **5**). The threshing efficiency was directly proportional to cylinder speed and it was negatively correlated with moisture content and forward speed. It increased from 97.18 to 99.81% as the grain moisture decreased from 22.4 to 18.1% and cylinder speed increased from 14.42 m s^{-1} to 16.64 m s^{-1} at forward speed of 4.5 km h^{-1} (**Table 4**). Higher threshing efficiency at higher cylinder speed was probably due to increased impact force on the grains. The minimum threshing efficiency at higher moisture content may be due to the fact that at higher moisture content the grains became slightly elastic and more impact force is required for the grain to get detached from the panicle. The results are in conformity with those reported by Manes et al. (2015) in axial flow threshing system.

Effect of Grain Moisture Content, Forward Speed and Cylinder Speed on Cleaning Efficiency in Paddy Variety Pusa - 1121

The regression coefficients of grain moisture content and forward speed were negative in equation (ii), which indicated that increase of these variables resulted in the decrease in cleaning efficiency. The positive value of regression coefficient of cylinder speed indicated that cleaning efficiency increased with the increase in cylinder speed. The coefficient of determination indicated that these variables contributed 98% in total variation of cleaning efficiency.

The effect of interactions of variables viz. grain moisture - forward speed and grain moisture - cylinder speed were significant but the interaction of cylinder speed - forward speed and grain moisture - forward speed - cylinder speed was non-significant (**Table 6** and **7**). The cleaning efficiency was the minimum at higher moisture content, forward

Table 6 Effect of grain moisture, forward speed and cylinder speed on cleaning efficiency in paddy variety Pusa - 1121

Grain moisture, (%)	22.4				20.3				18.1			
Forward speed, (km h^{-1})	3.5	4	4.5	Mean (clynder speed)	3.5	4	4.5	Mean (clynder speed)	3.5	4	4.5	Mean (clynder speed)
Cylinder speed (m s^{-1})												
14.42	97.251	97.352	96.803	97.135	98.021	98.121	97.983	98.042	98.851	98.89	98.91	98.883
15.53	97.412	97.504	96.955	97.290	98.19	98.292	98.15	98.211	99.053	99.144	99.131	99.109
16.64	97.392	97.480	97.171	97.348	98.123	98.241	98.102	98.155	99.091	99.121	99.112	99.108
Mean (Forward speed)	97.352	97.445	96.976		98.111	98.218	98.078		98.998	99.052	99.051	
Mean (Grain moisture)	97.258				98.136				99.034			
Mean (Forward speed)	(3.5 km h^{-1}) = 98.154				(4.0 km h^{-1}) = 98.238				(4.5 km h^{-1}) = 98.035			
Mean (Cylinder speed)	(14.42 m s^{-1}) = 98.020				(15.53 m s^{-1}) = 98.203				(16.64 m s^{-1}) = 98.204			
CD (P = 0.05)	MC = 0.052		FS = 0.052			CS = 0.052			MC × FS × CS = NS			

Table 7 Interaction between moisture content, forward speed and cylinder speed for cleaning efficiency in paddy variety Pusa - 1121

Grain moisture (%)	Forward speed,(km h^{-1})			Grain moisture (%)	Cylinder speed, (m s^{-1})			Forward speed (km h^{-1})	Cylinder speed,(m s^{-1})		
	3.5	4	4.5		14.42	15.53	16.64		14.42	15.53	16.64
22.4	97.352	97.445	96.976	22.4	97.135	97.290	97.348	3.5	98.04	98.217	98.287
20.3	98.111	98.218	98.078	20.3	98.042	98.211	98.155	4	97.98	98.15	98.257
18.1	98.998	99.052	99.051	18.1	98.883	99.109	99.108	4.5	97.897	98.078	98.21
Interaction	MC × FS = 0.090			MC × CS = 0.090				FS × CS = NS			

speed and lower cylinder speed. Cleaning efficiency increased as the grain moisture content decreased from 22.4 to 18.1% and forward speed increased from 3.5 to 4.0 km h-1and cylinder speed increased from 14.42 to 15.53m s^{-1}, but as cylinder speed increased from 15.53 to 16.64 m s^{-1} and forward speed increased from 4.0 to 4.5 km h^{-1}, the cleaning efficiency decreased (**Table 6**). The results are in conformity with Sangwijit and Chinsuwan (2010), who revealed that higher grain moisture caused difficulties in proper screening because of poor flow of threshed material on sieve. The results are in conformity with Manes et al. (2015) who revealed that cleaning efficiency increased with increased cylinder speed and then decreased with further increase in cylinder speed as throughput increases in axial flow threshing system.

Effect of Grain Moisture Content, Forward Speed and Cylinder Speed on Total Grain Losses in Paddy Variety Pusa - 1121

The regression coefficient of cylinder speed was negative in equation (iii), which indicated that increase of this variables resulted in decrease in total grain losses. The positive value of regression coefficients of grain moisture content and forward speed indicated that total grain losses increases with the increase in grain moisture and forward speed. The coefficient of determination indicated that these variables contributed 97% in total variation of total grain losses.

The effect of interactions of variables viz. grain moisture - forward speed, grain moisture - cylinder speed, cylinder speed - forward speed and grain moisture - forward speed - cylinder speed were significant (**Table 8** and **9**). The total grain losses were maximum at higher moisture content and it decreased as the grain moisture content decreased from 22.4 to 18.1% (**Table 8**). It may be due to the reason that at higher grain moisture content, unthreshed losses increases as more force is required to detach the grain from the panicle. However, at lower grain moisture content, the less energy is required to detach the grain from the panicle. The results are in conformity with those reported by Alizadeh and Khodabakhshipour (2010) and Chuan and Chinsuwan (2010). The total grain losses decreased as we increase the cylinder speed from 14.42 to 15.53 m s^{-1} at all levels of moisture content (**Table 8**). It might be due to the reason that with an increase in cylinder speed, the number of impacts between grain and cylinder increases which results in more threshing and less unthreshed grains. Total grain losses increased as we increased the cylinder speed from 15.53 to 16.64 m s^{-1} at 18.1% moisture content (**Table 8**). It might be due to the fact that at lower moisture content unthreshed grains becomes less but the damage incurred to grain becomes more which resulted in more total grain losses. These results are in conformity with Manes et al. (2015) and Lashgiri et al. (2008).

The unthreshed grain losses increased as moisture content and forward speed increased and decreased as cylinder speed increased (**Table 10**). It may be due to the reason that at higher seed moisture content, panicle grain attachment strength was more, which resulted in increased elastic behavior of crop and

Table 8 Effect of grain moisture, forward speed and cylinder speed on total grain losses in paddy variety Pusa - 1121

Grain moisture, (%)	22.4				20.3				18.1			
Forward speed, (km h^{-1})	3.5	4	4.5	Mean (clynder speed)	3.5	4	4.5	Mean (clynder speed)	3.5	4	4.5	Mean (clynder speed)
Cylinder speed (m s^{-1})												
14.42	3.269	3.470	3.736	3.492	2.838	2.827	2.893	2.853	1.749	1.638	1.773	1.720
15.53	3.094	3.375	3.561	3.343	2.633	2.637	2.658	2.643	1.564	1.428	1.618	1.537
16.64	3.089	3.198	3.328	3.205	2.403	2.397	2.418	2.406	1.598	1.437	1.590	1.542
Mean (Forward speed)	3.151	3.348	3.542		2.625	2.620	2.656		1.637	1.501	1.660	
Mean (Grain moisture)	3.348				2.634				1.599			
Mean (Forward speed)	(3.5 km h^{-1}) = 2.471				(4.0 km h^{-1}) = 2.490				(4.5 km h^{-1}) = 2.619			
Mean (Cylinder speed)	(14.42 m s^{-1}) = 2.688				(15.53 m s^{-1}) = 2.508				(16.64 m s^{-1}) = 2.384			
CD (P = 0.05)	MC = 0.007			FS = 0.007			CS = 0.007			MC × FS × CS = 0.022		

Table 9 Interaction for between moisture content, forward speed and cylinder speed for total grain losses in paddy variety Pusa - 1121

Moisture content (%)	Forward speed,(km h^{-1})			Moisture content (%)	Cylinder speed, (m s^{-1})			Forward speed (km h^{-1})	Cylinder speed,(m s^{-1})		
	3.5	4	4.5		14.42	15.53	16.64		14.42	15.53	16.64
22.4	3.151	3.348	3.546	22.4	3.492	3.343	3.205	3.5	2.619	2.43	2.363
20.3	2.625	2.620	2.656	20.3	2.853	2.643	2.406	4	2.646	2.48	2.344
18.1	1.637	1.501	1.66	18.1	1.720	1.537	1.542	4.5	2.801	2.617	2.445
Interaction	MC × FS = 0.013			MC × CS = 0.013				FS × CS = 0.013			

resulted in reduced effect of impact and frictional forces and resulted in more unthreshed grains. The broken grain losses increased as cylinder speed increased and moisture content decreased whereas, broken grains decreased as forward speed increased. It might be due to the reason that with an increase in cylinder speed, the number of impacts between grain and cylinder increases which resulted in more broken grains. At lower seed moisture content, the less energy was required to detach the grain from the panicle and the surplus energy resulted in more grain breakage. Alizadeh and Khodabakhshipour (2010) also reported that in axial flow threshing system the maximum broken grains of 0.68% was recorded at a speed of 850 rpm and moisture contents of 17 % whereas, the least value was obtained at a drum speed of 450 and 550 rpm and at 23% moisture content.

The cutter bar losses increased as moisture content decreased and forward speed increased (**Table 10**). It might be due to the fact that at lower moisture content the bonding of grain with the panicle is loosen and the grains shattered easily from the panicles after coming in contact with cutter bar. Similarly, at higher forward speed the shattering of grains are more due to more impact of cutter bar to cut the rice stem. However, with decrease in moisture content and increase in forward speed the conveyance losses increases, which are counted towards cutter bar losses in this head feed combine. The results are in conformity with Sangwijit and Chinsuwan (2010) and Abdi and Jalali (2013). The effect of cylinder speed, forward speed and moisture content were not observed significant on threshed grain losses, unthreshed grain losses and broken grain losses on sieve. The results are also in conformity with Manes et al. (2015) in axial flow threshing system.

Effect of Independent Variables on Threshing Performance in Paddy Variety HKR - 127

The prediction equation for paddy variety HKR 127 using multiple regression technique was:

T_E = *103.914 – 0.368 MC – 0.175 FS + 0.189 CS* ($R^2 = 0.99$) ..... (iv)

C_E = *103.085 – 0.354 MC – 0.066 FS + 0.157 CS* ($R^2 = 0.98$) ..... (v)

G_L = *– 1.141 + 0.285 MC + 0.094 FS*

Table 10 Total harvesting losses in paddy variety Pusa - 1121

Interaction	Collectable losses, %		Non collectable losses, %				Total losses, %	Threshing efficiency, %
				Sieve losses				
	Unthreshed losses, %	Broken losses, %	Cutter bar losses, %	Threshed losses, %	Un threshed losses, %	Broken losses, %		
M1F1C1	2.32	0.18	0.302	0.46	0.0061	0.001	3.2691	97.674
M1F1C2	2.12	0.22	0.302	0.445	0.0062	0.001	3.0942	97.874
M1F1C3	2.02	0.33	0.302	0.43	0.006	0.001	3.089	97.974
M1F2C1	2.55	0.15	0.324	0.44	0.0052	0.001	3.4702	97.445
M1F2C2	2.45	0.17	0.324	0.425	0.005	0.001	3.375	97.545
M1F2C3	2.21	0.24	0.324	0.418	0.0053	0.001	3.1983	97.785
M1F3C1	2.82	0.13	0.353	0.428	0.0041	0.001	3.7361	97.176
M1F3C2	2.65	0.145	0.353	0.408	0.0044	0.001	3.5614	97.346
M1F3C3	2.42	0.16	0.353	0.39	0.0042	0.001	3.3282	97.576
M2F1C1	1.48	0.25	0.682	0.42	0.0051	0.001	2.8381	98.515
M2F1C2	1.28	0.28	0.682	0.385	0.005	0.001	2.633	98.715
M2F1C3	0.95	0.42	0.682	0.345	0.0052	0.001	2.4032	99.045
M2F2C1	1.54	0.21	0.702	0.37	0.004	0.001	2.827	98.456
M2F2C2	1.32	0.25	0.702	0.325	0.039	0.001	2.637	98.641
M2F2C3	1.02	0.38	0.702	0.29	0.0041	0.001	2.3971	98.976
M2F3C1	1.58	0.19	0.804	0.315	0.0029	0.001	2.8929	98.417
M2F3C2	1.36	0.24	0.804	0.25	0.003	0.001	2.658	98.637
M2F3C3	1.12	0.29	0.804	0.2	0.0031	0.001	2.4181	98.877
M3F1C1	0.42	0.28	0.865	0.18	0.0028	0.001	1.7488	99.577
M3F1C2	0.24	0.32	0.865	0.135	0.0029	0.001	1.5639	99.757
M3F1C3	0.19	0.42	0.865	0.118	0.0035	0.001	1.5975	99.807
M3F2C1	0.45	0.18	0.885	0.12	0.0019	0.001	1.6379	99.548
M3F2C2	0.26	0.19	0.885	0.09	0.0019	0.001	1.4279	99.738
M3F2C3	0.19	0.25	0.884	0.11	0.002	0.001	1.437	99.808
M3F3C1	0.48	0.14	1.005	0.145	0.0018	0.001	1.7728	99.518
M3F3C2	0.28	0.17	1.005	0.16	0.0017	0.001	1.6177	99.718
M3F3C3	0.19	0.21	1.005	0.182	0.0015	0.001	1.5895	99.809

$– 0.178\ CS \qquad (R^2 = 0.93)$ .....(vi)

T_E = Threshing efficiency (%),
C_E = Cleaning efficiency (%)
G_L = Total grain losses (%)
R^2 = Multiple coefficient of determination (Significant at $p = 0.05$)

Effect of Grain Moisture Content, Forward Speed and Cylinder Speed on Threshing Efficiency in Paddy Variety HKR - 127

The regression coefficients of grain moisture content and forward speed were negative in equation (iv), which indicated that increase of these variables resulted in decrease in threshing efficiency. The positive value of regression coefficient of cylinder speed indicated that threshing efficiency increases with the increase in cylinder speed. The coefficient of determination indicated that these variables contributed 99% in total variation of threshing efficiency.

The effect of interactions of variables viz. grain moisture - forward speed, grain moisture - cylinder speed and cylinder speed - forward speed were nonsignificant but the interactions of grain moisture - forward speed - cylinder speed were significant (**Table 11** and **12**). The threshing efficiency was directly proportional to cylinder speed and it was negatively correlated with moisture content and forward speed. It increased from 97.68 to 99.72% as the grain moisture decreased from 22.3 to 18.1% and cylinder speed increased from 14.42 m s^{-1} to 16.64 m s^{-1} at forward speed of 4.5 km h^{-1} (**Table 11**). Higher threshing efficiency at higher cylinder speed was probably due to increased impact force on the grains. The minimum threshing efficiency at higher moisture content may be due to the fact that at higher moisture content the grains became slightly elastic and more impact force is required for the grain to get detached from the ear head. The results are in conformity with those reported by Manes et al. (2015) in axial flow threshing system.

Effect of Grain Moisture Content, Forward Speed and Cylinder Speed on Cleaning Efficiency in Paddy Variety HKR - 127

The regression coefficients of grain moisture content and forward speed were negative in equation (v), which indicated that increase of these variables resulted in the decrease in cleaning efficiency. The positive value of regression coefficient of cylinder speed indicated that cleaning efficiency increases with the increase in cylinder speed. The coefficient of determination indicated that these variables contributed 98% in total variation of cleaning efficiency.

The effect of interactions of variables viz. grain moisture - forward speed, grain moisture - cylinder speed and cylinder speed - forward speed were significant. The interaction of grain moisture - forward speed - cylinder speed was nonsignificant (**Table 13** and **14**). The cleaning efficiency was minimum at higher moisture content, forward speed and lower cylinder speed. Cleaning efficiency increased from 97.15 to 99.14% as the grain moisture content decreased from 22.3 to 18.1%. The cleaning efficiency increased as cylinder speed increased from 14.42 to 16.64 m s^{-1} at 18.1% moisture content and forward speed of 4.5 km h^{-1} (**Table 13**). The results are in conformity with Sang-

Table 11 Effect of grain moisture, forward speed and cylinder speed on threshing efficiency in paddy variety HKR - 127

Grain moisture, (%)	22.3				20.4				18.1			
Forward speed, (km h^{-1})	3.5	4	4.5	Mean (clynder speed)	3.5	4	4.5	Mean (clynder speed)	3.5	4	4.5	Mean (clynder speed)
Cylinder speed (m s^{-1})												
14.42	97.815	97.775	97.676	97.755	98.445	98.346	98.277	98.356	99.347	99.317	99.277	99.314
15.53	98.145	98.035	97.746	97.975	98.645	98.546	98.467	98.553	99.547	99.487	99.517	99.517
16.64	98.395	98.195	98.016	98.202	98.875	98.756	98.657	98.763	99.716	99.716	99.717	99.716
Mean (Forward speed)	98.118	98.002	97.813		98.655	98.549	98.467		99.537	99.507	99.504	
Mean (Grain moisture)	97.978				98.557				99.516			
Mean (Forward speed)	(3.5 km h^{-1}) = 98.770				(4.0 km h^{-1}) = 98.686				(4.5 km h^{-1}) = 98.594			
Mean (Cylinder speed)	(14.42 m s^{-1}) = 98.475				(15.53 m s^{-1}) = 98.682				(16.64 m s^{-1}) = 98.894			
CD (P = 0.05)	MC = 0.043		FS = 0.043			CS = 0.043			MC × FS × CS = 0.128			

Table 12 Interaction between moisture content, forward speed and cylinder speed for threshing efficiency in paddy variety HKR - 127

Grain moisture (%)	Forward speed,(km h^{-1})			Grain moisture (%)	Cylinder speed, (m s^{-1})			Forward speed (km h^{-1})	Cylinder speed,(m s^{-1})		
	3.5	4	4.5		14.42	15.53	16.64		14.42	15.53	16.64
22.3	98.118	98.002	97.813	22.3	97.755	97.975	98.202	3.5	98.536	98.782	99.002
20.4	98.655	98.549	98.467	20.4	98.356	98.553	98.763	4	98.48	98.706	98.886
18.1	99.537	99.507	99.504	18.1	99.314	99.537	99.716	4.5	98.41	98.577	98.783
Interaction	MC × FS = NS			MC × CS = NS				FS × CS = NS			

wijit and Chinsuwan (2010), who revealed that higher grain moisture caused difficulties in proper screening because of poor flow of threshed material on sieve. The results are in conformity with Manes et al. (2015) who revealed that cleaning efficiency increased with increased cylinder speed and then decreased with further increase in cylinder speed as throughput increases in axial flow threshing system.

Effect of Grain Moisture Content, Forward Speed and Cylinder Speed on Total Grain Losses in Paddy Variety HKR - 127

The regression coefficient of cylinder speed was negative in equation (vi), which indicated that increase of this variable resulted in the decrease in total grain losses. The positive value of regression coefficients of grain moisture content and forward speed indicated that total grain losses increases with the increase in grain moisture and forward speed. The coefficient of determination indicated that these variables contributed 93 per cent in total variation of total grain losses.

The effect of interactions of variables viz. grain moisture - forward speed, grain moisture - cylinder speed and cylinder speed - forward speed and grain moisture - forward speed - cylinder speed were significant (**Table 15** and **16**). The total grain losses were the maximum at higher moisture content and it decreased as the grain moisture content decreased from 22.3 to 18.1% (**Table 15**). It may be due to the reason that at higher grain moisture content, unthreshed losses increases as more force is required to detach the grain from the panicle. However, at lower grain moisture content, the less energy is required to detach the grain from the panicle. The results are in conformity with those reported by Alizadeh and Khodabakhshipour (2010) and Chuan and Chinsuwan (2010). The total grain losses decreased as we increased the cylinder speed from 14.42 to 16.64 m s^{-1} at all levels of moisture content (**Table 15**). It might be due to the reason that with an increase in cylinder speed, the number of impacts between grain and cylinder increases which results in more threshing and less unthreshed grains.These results are in line with earlier work carried out by Manes et al. (2015) and Lashgiri et al. (2008).

The unthreshed grain losses increased as moisture content and forward speed increased and decreased as cylinder speed increased (**Table 17**). It may be due to the reason that at higher seed moisture content, panicle grain attachment strength was more, which resulted in increased elastic behavior of crop and resulted in reduced effect of impact forces and resulted in more unthreshed grains. The broken grain losses increased as cylinder speed increased and moisture content decreased whereas, broken grains decreased as forward speed increased. It might be due to the reason that with an increase in cylinder speed, the number of impacts between grain and cylinder increases which resulted in more broken grains. At lower seed moisture content, the less energy was required to detach the grain from the panicle and the surplus energy resulted in more grain breakage. Alizadeh and Khodabakhshipour (2010) also reported that in axial flow threshing system the maximum broken grains of 0.68% was recorded at a speed of

Table 13 Effect of grain moisture, forward speed and cylinder speed on cleaning efficiency in paddy variety HKR - 127

Grain moisture, (%)	22.3				20.4				18.1			
Forward speed, (km h^{-1})	3.5	4	4.5	Mean (clynder speed)	3.5	4	4.5	Mean (clynder speed)	3.5	4	4.5	Mean (clynder speed)
Cylinder speed (m s^{-1})												
14.42	97.261	97.251	97.158	97.223	97.85	97.78	97.741	97.790	98.681	98.742	98.771	98.731
15.53	97.552	97.48	97.215	97.416	98.011	97.951	97.890	97.951	98.862	98.911	98.992	98.922
16.64	97.78	97.615	97.468	97.621	98.120	98.148	98.121	98.130	98.972	99.012	99.14	99.041
Mean (Forward speed)	97.531	97.449	97.280		97.994	97.960	97.917		98.838	98.888	98.967	
Mean (Grain moisture)	98.121				98.099				98.900			
Mean (Forward speed)	(3.5 km h^{-1}) = 98.770				(4.0 km h^{-1}) = 98.686				(4.5 km h^{-1}) = 98.057			
Mean (Cylinder speed)	(14.42 m s^{-1}) = 97.915				(15.53 m s^{-1}) = 98.096				(16.64 m s^{-1}) = 98.266			
CD (P = 0.05)	MC = 0.049			FS = NS			CS = 0.049			MC × FS × CS = NS		

Table 14 Interaction between moisture content, forward speed and cylinder speed for cleaning efficiency in paddy variety HKR - 127

Grain moisture (%)	Forward speed,(km h^{-1})			Grain moisture (%)	Cylinder speed, (m s^{-1})			Forward speed (km h^{-1})	Cylinder speed,(m s^{-1})		
	3.5	4	4.5		14.42	15.53	16.64		14.42	15.53	16.64
22.3	97.531	97.449	97.280	22.3	97.223	97.416	97.621	3.5	97.93	98.14	98.29
20.4	97.994	97.960	97.917	20.4	97.790	97.951	98.130	4	97.923	98.113	98.258
18.1	98.838	98.888	98.974	18.1	98.731	98.922	99.041	4.5	97.889	98.032	98.243
Interaction	MC × FS = 0.084			MC × CS = 0.084				FS × CS = 0.084			

850 rpm and moisture contents of 17 % whereas, the least value was obtained at a drum speed of 450 and 550 rpm and moisture content of 23%.

The cutter bar losses increased as moisture content decreased and forward speed increased (**Table 17**). It might be due to the fact that at lower moisture content the bonding of grain with the panicle is loosen and the grains shattered easily from the panicles after coming in contact with cutter bar. Similarly, at higher forward speed the shattering of grains are more due to more impact of cutter bar to cut the rice stem. However, with decrease in moisture content and increase in forward speed the conveyance losses increases, which are counted towards cutter bar losses in this head feed paddy combine. The results are in conformity with Sangwijit and Chinsuwan (2010) and Abdi and Jalali (2013). The effect of cylinder speed, forward speed and moisture content were not observed significant on threshed, unthreshed and broken grain losses on sieve. The results are also in conformity with Manes et al. (2015) in axial flow threshing system.

Conclusions

Moisture content of 18.1 per cent, cylinder speed of 15.53 m s^{-1} and forward speed of 4.0 km h^{-1} was found optimum for harvesting of scented paddy variety Pusa - 1121, whereas, moisture content of 18.1%, cylinder speed of 16.64 m s^{-1} and forward speed of 4.5 km h^{-1} was found optimum for harvesting of non-scented paddy variety HKR - 127. Moisture content was the most important factor influencing threshing efficiency, cleaning efficiency and total grain losses followed by cylinder speed and forward speed in all scented and non-scented varieties.

REFERENECS

Abdi, R. and A. Jalali. 2013. Mathematical model for prediction combine harvester header losses. International Journal of Agriculture and Crop Sciences,5: 549-552.

Alizadeh, M. R. and M. Khodabakhshipour. 2010. Effect of threshing drum speed and crop moisture on the paddy grain damage in axial-flow thresher. Cercetari Agronomice in Moldova, 4(144): 5-11.

Anonymous. 2015b. Agricultural statistics, Ministry of Agriculture and Farmers Welfare, Government of India.

Anonymous. 2015a. Rice market monitor, Vol. XVII, Issue No. 1: 1-39. Food and Agriculture Organization (FAO).

Chuan-udam, S. and W. Chinsuwan. 2010. Prediction equation for losses of axial flow rice combine harvester when harvesting Chainet 1 rice variety. KKU Research Journal, 15(6): 496-504.

Dhillon, B. S., P. Kataria and P. K. Dhillon. 2010. National food security vis-a-vis sustainability of agriculture in high crop productivity regions. Current Science, 98: 33-36.

Gupta, P. K., S. Sahai, N. Singh, C. K. Dixit, D. P. Singh, C. Sharma, M. K. Tiwari, R. K. Gupta and S. C. Garg. 2004. Residue burning in rice-wheat cropping system:

Table 15 Effect of grain moisture, forward speed and cylinder speed on threshing efficiency in paddy variety HKR - 127

Grain moisture, (%)	22.3				20.4				18.1			
Forward speed, (km h^{-1})	3.5	4	4.5	Mean (clynder speed)	3.5	4	4.5	Mean (clynder speed)	3.5	4	4.5	Mean (clynder speed)
Cylinder speed (m s^{-1})												
14.42	2.981	2.946	3.090	3.006	2.586	2.770	2.821	2.727	1.839	1.755	1.749	1.781
15.53	2.686	2.696	3.012	2.798	2.406	2.478	2.596	2.493	1.639	1.625	1.539	1.601
16.64	2.412	2.561	2.740	2.571	2.236	2.272	2.306	2.271	1.528	1.475	1.339	1.447
Mean (Forward speed)	2.693	2.734	2.947		2.409	2.508	2.574		1.669	1.618	1.542	
Mean (Grain moisture)	2.794				2.497				1.610			
Mean (Forward speed)	(3.5 km h^{-1}) = 2.257				(4.0 km h^{-1}) = 2.286				(4.5 km h^{-1}) = 2.354			
Mean (Cylinder speed)	(14.42 m s^{-1}) = 2.504				(15.53 m s^{-1}) = 2.297				(16.64 m s^{-1}) = 2.097			
CD (P = 0.05)	MC = 0.008			FS = 0.008			CS = 0.008			MC × FS × CS = 0.024		

Table 16 Interaction between moisture content, forward speed and cylinder speed for total grain losses in paddy variety HKR - 127

Grain moisture (%)	Forward speed,(km h^{-1})			Grain moisture (%)	Cylinder speed, (m s^{-1})			Forward speed (km h^{-1})	Cylinder speed,(m s^{-1})		
	3.5	4	4.5		14.42	15.53	16.64		14.42	15.53	16.64
22.3	2.693	2.734	2.947	22.3	3.006	2.798	2.571	3.5	2.468	2.24	2.059
20.4	2.409	2.508	2.574	20.4	2.727	2.494	2.271	4	2.492	2.25	2.103
18.1	1.669	1.618	1.542	18.1	1.781	1.608	1.447	4.5	2.551	2.383	2.142
Interaction	MC × FS = 0.014			MC × CS = 0.014				FS × CS = 0.014			

Causes and implications. Current science, Vol. 87 (12): 1713-1717.
IS: 8122-2 (2000): Test code for testing of combine harvester and threshers.
Lashgari, M. H., M. Mobli, R. Omid, Alimardani and S. S. Mohtasebi. 2008. Qualitative analysis of wheat damage during harvesting with John Deere combine harvester. Int. J. Agri. Biol., 10: 201-204.
Manes, G. S., A. Dixit, A. Singh, M. Singh and B. P. Singh. 2015. Comparative performance evaluation of axial flow and tangential axial flow threshing system for basmati rice (Oryza Sativa). Agricultural Research, DOI 10.1007/ s 40003-015-0169-3, 1-7.
Sangwijit, P. and W. Chinsuwan. 2010. Prediction equations for losses of axial flow rice combine harvester when harvesting Chainat-I Rice variety. KKURes J. 15(6): 496-504.
Sheoran, O. P. Online statistical programme for data analysis. CCS HAU, Hisar (www.hau.ernet.in).
Veerangouda, M., S. Sushilendra, K. V. Prakash and M. Anantachar. 2010. Performance evaluation of tractor operated combine harvester. Karnataka Journal of Agricultural Sciences, 23(2): 282-285.

■■

Table 17 Total harvesting losses in paddy variety HKR - 127

Interaction	Collectable losses, %		Non collectable losses, %				Total losses, %	Threshing efficiency, %
				Sieve losses				
	Unthreshed losses, %	Broken losses, %	Cutter bar losses, %	Threshed losses, %	Un threshed losses, %	Broken losses, %		
M1F1C1	2.18	0.14	0.295	0.36	0.0051	0.001	2.9811	97.815
M1F1C2	1.85	0.18	0.295	0.355	0.005	0.001	2.686	98.145
M1F1C3	1.6	0.2	0.295	0.34	0.0052	0.001	2.4412	98.395
M1F2C1	2.22	0.11	0.31	0.3	0.0051	0.001	2.9461	97.775
M1F2C2	1.96	0.14	0.31	0.28	0.0049	0.001	2.6959	98.035
M1F2C3	1.8	0.165	0.31	0.28	0.0051	0.001	2.5611	98.195
M1F3C1	2.32	0.102	0.338	0.325	0.0041	0.001	3.0901	97.676
M1F3C2	2.25	0.115	0.338	0.304	0.0039	0.001	3.0119	97.746
M1F3C3	1.98	0.132	0.338	0.285	0.0042	0.001	2.7402	98.015
M2F1C1	1.55	0.18	0.55	0.3	0.0051	0.001	2.5861	98.445
M2F1C2	1.35	0.22	0.55	0.28	0.0052	0.001	2.4062	98.645
M2F1C3	1.12	0.34	0.55	0.22	0.005	0.001	2.236	98.875
M2F2C1	1.65	0.15	0.615	0.35	0.0042	0.001	2.7702	98.346
M2F2C2	1.45	0.18	0.615	0.228	0.0041	0.001	2.4781	98.546
M2F2C3	1.24	0.192	0.615	0.22	0.004	0.001	2.272	98.756
M2F3C1	1.72	0.12	0.692	0.285	0.0031	0.001	2.8211	98.277
M2F3C2	1.53	0.16	0.692	0.21	0.0032	0.001	2.5962	98.467
M2F3C3	1.34	0.12	0.692	0.15	0.0029	0.001	2.3059	98.657
M3F1C1	0.65	0.25	0.785	0.15	0.003	0.001	1.839	99.347
M3F1C2	0.45	0.28	0.785	0.12	0.0031	0.001	1.6391	99.547
M3F1C3	0.28	0.35	0.785	0.108	0.0042	0.001	1.5282	99.716
M3F2C1	0.68	0.16	0.812	0.1	0.0029	0.001	1.7559	99.317
M3F2C2	0.51	0.21	0.812	0.09	0.0029	0.001	1.6259	99.487
M3F2C3	0.28	0.28	0.812	0.09	0.0038	0.001	1.4668	99.716
M3F3C1	0.72	0.09	0.855	0.08	0.003	0.001	1.749	99.277
M3F3C2	0.48	0.12	0.855	0.08	0.0026	0.001	1.5386	99.517
M3F3C3	0.28	0.12	0.855	0.08	0.0026	0.001	1.3386	99.717

Development of a Chopping Apparatus for Cactus Prickly Cladodes

by

H. M. Duran-Garcia
Professor
Universidad Autónoma de San Luis Potosí,
Instituto de Investigación de Zonas Desérticas.
Altair 200, Col. del Llano,
San Luis Potosí, SLP 78377
MEXICO

U. Marquez-Perez
Research student
Universidad Autonoma de San Luis Potosí,
Facultad de Ingeniería.
Manuel Nava 8, Zona Universitaria,
San Luis Potosi, SLP 78290
MEXICO

E. J. Gonzalez-Galvan
Research student
Universidad Autonoma de San Luis Potosí,
Facultad de Ingeniería.
Manuel Nava 8, Zona Universitaria,
San Luis Potosi, SLP 78290
MEXICO

E. D. Rössel-Kipping
Professor
Colegio de Postgraduados,
km 36.5 Carretera México-Texcoco,
Montecillo, Texcoco,
Estado de México. 56230
MEXICO

H. Ortiz-Laurel*
Professor
Colegio de Postgraduados,
km 36.5 Carretera México-Texcoco,
Montecillo, Texcoco,
Estado de México. 56230
MEXICO
hlaurel@colpos.mx

Abstract

Either under proper cultivation and growing in the wild, cactus prickly represents an important source to feed livestock. When properly cultivated, around 10 t/ha per year of fresh biomass is produced just from pruning. However, when the biomass is left over the soil it slowly degrades and fertilizes cactus prickly orchards, in contrast, when unattended it contributes to generate pests and diseases. A profitable alternative is to utilize this cactus prickly pruning to feed livestock, by mixing and balancing it with some locally feeds such as mesquite pod and hay from alfalfa. Thus this work shows the development an apparatus for continuously chopping cactus prickly cladodes; firstly by cutting strips and ended into small cubes. The apparatus is simple to handle, inexpensive and with the capacity of processing up to 10 t/h; besides it provides a profitable choice for an underutilized resource in a region with shortage of feeds for livestock

Keywords: mechanized chopping, cactus prickly biomass, mechanical processing, dryland feeds, dryland areas.

Introduction

Cactus prickly is one of the most important plants for rural communities in the semiarid regions of Mexico. It is being utilized as food for people, fodder for livestock and wild animals, a simple and inexpensive measure for averting soil erosion, for the pharmaceutical and cosmetology industries, among others uses. Cactus prickly spreads easily with good management; it is one of the few fodder resources readily available for livestock feeding in rural areas when there is shortage of pasture on grassland.

Although, cladodes (pencas) are provided as animal feed, there is no processing and no thorns removal, so their efficiency is low and animals are injured because of thorns and sometimes they suffer from diarrhea. Thus, instead of considering that fresh cladodes are a direct feed, they should be utilized as a complementary ingredient in order to elaborate a more nutritious animal diet, for example, through silage. To undertake this process, cactus prickly cladodes are the largest ingredient and they will be complemented with other local available feed materials, such as mesquite pod and hay from alfalfa. This composition could constitute an entire nutritious feed that would provide enough components for livestock growing (cattle, sheep and goats) during the dry season without losing live weight.

For elaborating silage it is essential to chop the cladode to particle sizes from 20 to 30 mm. Since cactus prickly is a succulent and fibrous material, technically, it demands a machine with certain mechanical and design features, so that its operating capacity should exceed the manual chopping as well as speed of the process is increased. Scorching is avoided, as soon as cladodes are chopped and silaged (combined with mesquite pods and hay from alfalfa), thorns are destroyed and up to 10 - 12% of crude protein is achieved, a quantity quite enough to sustain livestock during the dry season.

Generally, shape of cactus prickly cladode looks like a plane and thick ellipse, thicker when ageing near the junction with the plant (**Fig. 1**). Most of fresh cladodes are 200 to 300 mm long, 150 to 200 mm wide and up to 50 mm thick at the base (Durán-García et al., 2012). Thus, there is a need for mechanizing the chopping of cactus prickly cladode, either by getting continuously strips and square cuts. Uncomplicated manufacturing, inexpensive and high performance are fundamental.

Materials and Methods

In order to accomplish the above objective it was necessary to search compatible information about all kind of mechanisms as well as their operation principles, performance and capacities. These were fundamental to formulate straightaway a proper and simple design in order to successfully meet the above goal. Features, such as types and size of cutting blades, energy consumption, materials used in its construction, processing capacity, power transmission system, cutting methodology and other outstanding features in cutting equipment, were also investigated. Equally, the cutting principles described by Frank (1965) were widely analyzed. However, there were economic, design and technical restraints to undertake this project: the processing apparatus must be inexpensive with a capacity to process 10 t/h; capable of handing out different size, young and old cladodes. The construction should be simple and to utilize components readily provided by domestic industry in Mexico, in order to aid by reducing manufacturing costs and allowing to use typical available equipment from small workshops.

On the other hand, since cactus prickly has physiological adaptations which allow it to tolerate and grow under harsh and arid conditions, leads to generate itself great variations in the physical-mechanical attributes (Sánchez et al. (1994); Bustamante et al. (2000)). Processing machines are designed by wholly considering the different physical-mechanical qualities, because they are important in the evaluation of processing material as well as the selection of the working elements or mechanisms that intervene in the cutting process. **Table 1** shows average data for the physical-mechanical features attributed to cladodes used for livestock feeding and human consumption.

Development of the Apparatus

A single machine can be divided into several mechanisms, where each has a certain role for the good functioning. The proposed apparatus consists of two systems: the processing system and the auxiliary or support system. The processing system includes those components which together perform the target function i.e. cutting, separation or mixing, among others. The cladode chopping machine comprises in principle, a structure that supports a feeding tray in order to direct the fresh cladodes towards the cutting process (**Fig. 2**). Once there, a set of circular knives (disks) each spaced 25 mm perform the first cut (stripping), driven by an electric motor that transmits its power through a belt-pulley transmission. When the cladode is first cut, pieces slip towards a second slicing roll, formed with a pair of helical blades sup-

Fig. 1 Typical cactus prickly plants in the semiarid zones of Mexico

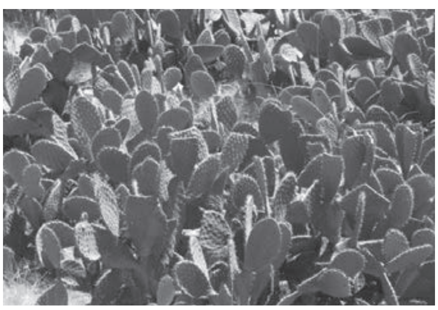

Table 1 Average physical-mechanical attributes of cactus prickly cladodes.

Coefficient of friction	
a) Static	0.7
b) Dynamic	0.56
Compression test	
a) Maximum load of proportionality according to Hooke's law	250 N
b) Deformation	8.75 mm
Shear strength	
Energy in the cut and to overcome resistance	1.51 J
Apparent density	1.11 g/cm^3

Source: Bustamante et al., (2000)

Table 2 Elastic modulus for four cactus prickly species

Species	Elastic modulus (kPa)
Nopalea cochenillifera	60.058
Opuntia robusta	98.197
Opuntia undulata	90.567
Opuntia ficus indica	55.614

ported on two disks which, when rotating, generate a traverse cut onto the strips. The speed reduction gear rotates at a speed adequate to the particular characteristics for the end product.

In order to know the forces acting on the system, it is necessary to calculate the critical intensity factor (K_N) and the elastic modulus of the cladode. The latter obtained under laboratory conditions for four species of cactus prickly are shown in **Table 2**.

Results and Discussion

Critical Intensity Factor (K_N) and Shear Force (F_c)

The critical intensity factor (K_N) can be obtained by using the following equation:

$K_N = E \cdot s \cdot p \cdot \sqrt[3]{(V_m / V_d)}$

It is calculated by considering the maximum value of the elastic modulus corresponding to the Opuntia robust specie (98.197 kPa). The velocity of cladode feeding was $V_m = 0.04$ m/s and the blade tangential velocity was $V_d = 13.74$ m/s; the rate of the speed reduction gear was 1:2, while the maximum thickness of the fresh cladode was 50 mm; thus the critical intensity factor is $K_N = 0.35$.

Once the critical intensity factor is known, the penetration force (F_N) is calculated as follows,

$F_N = K_N \cdot \tan\mathcal{E} / 2 \cdot \sqrt[2]{d} \cdot s \cdot p$

Where:

$\tan\mathcal{E} / 2 = (\pi / 12) / 2$

s = spacing generated by the cut (0.5 mm),

d = cutting disk diameter (300 mm);

p = maximum thickness of cactus prickly cladode (50 mm).

Therefore the penetration force is $F_N = 0.35 \times 0.13 \times 86.6 = 3.94$ N which, applied on the fourteen disks, generates a force of $F_N = 55.16$ N. By considering that geometry of the cactus prickly fresh cladode resembles an ellipse, it is assumed that a given time no all disks at cutting biomass, therefore it was considered that just eight of them could make instantaneous contact with the mass (predetermined working condition). This is the reason why the force is calculated based on only eight disks i.e., $F_N = 31.52$ N.

Finally, the cutting force (F_C) is obtained by utilizing the equation.

$F_C = (2K_N \cdot s \cdot d \cdot \tan\mathcal{E} / 2) / \sqrt[2]{p}$

$F_C = 2 \cdot 0.35 \cdot 0.5 \cdot 300 \cdot 0.13 / \sqrt[2]{50}$

$= 13.65 / 7.07 = 1.93$ *N per disk*,

For fourteen disks this force is 27 N.

Rotational speed

When processing biological materials by cutting, it is advisable to analyze the effect of speed of the cutting tools in order to get a final desirable particle size. Savani et al. (2004) obtained an optimum efficiency in cutting stems, operating between 500 to 600 revolutions per minute (rpm). López and Lozano (1995), when designing a chopper for size reduction of cactus prickly cladodes and conditioning it for forage, the best speed for cutting was 190 rpm. On the other hand, Torrey-brand chicken cutter has a cutting disk attached directly to an electric motor that consumes 0.37 kW, which is capable of cutting chicken bones by rotating at 750 rpm and equally, a sausage cutters from the same brand operates at speeds exceeding 600 rpm. From above, it indicates that for processing a hard, woody and fibrous biological material, larger speeds are required compared with soft materials, ranging from 500 rpm to 900 rpm. There-

Fig. 2 Main components for the cactus prickly cladode chopping apparatus

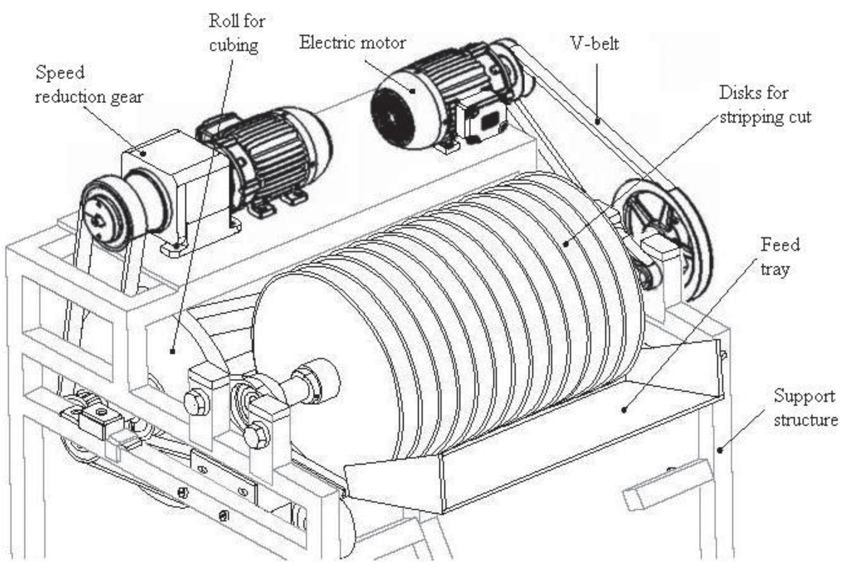

Fig. 3 Performance testing of the cactus prickly cladodes chopping apparatus

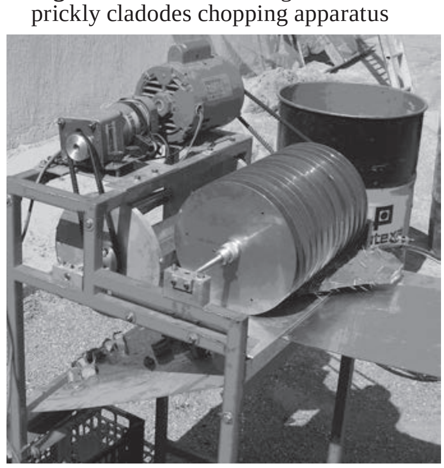

fore, during testing the machine the above figures were utilized as reference and a direct speed reduction gear of 1:2 was employed, since commercial electric motors usually operate at 1750 rpm. By undertaking a mathematical procedure, it was calculated that for a minimum power requirement to drive the machine must utilize a 1.1 kW electric motor (**Fig. 3**).

Conclusions

This machine is an alternative that could contribute to improve the efficiency of using cactus prickly as well as reducing losses. The apparatus it is easy to use, has a capacity to process fresh mass up to 10 t/h and has a cost of around 1,000 $US. The final size of chopping and conditioning of cladodes facilitates mixing with other local feed materials such as mesquite pod and hay from alfalfa for elaborating silage, thus reaching a crude protein from 10 to 12%, which is right enough to sustain cattle during the dry season.

REFERENCES

Bustamante, P., E. Parra and A. Sánchez. 2000. Diseño de una máquina desespinadora de nopal verdura. Bachelor Thesis. Department of Agricultural Mechanical Engineering. Autonomous University Chapingo. Chapingo, Mexico. 123p.

Durán-García, H. M., E. J. González-Galván and U. Márquez-Pérez. 2012. Conditioning of nopal cactus (Opuntia spp.) for food and dehydration. Journal of Food, Agriculture and Environment, 10(1): 49-52.

Frank, G. 1965. Apparatus and process for producing crinkle cut vegetables. Unites States Patent Office. No. 507,902.

López, D. and M. Lozano. 1995. Diseño de una máquina picadora de nopal para forraje. BSc Thesis. Department of Agricultural Mechanical Engineering. Autonomous University Chapingo. Chapingo, Mexico. 70p.

Sanchez, I., M. Cano and B. Hermida. 1994. Blanding, freezing and frozen storage influence texture of white asparagus. Journal of Food Science. 59: 821-823.

Savani J., V. Vagadia and R. Kathiria. 2004. Design and development of agricultural wastes shredder. Agricultural mechanization in Asia, Africa and Latin America, 35(2): 41-46.

■■

Modification of Rotary Power Tiller units for *Biasi* (Interculture Operation) Rice Cultivation in Eastern India

by

Ajay Kumar Verma
Professor & Principal Scientist
Dept. of Farm Machinery and Power Engineering,
Faculty of Agril. Engineering,
IGKV, Raipur, Chhattisgarh
INDIA
ajayaverma@rediffmail.com

Samir Santiya
Subject Matter Specialist (Agril. Engineering)
Universidad Autonoma de San Luis Potosí,
KVK, IGKV, Janjgir, Chhattisgarh
INDIA

Abstract

Biasi (Beushening) is a traditional method of rice cultivation in rain fed risk prone areas of Eastern India. It is performed by animal drawn plough. The productivity of rice drastically reduces due to delayed in *Biasi* operation because of the use of animal drawn implement. Therefore, focus was initiated on developing a rotary tiller unit *Biasi* implement. To develop it, soil condition during *Biasi* operation for Inceptisols and vertisols soils were characterized [Soil moisture content 60-65% (d.b.) flooded, specific weight 14-18 kN/m^3 & Cone index 48-54 kPa]. Accordingly, the cage wheel parameters (73 cm wheel diameter, 30 cm wheel width, 450 lug angle and 20 cm lug pitch) for *Biasi* operation were optimized. The rotary unit of 13 hp power tiller was modified for *Biasi* operation. The rotary unit with 8 tines, 152 rpm rotor speed for 70 cm working width, blade distance 18 cm, length of soil slice 7-9 cm at 0.4 m/s forward speed was found suitable. The study revealed that the modified rotary unit of power tiller was found suitable for *Biasi* operation under rainfed rice cultivation because of its higher field capacity, better quality of work and more benefit cost ratio as compare to traditional method.

Introduction

Biasi or Beushening method of rice cultivation is commonly used under highly variable climates and a poor resource base. In this system rice seeds are broadcasted in dry or wet soils after normal field preparation. The rice plants as well as weeds grow simultaneously up to 30-40 days and thereafter shallow ploughing (Single or cross) is done in presence of 5-10 cm of water in standing rice crop by animal drawn indigenous plough followed by manual weeding and gap filling. This operation is called *Biasi*. Under rainfed situation *Biasi* is necessary because it helps to maintain the plant population, better plant growth and development of roots. In India more than 1.5million ha area of rice is under *Biasi* system of rice cultivation. Indian farmers, particularly the small and marginal, have been dependent on human and animal power for performing various farm operations. Animals meet the power requirements of small and marginal farms with associated limitations. The availability of draught animals power has come down from 0.133 kW/ha in 1971-72 to 0.094 kW/ha in 2012-13 (Mehta et al., 2014), whereas the share of tractors and power tillers has increased during the same period. Since the traditional method of *Biasi* gives low output results in delayed operation with high cost. Mechanization of this particular operation through mechanical means would play a major role to enhance the field efficiency with minimum waste of time, energy and materials. Chandravanshi (1989) informed that direct seeded rainfed *Biasi* cultivation of rice occupies 87% of the rice area in Chhattisgarh. Fujisaka (1991) emphasized that *Biasi* (Beusani) is a common crop establishment practice in rainfed lowland rice. *Biasi* is used in dry seeded lowland fields to control weeds. *Biasi* reduces not only the weed population, but also the rice plants population. Kawade (2001) reported that farmers adopted *Biasi* method to minimize the labour requirement in weeding operation and to enhance the plant growth. Mishra (2010) developed animal drawn *Biasi* implement. The field capacity of 0.80 ha/day was found to be highly significant. It was more than 4 times higher than that of local *Biasi* plough with 0.18 ha/day. It was due to proper shape and arrangement of curved tines in the developed *Biasi* implement which facilitated self- unclogging and minimized the time wastage in removal of clogging. The draught requirement of developed *Biasi* implement was within the draught capacity of local bullocks (55-65 kgf).

As the traditional method of *Biasi* gives low output resulting in delayed operation with high cost. Mechanization of this particular operation plays a major role to enhance the field efficiency with minimum waste of time, energy and materials. But mechanization of above operations is not up to the level of farmer's expectations till to date. So if an intercultural power operated implement can be introduced, it will reduce drudgery of farmers and also increase the yield due to timeliness of field operation. In order to bring down the area work pressure on animate power and to assess the possibility of mechanization of the *Biasi* operation, the power operated *Biasi* implement was proposed to be designed, developed and tested.

Material and Methods

To develop a rotary tiller unit *Biasi* implements, various research findings on crop and soil parameters for *Biasi* operation available in literature taken in to consideration are given in **Table 1**.

Features of Power Tillers That Outfit the *Biasi* Operation

The reasons for taking power tiller to perform *Biasi* operation was its compact construction and good trafficability. The lightness and low centre of gravity facilitate easy operation, low sinkage on submerged soils and rare casualties. The narrow wheel tread enables these to go through the narrow patch in the country side. Due to absence of two front wheels and narrow wheel tread, power tillers have short turning radius. Thus less land was left untilled during field operations. Rotary type power tiller have been selected for *Biasi* operation because the reduction in traction demanded of power tiller driving wheels due to the ability of the soil working blades to provide some forward thrust (Benny et.al., 1970).

Modification in rotary power tiller unit for *Biasi* operation

Modification work in rotary power tiller units for *Biasi* rice cultivation was carried out during the year 2013 to 2015. During this period the cage wheel parameters such as types and number of blades and their combinations were optimized through field experiments for *Biasi* operation. The technical specifications of the power tiller taken for development of rotary *Biasi* are given in **Table 2**.

Development of Rotary Unit for *Biasi* Operation

Various research findings have supported to choose C-shaped rotary blades for *Biasi* operation because of hooking character between the rotary blades and plants (low plant mortality), less torque and power consumption (unclogging in submerged rice field). Salokhe et al. (1993) studied on the power requirement and puddling of a rotavator in wet clay soil. It was observed that rotor of C-shaped blades consumed less power than the rotor of L-shaped blades. Chertkiattipol, et.al. (2007) explained that it was the phenomenon of reaction forces between soil and tillage tool that related to soil failure pattern. The torque acting on the rotary shaft of

Table 1 Crop and soil parameters for Biasi operation

Particulars	Value	Reference
Soil type	Loam, silt clay loam, clay loam	Verma et. al. (2006)
Field preparation	Two cross ploughing by tractor with cultivator depth of ploughing 8-12 cm, bulk density 1.3-1.4 Mg/m^3	Verma et. al. (2006)
Seed rate	80-100 kg/ha	Lakpale and Shrivastava (2012)
Time of Biasi	30-40 days after sowing	
Depth of water in the field at the time of Biasi	5-10 cm	
Distance of Biasi (distance between furrow)	20 ±3 cm	Kawade (2001)
Depth of Biasi	6-8 cm	
Gap -filling process	Within 3 days of Biasi operation	Lakpale and Shrivastava (2012)
Plant population/m^2	125 plants/ m^2	

Table 2 Technical specifications of power tiller

Specification	Value
Engine Type	Vertical Diesel Engine
Number of cylinder	1
Engine maximum power at 2400 rpm	(9.7 kW) 13 hp
Engine maximum torque at 1900 rpm	4.2 kNm
Tilling Width	800 mm
Tilling Depth	160-220 mm
No. of Tynes	24
Gears	6 forward & 2 reverse
Rotational speed PTO shaft	540 rpm
Total weight	120 kg

L- shaped blades was slightly higher than for the Japanese C-shaped blade. Design of rotary tiller blades depends on soil types, no. of blades and working condition. The specific work carried out by rotary tiller at each rotation of tillage blades was considered as the volume of tilt soil. Specific work can be calculated by following equation (Bernacki et al, 1972).

$A = A_O + A_B$ kg-m/dm³ .....(1)

Where: A is specific work of rotor, A_O is static specific work, A_B is dynamic specific work. A_O and A_B were obtained by using following relationship:

$A_O = 0.1\ C_O\ k_O$ kg-m/dm³ .....(2)

$A_B = 0.001\ a_u\ u^2$ kg-m/dm³ .....(3)

$A_B = 0.001\ a_v\ v^2$ kg-m/dm³ .....(4)

Where, C_0 is coefficient relative to the soil type (for clay loam C_0 = 2.5) k_0 is specific strength of soil (60 kg/dm³), u is the tangential speed of the blades (m/s), v is tractor forward speed. a_u and a_v are dynamic coefficient and it can be calculated by

$a_v = a_u\ (u / v)^2$ ....(5)

$\lambda = u / v$.

The static specific work Ao which is related to the cutting soil slice must be greater than the specific work of rotary tine and of other passive tools, because each rotary unit was bound to cut a considerably greater part of the soil surface than the tine. The larger the slices the lower the specific work and other portion represent the dynamic specific work resulting from striking the soil by the blades while penetrating and from acceleration of the soil slices during the *Biasi* operation. Dynamic work determines the magnitude of power consumed by the rotary units.

Calculation of Performable Work of the Power Tiller for *Biasi* Operation (A_C)

The maximum performable work of the power tiller can produced was calculated by the following equation:

$A_C = (7.5\ N_c\ \eta_c\ \eta_z) / (V.a.b)$ .....(6)

Where: N_c is the power tiller (hp); η_c is the efficiency of power tiller for forward rotation of the rotary tiller shaft which is equal to 0.9, η_z is the coefficient of reservation of power tiller power (0.7-0.8); V is the forward speed of power tiller (m/s); a is rotary tiller working depth (dm); b is tiller working width (dm). The values of different parameters used in designing of rotor of *Biasi* implement and values of specific work of rotary tiller and maximum power tiller work for different values of V & λ are given in **Table 3** and **Table 4**.

Table 3 Values of different parameters used in designing of rotor of *Biasi* implement

Particulars	Values
C_o, coefficient relative to the soil type	2.5
K_o, specific strength of soil.(kg/dm³)	60
A_u, dynamic coefficient	400
N_c, the power tiller (hp)	(9.7 kW) 13
η_c, traction efficiency	0.9
η_z, coefficient of reservation of power tiller	0.8
a, rotary tiller working depth (dm)	0.982
Sy, Yield stress MPa	520
K, Coefficient of stress concentration	0.75
Cs Reliability factor non rocky soil.	2
FS factor of safety	2
V, m/s	0.2-0.6
R, cm	25
U_{min}, m/s	1.19

Table 4 Values of specific work of rotary tiller and maximum power tiller work for different values of V & λr

Velocity (m/s)	λ	$a_v = a_u(u/v)^2$	$A_B = 0.001a_v v^2$	$A_0 = 0.1C_o\ k_o$	$A = A_0 + A_B$ kg/dm³	A_c kg.m/dm³
0.2	22	193,600	7.74	15	22.74	51.06
0.3	18	129,600	11.66	15	26.66	34.04
0.4	10	40,000	6.4	15	21.4	25.53
0.5	4	6,400	1.6	15	16.6	20.42
0.6	2	1,600	0.576	15	15.57	17.02

Power Requirement of Rotary Power Unit

Drawbar power requirement of rotary tiller was calculated by the following equation:

$P = (V \times D_f) / 3.6$ .....(7)

Where; P is the drawbar power (kW); V is the forward speed (km/h); D_f is the drawbar force (kN).

$D_f = (D_r \times a \times b) / 1000$ .....(8)

$D_f = (25 \times 9.0 \times 70) / 1000$

$D_f = 15.6$ kN

$P = (2.16 \times 16.6) / 3.6$

$P = 9.36$ kW

Where; D_r is average rotary tiller specific resistance (kN) (21 N/cm² loam & silt-clay loam), 25 kN/cm² for clay soil. a & b are working depth and working width of *Biasi* operation respectively in cm.

Design of rotary tiller blades

In this design C-type rotary blades were considered. Design of rotary tiller blades depends on the following parameter: Soil types, no. of blades and working condition.

The no. of rotary tiller flange (f) was calculated by following equation;

$f = (b / bi) = 70 / 18 = 3.88$ .....(9)

Where, b is the working width (cm) and bi is the distance between the flange on the rotor (cm). Two blades were consider on each flange (z = 2). So total no. of blades was obtained by following relationship:

$N = f \times z = 4 \times 2 = 8$. Arrangements of blades on rotory unit is shown in **Fig. 1**.

Table 5 Total possible selections for the rotary tiller working width, forward speed and rotational speed of rotor

S. No.	Working width (cm)	Forward speed (m/s)	Rotor speed (rpm)	λ	Length of sliced soil (L) (cm)
1		0.2	168.08	22	3.57
2		0.3	206.28	18	4.36
3	60 cm	0.4	152.8	10	7.85
4		0.5	76.4	4	19.63
5		0.6	45.84	2	39.27
6		0.2	168.08	22	3.57
7		0.3	183.36	16	4.91
8	**70 cm**	**0.4**	**122.24**	**8**	**9.82**
9		0.5	57.3	3	26.18

Table 6 Modification in rotary unit of Power Tiller for Biasi operation

Particulars	General Operation	Biasi operation
Blades (tines) numbers	20 numbers	6/8 numbers
Blades (tines) Distance	2-4 cm	18 cm
Gear	I Forward heavy	I Forward heavy
RPM	2000-1800	2000-1800
Blade specification	C-shaped blade (4.5 cm tilling blade width), Length 28 cm, Heat -Treatment process	15° lengthwise slice angle, 2.5 cm tilling blade width Length 32 cm, Heat -Treatment process

Diameter of Rotor

The factors which affect the rotor diameter include torque and bending moment. Torque was important factor that was affected by the dimension of rotor diameter. For safe design of rotor diameter, selection of rotor axle and torque were important. Diameter was calculated by following relationship

$d = \sqrt[3]{16\ M_s / \tau}$ .....(10)

Where; d is the diameter of the rotor (cm); M_s is maximum torque at rotor axle in N.cm; τ is allowable shear stress at the rotor axle N/cm^2.

$\tau = (0.577\ K\ S_y) / F_S$ .....(11)

$\tau = (0.577 \times 0.75 \times 520) / 2$

$\tau = 112.5$ N/cm^2

Where; k is coefficient of stress concentration, S_y is yield stress (MPa) based on material of rotor; FS is factor of safety.

$M_s = K_s \times R$ .....(12)

$M_s = 294.95$ kN.m

Where, R is the rotor radius (mm)

$K_s = (75\ C_s\ N_c\ \eta_c\ \eta_z) / umin$ .....(13)

$K_s = 1179.83$ kg

Where, K_s is the maximum tangential force at the rotor axle (kg); u is minimum linear velocity of rotor (m/s); C_s is reliability factor taken as 1.5 for non-rocky soil and 2 for rocky soil. By using the equation (11, 12 & 13) the optimal diameter of rotor was calculated as 5.03 cm.

Development of Rotary Unit of Power Tiller for *Biasi* Operation

In the rotary unit, power was transferred to the tiller from the engine via the power-take-off drive. A shaft containing blades was located at 90° to the line of travel and rotated in the same direction as the forward travel of the power tiller. Since the shaft turns at a rate that was considerably faster than the corresponding power tiller speed, soil churning was accomplished. The proper selection of forward speed was dependent on the tangential speed of the blades (that is a function of rotational speed of rotor) and the length of sliced soil. The tangential speed of the blades (u), the rotational speed of the rotor (N), and the length of sliced soil (L) could be obtained by the following equations:

$U = (2\ \pi nR) / 6000$ .....(14)

$n = (6000\ \lambda v) / 2\ \pi R$ .....(15)

$L = (2\ \pi R) / \lambda Z$ .....(16)

Where, R = rotor radius (cm), v = forward speed (m/s), Z = number of blades on each side of the rotor flanges.

In this design, two blades were considered on each side of the flanges (Z = 2). Lakpale and Shrivastava (2012) found that, for better rice yield the *Biasi* operation can be performed at the working width of 20 ± 3 cm and 8-10 cm depth. Therefore, the designed parameter considered for the development of rotary *Biasi* unit was having a definite line of spacing and 10 cm depth of operation. Matyashin (1968) suggested that the radius of rotor for rotary tillers selected should be greater than the working depth. Considering these explanations, a 50 cm diameter was diagnosed to be appropriate for the rotary tiller rotor. By executing the selected values for the rotor diameter in the equations (15) and (16) becomes

Fig. 1 Arrangements of blades on rotory unit

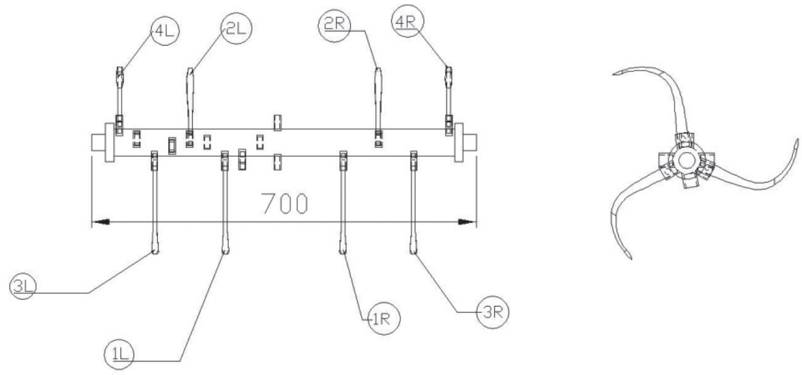

Fig. 2 Modification of number of blades, size and spacing on rotary unit

Fig. 3 Arrangements of blade unit in rotary unit of power tiller

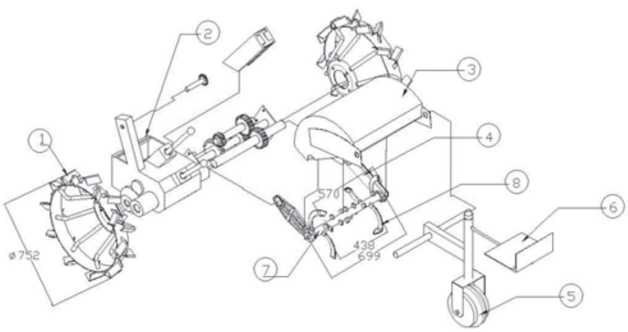

S. NO.	ITEMS	Qty.
1	CAGE WHEEL	2
2	GEAR BOX	1
3	MUD COVER	1
4	CHAIN COVER	1
5	GROUND WHEEL	1
6	OPERATOR SEAT	1
7	SHAFT	1
8	C-TYPE TYNE	6

$$n = (6000\,\lambda v / 2\,\pi R) = 38.21\,\lambda v \quad .....(17)$$

$$L = (2\,\pi \times 25) / (\lambda \times 2) = (25\,\pi) / \lambda \quad .....(18)$$

The net possible selections for the rotary tiller working width (b), forward speed (v) and rotational speed of rotor (n) are presented in **Table 5** and **Table 6** that were obtained through equations (17) and (18). For each of the selected working width, the closest values of the rotary tiller specific work of the power tiller were determined at each of the forward speed. Then the corresponding values of λ for each forward speed were determined to calculate the rotor speed and the length of soil sliced. By selecting the rotary tiller specific work and the performable work of the power tiller close together at each of the forward speeds, an appropriate conformity will be continued between the rotary tiller and power tiller. Considering the suitable domain obtained for the rotor speed, the length of sliced soil and the forward speed, at the working width of 70 cm, this width was selected as a proper working width for the power tiller (**Table 5**).

Considering the results presented in **Tables 1** and **5**, it becomes evident that the selected power tiller for this design only at the gear one can supply a rotary tiller with the working width of 70 cm at a working depth of 9.82 cm. After specifying the appropriate working width for the power tiller, the length of sliced soil, the rotational speed of the rotor and the tangential speed of the blades should be calculated at the selected gear (the forward speed of 0.40 m/s). Before performing the mentioned calculations, the appropriate value of λ, proportional to the selected forward speed for the power tiller should be obtained. For this purpose, the specific work of the rotary tiller and the performable work of the power tiller should be equal together. Therefore, gear no. 1 (forward heavy) was selected for *Biasi* operation.

Gear No. : 1 Forward heavy → v = 0.4 m/s, λ = 8

By obtained value for λ at the equations (14), (15) and (16) we will have, L = 9.82 cm, n = 122 rpm. On the basis of these calculations the following modification were made in the rotary unit of tiller **Table 6** and **Fig. 2** & **3**.

Result and Discussion

Comparative Performance of *Biasi* Implements

The comparative performance of the improved implements over that of traditional plough (**Fig. 4**) was assessed in terms of operational indicators as well as yield indicators.

Operational Indicators

The mean performance of different *Biasi* implements/ploughs in terms of operational indicators such as field capacity, distance of *Biasi*, plant mortality and weeding efficiency is shown in **Table 7**.

Fig. 4 Different operational views of *Biasi* implements

Study indicates that by the use of improved *Biasi* implements the field capacity was higher as compared to traditional method. The qualities of work indicator were Plant mortality (%), Weeding efficiency %, Plant population/ m^2, and Effective Tillers No./m^2.

The developed *Biasi* implement had shown significant increase in grain yield due to minimized plant mortality and better root stimulation that led to better crop growth and development of yield attributes. The B:C ratio was highest for Power Tiller operated modified rotary tines (2.34) and lowest for Traditional method (1.65). The studies clearly indicated that by mechanization timeliness of operation can be achieved and the cost of production was reduced and significant increase in yield was observed.

Yield Indicators

The comparative performance of different *Biasi* implements in terms of rice yield is shown in **Table 8**. All the implements used for *Biasi* operation performed better with regards to grain yield of rice as compared to that of the traditional plough used for *Biasi*. The highest grain yield was recorded in Trifal *Biasi* plough followed by power operated 5 tines plough and power tiller operated modified rotary *Biasi* implement. The lowest yield was recorded in traditional plough which served as control. The rice grain yield was recorded as 39.2 qha^{-1} (Trifal), 36.2 qha-1 (power tiller operated modified rotary *Biasi* implement), and 32.4 qha^{-1} (traditional). Significantly highest rice yield over traditional plough was obtained in Trifal *Biasi* plough (21%), followed by power tiller operated modified rotary *Biasi* implement power tiller operated modified rotary *Biasi* implement (17.9%).

Conclusions

The study revealed that the mechanized *Biasi* implements were found suitable under rainfed *Biasi* rice cultivation. The improved *Biasi* implements were found suitable because of their higher field capacity, better quality of work and better benefit-cost ratio.

Acknowledgement

The authors are grateful to ICAR New Delhi, Niche Area of Excellence Programme- Farm Mechanization in Rainfed Agriculture, for granting financial assistance during the course of investigation.

REFERENCES

Beeny and D. C. P. Khoo, 1970. Preliminary investigations into the performance of different shaped blades for the rotary tillage of wet rice soil. J. Agric. Engg Res. 15 (1): 27-33.

Bernacki, H., J. Haman and C. Z. Kanafojski. 1972. Agricultural machines, theory and construction. US Department of Commerce, National Technical Information Service, Springfield, Virginia 22151.

Chertkiattipol, S., T. Niyamapa and V. M. Salokhe. 2007. "Influence of rotary blade shapes of three rotary blade types on characteristic of tillage resistance torque and specific tilling energy", Proceedings of International Conference on Agricultural, Food and Biological Engineering and Post Harvest/ Production Technology, Khon Kaen, Thailand: 8-15.

Chandravanshi, B. S. 1989. "Rice farming in Chhattisgarh "A report of IGAU Raipur.

Fujisaka, S., K. T. Ingram and K. Moody. 1991. Crop Establishment (Beusani) in Cuttak District, India, IRRI, Research paper series Number 148 : 2-7

Kawade, S. C. 2001. Design, Development and Evaluation of *Biasi* Implement, Unpublished M.Tech. thesis, Faculty of Agricultural

Table 7 Impact of different implements on various parameters affecting rice production (Date of Biasi, DAS-35)

Parameters	Biasi implement		
	Animal Drawn		Power Tiller with modified rotary tines
	Local Deshi plough	*Biasi* plough	
Seed rate kg/ha	100	100	100
Variety - Mahamaya			
Distance of *Biasi*	20 ±3 cm	20 ±3 cm	18 ±3 cm
Plant mortality, (%)	22-37	10-18	21-29
Plant population/ m^2	114	129	118
Weeding efficiency, %	47	62	60
Effective Tillers, No./m^2	222-298	324-419	301-412
Field Capacity, ha/h	0.034	0.127	0.215

Table 8 Modification in rotary unit of Power Tiller for Biasi operation

Biasi Plough	Yield qha^{-1}	% yield increase*	B : C ratio
Trifal *Biasi* plough	39.2	21**	2.11**
Power Tiller operated modified rotary *Biasi* implement	38.2	18**	2.34**
Traditional (Control)	32.4	--	1.65

* - As compared to using traditional Biasi plough, ** - significant
qha^{-1} (quintal per hectare) 1 Quintal = 100 kg

Engineering, Indira Gandhi Krishi Vishwavidyalaya, Raipur (Chhattisgarh).
Lakpale and Shrivastava. 2012. Traditional system of rice cultivation in Chhattisgarh (*Biasi*): limitation, advantages and practices for improvement Model Training Course on Rice Production Technology Directorate of Extension Services, IGKV, Raipur (CG) Feb., 22-29: 101 -107
Matyashin, Yu. 1968. Means of decreasing energy requirements of rotary tillers. Vestink Selskokhozyais Ven noi Nuaki 1968; 9:131-133.
Mehta, C. R., N. S. Chandel and T. Senthil Kumar. 2014. Trends of Agricultural Mechanization in India, CSAM Policy Brief, Issue No. 02, June 2014:2-3
Mishra, B. P. 2010. "*Biasi* Equipments and Improved Practices for Broadcast *Biasi* System of Rice Cultivation". Faculty of Agricultural Engineering, Indira Gandhi Krishi Vishwavidyalaya, Raipur (Chhattisgarh).
Salokhe, V. M., M. H. Miah and M. Hoki. 1993. Effect of blade type on power requirement and puddling quality of a rotavator in wet Clay soil, Journal of Terramechanics, Vol. 30, No. 5: 337-350
Verma, A. K. and M. L. Dewangan. 2006. "Efficiency and energy use in puddling of lowland rice grown on Vertisol in Central India " Soil & Tillage Research, The Netherlands Vol. 90: 100-107

■■

EVENT CALENDAR

2019

◆ **IDF World Dairy Summit**
September 23-26, Istanbul, TURKEY
http://www.idfwds2019.com/

◆ **22nd FOODAGRO AFRICA 2019 in Kenya**
October 3-5, Nairobi, KENYA
http://africabizevents.com/fc/

◆ **22nd FOODAGRO AFRICA 2019 in Tanzania**
October 17-19, Dar-es-Salaam, TANZANIA
http://africabizevents.com/fc/

◆ **ASIA AGRI-TECH EXPO & FORUM**
October 31-November 2, Taipei, TAIWAN
https://www.agritechtaiwan.com/en-us/

◆ **Agritechnica**
November 10-16, Hanover, GERMANY
https://www.agritechnica.com/en/

■■

Design and Experiment of Associated Baler for Combine Harvester

by
Li Baoqian
Electromechanic Engineering College of
Hunan Agriculture University,
Zhengzhou 450002
CHINA

Wu Gaofeng
Electromechanic Engineering College of
Hunan Agriculture University,
Zhengzhou 450002
CHINA

Liu Yunpeng
Electromechanic Engineering College of
Hunan Agriculture University,
Zhengzhou 450002
CHINA

Lv Fengzhao
Electromechanic Engineering College of
Hunan Agriculture University,
Zhengzhou 450002
CHINA

Shi Dongsheng
Anyang Yugong Agriculture Machinery Co., Ltd.,
Anyang 456400

Abstract

Matching straw baler for combine harvester is designed against the shortcomings, such as high energy-consuming, time-consuming, re-crushing of farmland and lower purity of recovered straw, of existing baler for straw picking. The matching baler is directly side-placed and installed on the combine harvester, gets power from axial flow of the combine harvester and straightly compresses the straws thrown out by the combine harvester into bales, achieving synchronization of bundling & gathering and crop harvest. This paper describes design and parameter calculation for how the matching baler is installed on the combine harvester, components of power transfer system of the matching baler, feeding mechanism and compressing mechanism and other main mechanisms. The matching baler saves the time it takes to collect the straw after grain harvesting and avoids secondary crushing of the farmland. It can be used for the mechanical harvesting of straws of wheat and rice, and provides technical support for new grain harvest and the design of straw harvesting integrated machine. Field experiments demonstrate that: the machine is safe and reliable with the bundled rate reaching up to 99.5%, regular straw baling rate of 96% and straw baling density of 120 kg/m^3. It cooperates well with the combine harvester, and the whole machine has good compatibility. Although the harvesting efficiency of the combine harvester is decreased, the yield of straw is increased and the economic benefits are increased by \$85.0-147.5 /hm^2 comprehensively, so it has great promoting value.

Keywords: Matching baler; Integrated machine; Straw; Mechanical harvest

Introduction

China is rich in straw resources. But because of its small density and collection and storage difficulties, it has not been effectively used [1-3]. At present, straws of rice and wheat are packed after reaped by the harvester or bundled on the field after being picked up. The machine used is self-propelled or trailed pick-up baler, which picks up and bundles the straws thrown on ground after the crop is harvested, existing the disadvantages of picking small amount of straws and increasing the walking times in the field; the second is the field work baler, which has the disadvantages such as collecting a small quantity of straws under the cross regional joint conditions. Now, there are few field work balers [4-6].

The matching baler is side-placed and installed on the combine harvester, directly obtains power from roller cylinder of the harvester, and compress and knot the straws discharged from straw outlet of the combine harvester into bundles, so as to realize automatic synchronization of bundle collection of straws and crop harvest. Directly obtain compressed and bundled straws in acquisition of wheat and rice, the amount of straws harvested is large, which is convenient for storage and transportation of straws, and beneficial to recycling of straws, providing technical basis for design of food and straw harvesting integrated machine in the future.

Overall Structure and Working Principle of the Matching Baler

The matching baler consists of feeding mechanism, compression device, knotting device and rack, transmission, shell and so on, which complete slowdown input of power, straw feeding, compression, knotting and other actions respectively and achieve automatic synchronization with the combine harvester to bundle the straws. The matching baler turns the straw picking mechanism into the feeding mechanism based on the trailed or self-propelled straw baler, and passes the straws discharged from outlet of the combine harvester into the collection box by way of the feeding mechanism. The baler is powered by the combine harvester's axial flow, and the input speed is 750-850 r/min generally. Too slow revolving speed will affect the performance of the machine, and too high revolving speed is of high failure rate, which has great influences on reliability of the baler.

The matching baler is side-placed and mounted on the left side of the combine harvester; its feeding mouth is docked to the grass outlet of the harvester, making a harvesting-bundling integrated machine through welding and bolted connection. The installation structure is as shown in **Fig. 2**.

During the working process, the straws are passed into the collection box through stirring-into movement of the feeding device in the feeding mechanism and compression movement of the upper piston after discharged from the straw outlet of the combine harvester. After that straw is compressed by the reciprocating motion of the main piston, making the straws in the compressed body constantly shaped from slices. As the straws continuously feed in, the

Table 1 Performance parameters of the matching bailer

Technical parameters	Design value
Size of the baling section / mm	300 × 450
Length of bales / mm	300-1200
Operating frequency of main piston / ($r{\cdot}min^{-1}$)	80-100
Input rotate speed / ($r{\cdot}min^{-1}$)	750-850
Overall dimension / mm	2800 × 800 × 1400
Weight of the bailer / kg	650
Input power / kW	5-6

Fig. 1 Structural sketch of matching baler

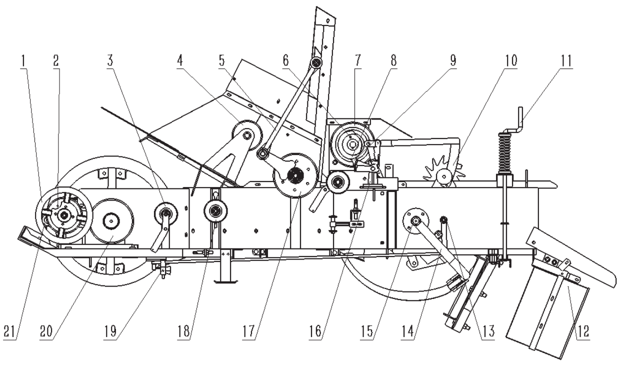

1. Hand wheel, 2. Uniaxial fuse, 3. Elastic tensioning wheel, 4. Swath roller sprocket, 5. Upper piston-connecting rod, 6. Knotting shaft safety, 7. Knotting keyboard, 8. Knotting cam, 9. Clutch separation block, 10. Bale length regulator, 11. Bale intensity regulator, 12. Bale rope box, 13. Safety assembly, 14. Needle frame, 15. Needle frame bearing, 16. Clutch support, 17. Upper piston sprocket, 18. Tensioning wheel, 19. Safety stop, 20. Output shaft sprocket, 21. Connecting rod bearing.

Fig. 2 Installation and structural drawing for matching baler and combine harvester

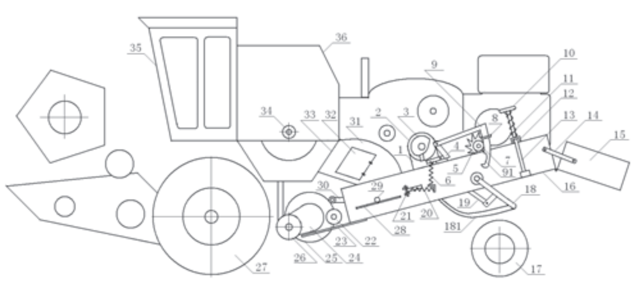

图 1

1. Knotter, 2. Chain wheel, 3. Limit plate, 4. Crank arm, 5. Ratchet wheel, 6. Spring, 7. Gear wheel, 8. Stopper, 9. Bent lever, 91. Adjusting tooth, 10. Operation, 11. Spring, 12. Hold down strip, 13. Montant, 14. Connecting plate, 15. Bundle placing board, 16. Baling box, 17. Rear wheel, 18. Needle-threader, 181. Threading needle, 19. Needle-threading rack, 20. Spring, 21. Check plate, 22. Chain wheel, 23. Supporting plate, 24. Reducer, 25. Drive plate, 26. Chain drive wheel, 27. Front wheel, 28. Piston guide rail, 29. Guide wheel bearing, 30. Connecting rod, 31. Passage, 32. Running wheel, 33. Grass outlet, 34. Output shaft of the combine harvester, 35. Cab, 36. Barn.

Fig. 3 Transmission system structure diagram

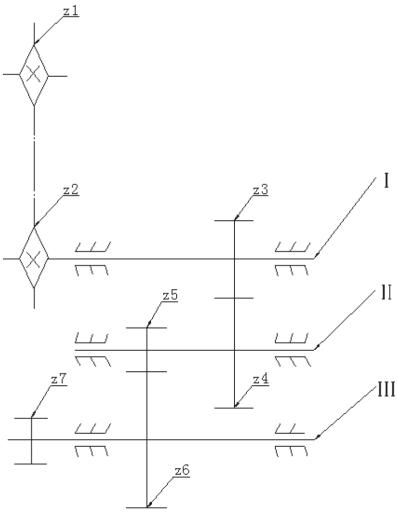

Note: *I* is the input shaft; *II* is intermediate shaft; *III* is output shaft; Z_1 is the chain wheel of the axial flow shaft, 22 teeth; Z_2 is the chain wheel of the input, 29 teeth; Z_3 is the output straight gear, 19 teeth; Z_4 is the input straight gear of the intermediate shaft, 46 teeth; Z_5 is the output straight gear of the intermediate shaft, 16 teeth; Z_6 is the straight gear of the output shaft, 53 teeth; Z_7 is the output chain wheel, 36 teeth.

baled straws drive the dosing wheel to rotate. When the length of baled straws reaches the predetermined value, the knotter clutch is released; the threading needle goes upward to pass the bundled rope; the knotter clamps the rope and finish rope knotting to form a complete bundle. With the continuous increase of straws inside the collection and reciprocating movement of the piston, the bundled straws are pushed out of the compression chamber. The straw in the compression chamber continues to be compressed into pieces, forming the next bale. The continuous formed bales slide off to the ground through the bale unloading slide carriage, thus completing the continuous bundling. And the bundled straws fall off to the ground.

The matching baler is placed on the left side of the combine harvester, and the harvester mounted with the matching baler will produce center-of-gravity shift to a certain extent. According to data analysis of promoting throughout the country over the past three years, the center-of-gravity shift does not affect the normal operation of the combine harvester. The design of this paper does not involve transformation of the combine harvester, and the problem of center-of-gravity shift will be thoroughly solved when the crop-straw harvesting machine is designed in the future.

The minimum clearance of the combined harvester above ground is 270 mm after installation of the matching baler, which still meets the requirements of the national standard of “Outline for Agricultural Machinery Promotion and Accreditation” (DG / T 014-2009 Grain Combine Harvester) without affecting the adoption of the combine harvester. And can satisfy the requirements of field adoption of the combine harvester in the Henan, Shandong, Anhui and northeast of China, the main producing areas of grain.

Design of Key Components

Design of Power Transfer System

The matching baler is powered by the combined harvester, and the power connection is the axial flow shaft of the combine harvester. According to Agricultural Machinery Designing Handbook in literature [8], total power required for each unit of the combined harvester is generally 64 kW, and the combined harvester engine shall be equipped with sufficient reserve power.

$$N = 1.33\, N_p \quad .....(1)$$

Where: N_p is the average power required for operation of the combine harvester, kW.

So, the power should generally be above 85 kW after matching baler is mounted. After verified by field production, on this basis, the combined harvester additionally mounted with the matching baler can still fully meet the requirements of normal harvesting. In design of the transmission system, input shaft of the reducer is equipped with safety bolts to protect the machine to work properly, avoid overloading operation of the baler, and result in accidents caused by damaged parts.

The output dynamic design is preliminarily determined as the overall plan of the transmission system: Level 1 power transmission is delivered to the reduction gearbox from the axial flow shaft and is driven by chains. Straight gear level 2 is adopted for speed reduction of the reducer, as shown in **Fig. 3**. Rotate speed of axial flow shaft of the harvester is generally about 750-850 r/min, the compression frequency of the baler is about 80-100 r/min after speed reduction. The transmission

Fig. 4 Feeding mechanism structure sketch

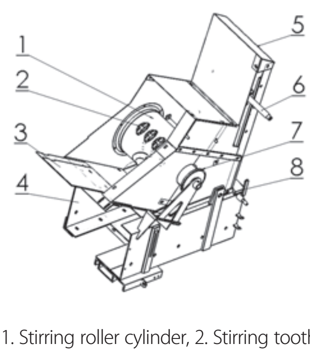

1. Stirring roller cylinder, 2. Stirring tooth, 3. Air duct tongue depressor, 4. Collection box, 5. Upper piston damper, 6. Upper piston, 7. Stirring roller sprocket, 8. Upper piston sprocket supporting plate

Fig. 5 Stirring roller structure diagram

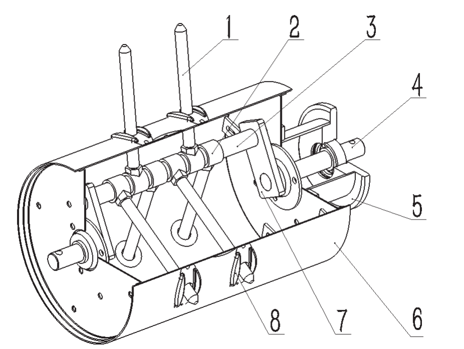

1. Stirring tooth, 2. Stirring tooth seat, 3. Stirring tooth shaft, 4. Driving shaft, 5. Chain wheel, 6. Barrel, 7. Crank, 8. Resin ball sleeve

ratio of the transmission system can be obtained through Formula (2), and level I speed reducing & transmission ratio is 1.32, level II speed reducing & transmission ratio is 2.42, the level III speed reducing & transmission ratio is 3.31. Refer to annotations of Fig. (2) for the quantity of transmission gears.

$i = z1 / z2$ .....(2)

Design of Feeding Mechanism

Working principle diagram

Straw feeding is the first action of the matching baler, and straw feeding mechanism is an important part of the baler. It is far from perfect that straw feeding of the matching baler only depends on power obtained from the fan on the combine harvester. If the feeding mechanism is not set, large amounts of straws will be accumulated at inlet of the baler, leading to blockage, affecting the straws enter into the bundling room and impeding normal reciprocating motion of the piston [7].

Stirring roller design

Stirring roller of the feeding mechanism is based on the principle of flexible stirring tooth, preventing the blockage caused by straws twining the stirring roller. As shown in **Fig. 5**.

At present, the matching baler can be equipped and installed to meet the power equipment. The standard for feed quantity setting of the combine harvester is 4 kg/s, and the density of wheat straws is 20-25 kg/m^3. After threshing and purification, the yield at outlet of the combine harvester is 0.7 kg/s. Feed quantity of feeding mechanism of the matching baler designed in this paper is 1 kg/s [8].

Fig. 6 Stirring tooth length and eccentricity

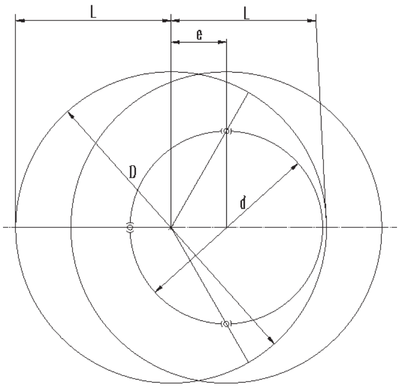

Note: L for the stirring tooth length, mm; D for the stirring tooth rotation radius, mm; d for the barrel diameter, mm; e for the eccentricity, mm

Fig. 7 Add a constraint stirring stick simulation model

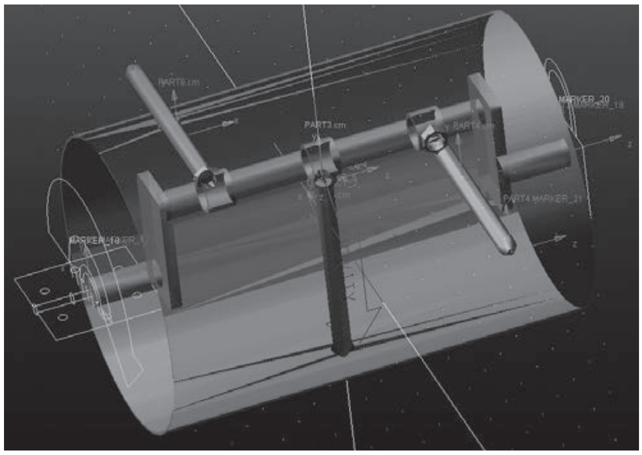

Length of the stirring tooth is 185 mm, and radius of the stirring roller is 132 mm. Rotating the stirring roller for a cycle can get an approximate cylinder, its feeding volume is as shown in Formula (3)

$V = \pi r_2^2 h - \pi r_1^2 h$ .....(3)

The feeding amount for the stirring stick rotating for one circle is

$m = \rho_0 kV$ .....(4)

In the equation: h is the feeding width, taken as 0.45 m; r_2 is the stirring tooth length, m; R_1 is the radius of the stirring stick, m; ρ_0 is the density of wheat straw, kg/m^3; is the filling coefficient of the stirring stick, taken as 0.1. Through calculation, at this time, the speed of the stirring stick n = 138 r/min.

The design of the stirring stick consists of three sets of stirring teeth being hinged side by side on the axle of stirring stick, every two is a group. The three sets of stirring teeth are arranged at 120° apart. In order to prevent fingertip from wear, save 8 mm margin of the stirring tooth outside the barrel, stirring tooth length L = 185 mm, diameter Φ = 16 mm. Eccentricity e = 33 mm, cylinder diameter 264 mm. The motion curve is as shown in **Fig. 6**

In the case shown in **Fig. 6**, the stirring tooth endpoint displacement, velocity, acceleration equation is as shown in equation (5)

$$\begin{cases} a = (r_2 + \sin \omega t \cdot e)\omega^2 \\ v = (e + \sin \omega t \cdot r_2)\omega \\ s = (e + \sin \omega t \cdot r_2)\omega t \end{cases} \quad .....(2)$$

Where the spindle is the reference, e is the eccentricity, m; r_2 is the stirring tooth length, m.

Use ADMAS software to do simulation verification of stirring tooth motion trial, add a fixed constraint to the crank and the ground in the ADMAS, add revolute which is relative to the crank to the sticking stick barrel and set into the active motion. The speed is 828 d/time. Add physical contiguity to the stirring tooth and the crank, the stirring tooth and the shell, add revolute which is relative to the crank to the stirring tooth. Add the constraint diagram as shown in **Fig. 7**. Observe the complete motion simulation situation, observation time is greater than a cycle, a cycle time is 1 / 2.3 = 0.436 s, here take End Time = 1.5 s, Steps = 500.

After simulation analysis, the speed curve is as shown in **Fig. 8**. In order to accurately analyze the movement of the stirring tooth, the bottom of the stirring tooth movement is set as Point 1. The Point 1 is the position where the stirring tooth rolls out of stirring stick. Every time, a rotation of 90°, set a point, the points respectively are Point 2, Point 3 and Point 4. Analysis motion characteristics of 4 regions, corresponding speed of 4 points is as shown in **Table 2**.

Run from Point 1 to Point 2 is the stage of the stirring tooth initially roll out of the stirring stick, speed at Point 1 on Y direction is almost 0, the resultant velocity and the horizontal speed are basically the same as 1.9131 m/s. The resultant velocity and Y speed gradually increase, when reaching Point 2, X speed is almost zero, at this time the straw began to be fed by stirring tooth, so that enough straw can be fed into the straw-collecting box.

Run from Point 2 to Point 3, the resultant velocity and X speed continue to increase, the extension length of the stirring tooth continue to increase, the straw feeding force shall be increased. At Point 3, the resultant velocity and X speed reach the maximum, at this time the feeding force is the strongest, compared with Point 1, Point 3 has higher feeding efficiency, Point 1 is the shortest point for the extension of the stirring tooth, both of speed and force are the smallest, which can achieve the optimal use of energy consumption.

Run from Point 3 to Point 1, the resultant velocity gradually reduces, the extension length of the stirring tooth gradually decreases to prevent the straw from twining barrel and to prevent the inside straw from rolling out.

Table 2 The speed of stirring tooth endpoint of stirring stick

	Corresponding time / s	V/(m·s^{-1})	VX/(m·s^{-1})	VY/(m·s^{-1})
1	0.144	1.9131	1.9131	0.0055
2	0.290	2.9051	0.0219	2.9049
3	0.364	6.1755	-6.1751	-0.0489
4	0.436	2.8640	0.0684	-2.8642

Upper piston design

After the stirring stick pull the straw into the straw-collecting box, in order to increase the straw density in straw-collecting box, the piston that can do upper and lower reciprocating motion is equipped in the straw inlet device, known as upper piston, the upper piston consists of piston cap, cross bar, piston plate, piston wheel, hinge plate and other components. The power is driven by the upper piston sprocket mounted on the baler's case, in right time order, when the main piston runs to the farthest position of the stroke, the upper piston runs to the top of the most stroke. During operation, when upper piston locates in the downlink, the hinge and straw contact to fold the hinge to the specified direction, at this moment, the hinge presses the straw into the straw box in a way of imitating the press gesture of the palm. As shown in **Fig.** 9.

Compression Mechanism Design

The compressor is mainly composed of flywheel, main piston and connecting rod. The flywheel receives the power from the reducer and stores and releases the kinetic energy. In order to avoid machine damage caused by sudden time disorder, the flywheel is welded with the impact insurance point. The connecting rod is used to connect the flywheel and the main piston for power transmission and ensures that the piston moves according to the intended track path. The main piston is used to compress the straw in the straw-collecting box for compression molding in the compression chamber.

Operation frequency analysis

The structure reasonableness of the flywheel, connecting rod and piston is one of the key factors of the normal operation of the baler. When the piston pressure changes from zero to the maximum, the straw bale density also changes from the minimum value to the maximum value; when the piston reverses, because of the characteristics of the material, the straw bale first maintains this density for some time, then due to the stress relax-

Fig. 8 Speed curve of stirring tooth endpoint

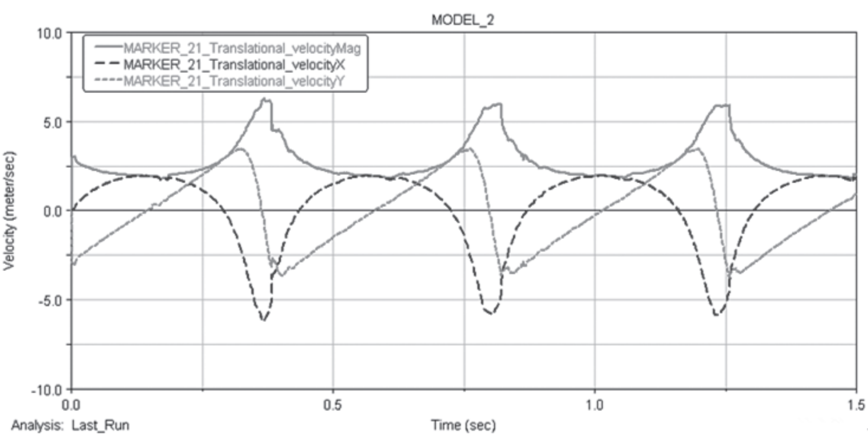

Fig. 9 Schematic diagram of the structure of upper piston

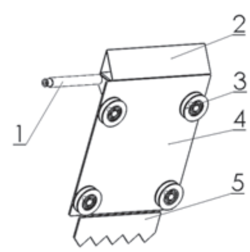

1. Cross-bar, 2. Piston cap, 3. Pulley, 4. Piston plate, 5. Hinge

ation, the straw begins to expand. If the compression piston implements the second compression before the straw has not yet expanded, the straw will be able to get a higher density, so the design frequency of the crank piston. Not only need to satisfy the time required for the threading and knotting operation of the baler, but also need to minimize the expansion and transformation of the compressed bundles of straw between the second compression and the first compression [9-11].

Though increasing the reciprocating frequency of the piston can increase the productivity of the baler, the increase of the reciprocating frequency of the piston can cause many new problems. First, the increase of the reciprocating frequency leads to a significant increase of the consumption power of the baler. Since the baler is placed on the side of the combine harvester, which has caused a rolling tendency of the harvester. When the flywheel drives the piston to run at high speed, the resulting imbalance and vibration phenomenon of the baler are more obvious. On the basis of ensuring the combine harvester and matching baler in normal working condition, combined with the above power transmission system deceleration, the piston reciprocating frequency of the baler is determined as 80 to 100 timesmin [1].

Main piston design

In order to distinguish the upper piston doing up and down reciprocating motion, It was called the piston doing left and right reciprocating motion the main piston. In order to overcome the vibration and friction resistance caused by the reciprocating motion of the piston, the bottom and side position of the piston are equipped with a sliding roller. When the piston is doing reciprocating motion, the roller on the piston rolls along the track on up, down, left and right sidewall of the compression chamber, so that the piston movement is smooth and reliable, greatly improving the performance of the piston. The compression piston is set in the compression chamber, and its main components include piston, upper slide, roller, hay knife and so on. Top and bottom of the piston have open slot of straw retaining plate, the midst of piston body has needle threading slot, which can ensure that compression piston does not interfere with grass board and the needle threading during compression work [12-13].

Motion analysis of compression mechanism

When the baler is installed in the combine harvester, due to the installation position and the matching power transmission design, the machine adopts the central crank slide block mechanism. As the compression mechanism is limited to the entire machine frame and compression chamber structure, some parameters are default value. From the analysis of the relationship between the baling density and the effective stroke, the density increases when the effective stroke increases. When the effective stroke reaches a certain value, the density is basically maintained at a level with the increase of the effective travel [15]. The effective stroke of square baling machine generally is 630-800 mm [8], the design compression crank AB length s = 660 mm, connecting rod L = 1400 mm. **Fig. 12** is the geometric relationship figure of the two poles positions of central crank slide block.

In order to ensure the stability of piston operation, the bottom of the machine body is equipped with running rails and tracks. The bottom and side of the piston itself are equipped with multiple sliding rollers to reduce power consumption and reduce vibration.

Stress analysis of compression mechanism

According to the law of motion and operation characteristics of compression mechanism [14], as shown in **Fig. 13**, establish XOY coordinates, OA is the crank of compression plate, Point O is the motion center of compression crank, AB is the compression connecting rod, X circumferential direction is the compression stroke direction, the crank conducts uniform rotation with ω, the rotation

Fig. 10 Schematic diagram of compression mechanism

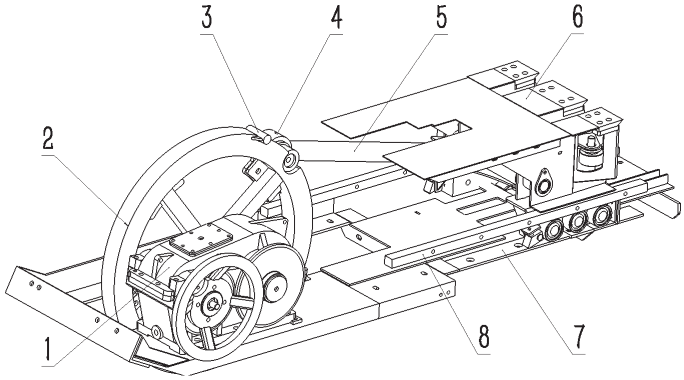

1. Reducer, 2. Crank round wheel, 3. Impact insurance point, 4. Connecting bearing, 5. Connecting rod, 6. Main piston, 7. Path, 8. Glide path

Fig. 11 Schematic diagram of the structure of main piston

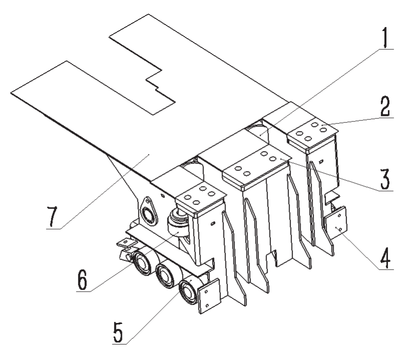

1. Needle threading slot, 2. Hay knife 1, 3. Hay knife 2, 4. Retaining leather, 5. Lower roller, 6. Side roller, 7. Grass board

angle is ϕ(t).

$$\varphi(t) = \omega t \qquad .....(6)$$

$$\theta(t) = art\,(-r \sin \varphi(t) / L) \qquad .....(7)$$

$$F_t = -F_1 \bullet \cos \theta(t) \qquad .....(8)$$

$$F_n = F_1 \bullet \sin \theta(t) \qquad .....(9)$$

Where: $\theta(t)$ is the function of included angle between connecting rod and crank to time t; $\varphi(t)$ is the function of included angle between crank and y axis to time t.

During the operation of baler, the power on the connecting rod is passed to the piston through the connecting rod, wherein, the connecting rod is hinged to the connecting pin axis, the direction of acting force received by the connecting rod axis continuously rotates along the circumferential direction and the size is constantly changing, because the connecting pin rod is more easily to have fatigue failure under the action of alternating load; during operation, the connecting rod is two-force bar, the direction receiving piston resistance is collinear with the direction of driving force of connecting pin axis, but the size of resultant force isn’t zero and constantly changes with the motion of crank slide mechanism, therefore, under the action of alternating load, the connecting rod is also easily have fatigue rupture, in this design, it utilizes the ANSYS Workbench software to conduct fatigue analysis on the connecting pin axis and connecting rod.

The material of connecting pin axis adopts 45 steel, the density is 7 850 kg/m^3, the elasticity modulus is 2.1×10^{-5} MPa, the Poisson’s ratio is 0.31, the yield strength is 353 MPa, the tensile strength is 598 MPa. A half of cylindrical surface in the connecting pin axis in the baler is welded in the notch of flywheel, therefore, in ANSYS Workbench simulation process, equivalently exert fixed constraint on this weld face, meanwhile, in order to simulate the load with changing direction received by the connecting pin axis in actual operating process, respectively exert F_1 = 1500 cos (360 time) along the horizontal direction and F_2 = 1500 sin (360 time) along vertical direction to the connecting pin axis to equivalently simulate the actual stress status of the connecting pin axis.

The simulation result demonstrates that in static analysis, the maximum stress that the connecting pin axis receives is located at the inside wall of root of the connecting pin axis, the value is 5.9669 MPa. The maximum deformation is about 0.0013mm at the contact top end. As shown in **Fig. 14a** and **Fig. 14b**, it can be known from the equivalent stress distribution cloud picture and the total deformation distribution cloud picture of static analysis. This region is easy to have fatigue. In fatigue analysis, the design life is 1e6, the minimum load range ability in fatigue sensitivity is 50%, the maximum load range ability is 200%, as shown in **Fig. 14c**, the design life in fatigue analysis is 1e6, in the safety coefficient of cycle index and curve graph of fatigue sensitivity, wherein, with the gradual enlarging of load, when the load increases to about 1700 N, the life of connecting pin axis gradually reduces.

Similarly, divide 54107 units of finite element analysis grid for connecting rod in ANSYS Workbench, obtain 79566 nodes, similar to connecting pin axis, it will not give unnecessary details for finite element analysis graphics. The load exerted on connecting rod within ANSYS is the maximum load that the connecting rod receives during actual operating, its value is still 1500 N, the simulation result demonstrates that in static analysis, the maximum stress the connecting road receives is at the joint with the flywheel, the value is 8.4795 MPa. When the maximum deformation of alternating stress is still at the outer end of joint with flywheel, the maximum stress value is 84.795MPa. When conducting fatigue analysis, the design life of connecting rod takes 1e6, the minimum load range ability in fatigue sensitivity is 50%, the maximum load range ability is 200%. Through comparing the cloud pictures of equivalent stress

Fig. 12 Schematic diagram of the operation of the compression mechanism

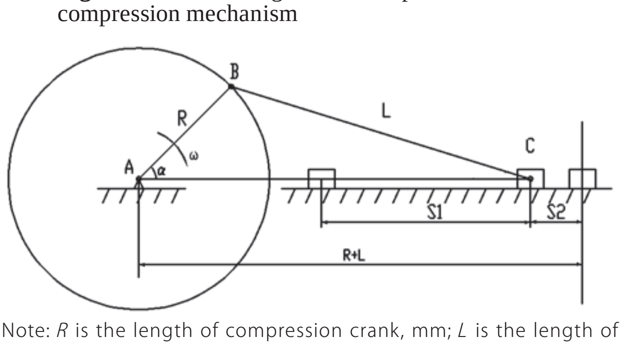

Note: R is the length of compression crank, mm; L is the length of connecting rod, mm; α is the crank angle, °; ω for the crank speed, r · min^{-1}; the sum of S_1 and S_2 is the stroke of piston, mm

Fig. 13 Stress model of compression mechanism

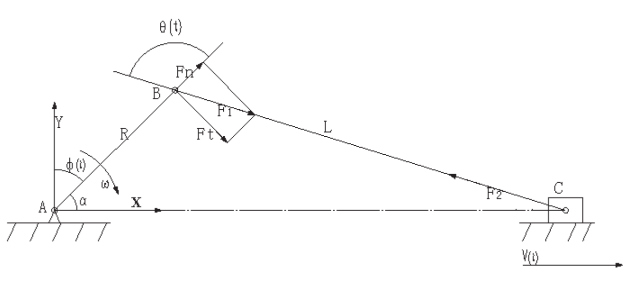

Note: R is the length of the compression crank, mm; L is the length of connecting rod, mm; α is the corner of crankshaft, °; ω is the rotating speed of crank, r/min; F_1 is the force the crank acts on the connecting rod, N; F_2 is the force the piston acts on the connecting rod, N; F_n is the component force on crank acted by crank itself in normal direction, N; F_t is the tangential component force of crank itself, N.

respectively under static load and alternating load of connecting rod, we can get to know that compared with the connecting rod under static load, under the action of bearing alternating load, the stress of connecting rod obviously increased, thus, under the action of alternating load, the connecting rod is more easily to have fatigue rupture. Wherein, with the gradual enlarging of load, when the load increases to about 1500 N, the lifetime of connecting rod also starts to reduce gradually.

Analysis of reciprocating inertia balance

The centric slider-crank mechanism causes bigger imbalance of centrifugal inertia force in vertical direction when avoiding full balance [8]. It only conducts partial balance analysis of reciprocating inertia force, the simplified stress is calculated according to Formula (10).

$$\lambda(M_d + (2/3)M_l)r + (1/3)M_l r = M_p r_p \quad .....(10)$$

Where: M_d is the mass of piston, taking 42 kg; M_l is the mass of connecting rod, taking 8 kg; M_p is the mass of crank plate after adding additional weight, taking 48 kg; is the radius of crank, m; r_p is the turning radius of center of gravity of crank, m. Generally, $\lambda = 0.25 – 0.5$, λ takes 0.3 here, thus the additional weight of crank plate is 1.88 kg.

Performance Test

Test Conditions

The experiment time is in June, 2016, the location is in Baliying Village, Huaxian County, Henan Province (35° 52′ N, 114° 80′ E), it is conducted in wheat farmland, the experimental farm is flat without slope, the soil layer is thick, belonging to cinnamon soil; the soil texture is relatively adhesive and heavy without rock debris. The wheat variety is Zhongyu 9307 mostly planted in local Huaxian County, the operation area is 8 hm^2. The planting density of wheat is 6 million plants/hm^2, the average height is 880 mm and the moisture content is 17-20%. The matching harvester is Guwang-TB60 (ZOOMLION), the operating speed is Gear II (1.1 m/s). The effect of field experiment is shown in **Fig. 15**.

Experimental Method

The experiment is based on Rectangular bale baler (Rectangular bale baler) and determined the experimental indexes according to the actual situation: straw bale density, baling twine consumption, oil consumption, regular straw baling rate, anti-drop rate, etc [16-17]. The main apparatuses of the experiment mainly include 1 set of Guwang-TB60 combine harvester equipped with matching baler, YP50001 type electronic balance scale (Shanghai Precision Instrument Co., Ltd.),

Fig. 14 Connecting pin axis stress cloud picture, displacement cloud picture and fatigue curve

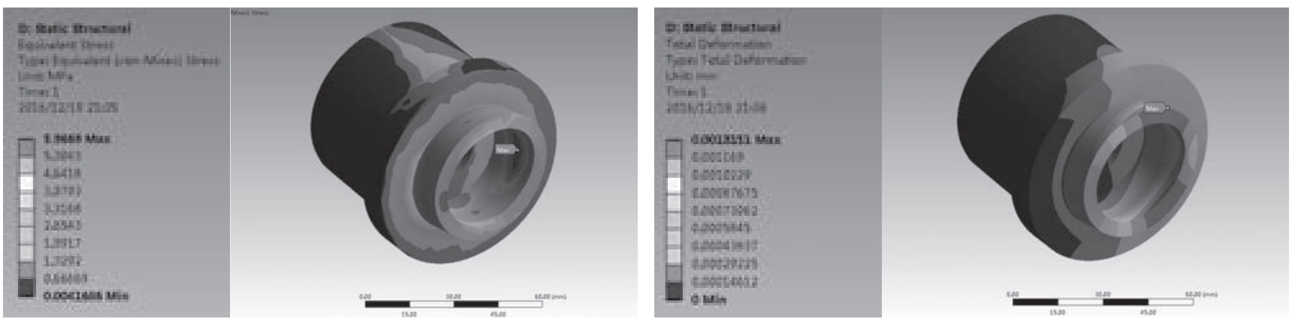

a. Stress cloud picture

b. Displacement cloud picture

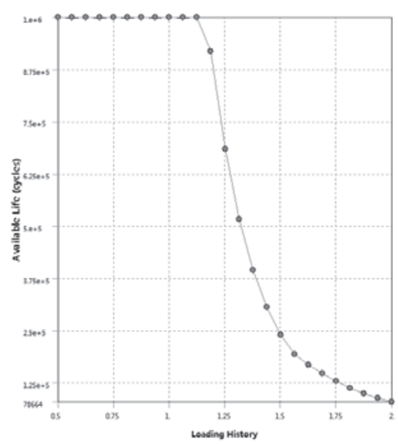

c. Fatigue sensitivity curve graph

Fig. 15 Field experiment of matching baler of combine harvester

DM1-102 type stopwatch (Shanghai Precision Instrument Co., Ltd.), JC151 type steel tape, meter ruler, etc.

Straw bale density and baling twine consumption

Take 5 points on diagonal line on experimental site, sample for 3 times to measure for each point. The experimental baling twine adopts SPPK-320 type polypropylene baling twine provided by JB/T 5167-2007, measured the size of straw bale shape after falling on ground, and respectively weigh the masses of bale straw and baling twine. One straw bale was tested for each one-way stroke. The equivalent density of straw bale is calculated according to Formula (11), the consumption of baling twine is calculated according to Formula (12).

$$P_d = (10^6 W_{kd}) / V_k \quad .....(11)$$

$$G_k = (10^3 W_{sk}) / (W_{kd} - W_{sk}) \quad .....(12)$$

Where: W_{kd} is the equivalent mass of the tested straw bale, kg; P_d is the equivalent density of the straw bale, kg/m^3 ; V_k is the volume of the tested straw bale, cm^3; G_k is the consumption of baling twine, kg/t; W_{sk} is the mass of baling twine, kg.

Regular straw baling rate and anti-drop rate

Used a steel ruler to determine the sizes of 4 side lengths of straw bales, when the difference of the maximum value and the minimum value isn't bigger than 10% of the average value of the long side, it should be determined as regular straw bale, otherwise, it should be determined as the irregular straw bale. Test 5 straw bales for each one-way stroke, calculate as per Formula (13); took 2 straw bales from each one-way stroke, freely fall from the height of 5m, dropped for 3 times for each bale, record the dropped and scattered straw bale quantity, calculate according to Formula (14);

$$S_g = ((I_{gc} - I_{gb}) / I_{gc}) \times 100 \quad .....(13)$$

$$S_{kc} = ((I_{kc} - I_{ks}) / I_{kc}) \times 100 \quad .....(14)$$

Where: S_g is regular straw baling rate %; I_{gc} is the tested straw bale quantity; I_{gb} is the irregular straw bale quantity, bale; S_{kc} is the anti-drop rate, %; I_{ks} is the accumulated dropped and scattered straw bale quantity, bale; I_{kc} is the tested straw bale quantity, bale.

Analysis of experimental result

The experimental result demonstrates: The operation machines and tools are stable, the performance is good, the handling is safe and reliable. The performance parameters of model machine are shown in **Table 3**.

After the combine harvester is equipped with matching baler, it could directly bale and harvest 3-4 t/hm^2 straws, the increased total production cost is \$54.5 /hm^2, the selling price of straws is \$46.5-50.9 /t, it could obtain an income of \$139.5-203.4 /hm^2, the net profit could reach \$85.0-147.5 /hm^2.

Table 3 Experimental parameters of main performance indexes

Item	Standard index	Measurement value
Baled rate/%	≥98	99.5
Straw baling density/(kg m^{-3})	≥100	120
Regular straw baling rate/%	≥95	96
Straw bale anti-drop rate/%	≥90	95
Baling twine consumption/(kg·t^{-1})	≤1.15	0.89

Conclusions

1) A match baler matched and integrated with the combine harvester was developed, compared with straw balers of other types, it has advantages of low energy consumption, high cleanliness of straws harvested and saving time, effectively solve the problems of straw harvesting and hurrying in farming season and the collection and disposal of crop straw. The field experiment demonstrates that the baled rate is 99.5%, the regular straw baling rate is 96%, the straw baling density is 120 kg/m^3, the anti-drop rate of straw bale is 95%, the baling twine consumption is 0.89 kg/t. The economic benefit is \$85.0-147.5 /hm^2.

2) The matching baler installed on side place has little effect on the center of gravity of the combine harvester, but it doesn't have any adverse effect on the normal function of the combine harvester. The minimum ground clearance after the installation of matching baler is 270 mm, which is still in the national standard scope and doesn't affect the field throughput capacity of combine harvester. Lay a good technological foundation for the design of grain straw harvest AIO.

3) The designed seed feeding mechanism adopts the combined working of stirring stick with telescopic stirring tooth principle and upper piston running up and down, effectively feeds the straws blown out by the combine harvester into the straw collection box, which isn't easily to get clogged. The operating speed of stirring stick is 138 r/min., the feed quantity is 1 kg/s.

4) The compression device of the matching baler adopts centric slider-crank mechanism, the operating frequency is 80-100r/min. and the stroke is 660 mm. The stress analysis and finite element analysis could obtain that the set mechanism could satisfy the strength requirement. The field experiment demonstrates that the piston operation has less polarization effect on combine harvester and matching baler, the operation stability is good.

REFERENCES

[1] Yu, T.E., B. C. English and LX.

He. Analyzing economic and environment performance of switchgrass biofuel supply chains. Bioenergy research, 2016, 9(2): 566-577.
[2] Omar Ahmad Bamaga, T. C. Thakur and M. L Verm. Assessment of cereal straw availability in combine harvested fields and its recovery by baling. Agricultural Mechanization in Asia, Africa and Latin America: AMA, 2003, 34(2): 100-105.
[3] Bi Yuyun, Gao Chunyu, Wang Yajing, et al. Estimation of straw resources in China. Transactions of the Chinese Society of Agricultural Engineering, 2009, 25(12): 211-217. (in Chinese)
[4] Brian Bell. Bale handling part II. Vintage Tractor, 2009, 1(4): 97-99.
[5] Lopez, R. M., H. E. Hetz and B. C. Maturana. Economic evaluation of collection, transport and utilization of straw in the swath of wheat stubble. Agricultural Mechanization in Asia, Africa and Latin America: AMA, 2010, 41(3): 52-58.
[6] Shito, H., N. Yamana, Y. Shibuya, et a1. Development of the Roll Baler for Chopped Materials. Agricultural Research Quarterly, 2006, 40(3): 233-237.
[7] Guo Jiyan, Guo Zhanyong, Shi Dongsheng. Grass feeding device of matching baler for combine harvester. China: ZL201010513972.2, 2012.05.23(in Chinese)
[8] Chinese Academy of Agricultural Mechanization Sciences. Agricultural Machinery Design Manual. China, Beijing: Machinery Industry Press, 2007.
[9] Nazari, Galedar M., A. Tabatabaeefar and A. Jafari. Influence of moisture content, rate of loading and height regions on tensile strength of alfalfa stems. International Agrophysics, 2009, 23(1): 27-31.
[10] Miao, Z., W., J. W. Phillips and T. E. Grift. Measurement of Mechanical Compressive Properties and Densification Energy Requirement of Miscanthus x giganteus and Switchgrass. Bioenergy Research, 2015, 8(1): 152-164.
[11] Lee, D. H., C. H. Choi and S. O. Chung. Evaluation of tractor fuel efficiency using dynamometer and baler operation cycle. Journal of the Faculty of Agriculture Kyushu University, 2016, 61(1): 173-182.
[12] Franco, W., F. Iarussi and G. Quaglia. Human powered press for producing straw bales for use in construction during post-emergency conditions. Biosystems Engineering, 2016, 150(8): 170-181.
[13] Afzalinia, S. and M. Roberge. Modeling of pressure distribution inside the compression chamber of a large square baler. Transitions of the ASABE. 2008, 51(4).
[14] Afzalinia, S. and M. Roberge. Modeling of the pressure-density relationship in a large cubic baler. Journal of Agricultural Science and Technology, 2013, 15(1): 35-44.
[15] Dogherety, M. J. O., J. A. Huber and J. Dyson. A study of the physical and mechanical properties of wheat straw. J. Agric Engng Res, (1995)62, 133-142.
[16] GB/T 25423-2010 Rectangular baler. (in Chinese)
[17] JB/T 9700 Rectangular baler test methods. (in Chinese)

■■

The Role of Agricultural Mechanization in the Process of Modernization of Agriculture in Vietnam - Contribution of Agricultural Engieering to Production After Years of Conducting Renovation

by
Pham Van Lang
Prof. Dr. Sc.
Vietnam Institute of Agricultural Engineering and Post Harvest Technology, Hanoi
VIET NAM
langttcd16@gmail.com

Nguyen Hay
Prof. Dr.
Nong Lam University,
Ho Chi Minh City
VIET NAM
nguyenhay@gmail.com

Đo Thi Tam
Ph. D.
Thai Nguyen University of Technology
VIET NAM

Nguyen Tien Han
Ph. D.
University of Industry of Hanoi
VIET NAM

Summary

Agricultural Mechanization plays an important role in the production process that directly affects modernization of the agriculture in Vietnam. The higher the rate of operations being mechanized in production and post-harvest processing, the higher contribution level to job creation and income rising for labors in economic regions nationwide.

In this paper, the regression analysis methodology based upon Cobb-Douglas production function has been applied in evaluating the results on application of agricultural engineering and machinery and identifying its relationship with production growth rate. Up to present, the agricultural mechanization in Vietnam has got significant achievements. The mechanized rate on land preparation reaches up approx. 68-70%; of sowing, planting and transplanting: 35%; crops care: 60-80%; rice harvesting: 60%; etc., Based upon the studies and analysis of current status, the contents have been made and approaches have been recommended aiming to promote agricultural mechanization in the forth coming period.

Keywords: Agricultural mechanization, Cobb-Douglas production function, Agricultural engineering and Machinery investment.

Abstract

Agricultural mechanization plays an important role in the entire career of industrialization-modernization. Likewise, implementing mechanization and electrification in agriculture and rural areas is to contribute to the economic restructuring in agriculture. The 10th National Congress of the Communist Party emphasized: "...Put priority for the industrialization-modernization of agriculture towards mass production, linking processing industries to the market, carrying out mechanization-electrification so as to increase productivity and product quality compatible to characteristics of individual regions and localities...".

In order to contribute realizing the Resolutions of the Central Committee and the Government on "Renovating agriculture towards added value and sustainable development", it's necessary to review the practical investments, equipment and operation, thereby working out

Table 2 Mobile motive power machines by types and sizes invested/applied nation-wide Unit: piece

Big Tractor: 16,717		Medium size tractors: 221,293		2-wheel tractors: 294,569		Total: 532,579	
Ave. rate over 100 ha agri.'l households	Ave.rate over 100 ha agri.'l land	Ave. rate over 100 ha agri.'l households	Ave.rate over 100 ha agri.'l land	Ave. rate over 100 ha agri.'l households	Ave.rate over 100 ha agri.'l land	Ave. rate over 100 ha agri.'l households	Ave.rate over 100 ha agri.'l land
0.174	0.057	2.31	0.76	3.07	1.01	5.55	1.82

Source: General Statistical Office, 2014. Calculation Results and Summary of the Project, 2017

forecast on the level of agricultural engineering and equipment investment in the near future. Based on data and documents collected from the Census of Agriculture and Rural Development (2003-2013) together with forecasts from related experts, references on agricultural mechanization strategies from localities, relationship between "INPUT" factors and derived "OUTPUT" processes has been established by using Cobb-Douglas function; this helps to estimate the contribution level of agricultural mechanization sub-sector. Along with the data processing methodology over Cobb-Douglas function, energy balance method for individual mechanization operation in production and processing has been applied.

I. Current Status of Agricultural Engineering and Machinery Investment

By 2014, total output of the engines installed on the tractors used in field operations has increased by 85% over the figure of the previous 7 years; especially, there is a rapid increase of the engine output of tractors in the provinces of South-East, Central Highlands and Mekong River Delta, for use primarily in such farming operations as cultivation on the land for industrial crops and forest trees - which are the agricultural strengths of these regions. The following table summarizes the output invested rates (hp) of all types of mobile motive power sources being applied in 7 production regions (**Table 1**).

Table 1 Average output rate of mobile motive power sources being applied among region Unit: horse power, hp

No.	Regions	Total mobile output	Over 100 agri.'l labors	Over 100 ha agri.'l land
1	Red River Delta	1,032,668	33.78	107.3
2	Midlands & North Mountains	2,009,920	46.85	26.00
3	North Central Coast	1,035,124	30.46	25.51
4	South Central Coast	573,913	29.43	17.04
5	Central Highlands	2,265,857	70.34	46.99
6	Southeast	975,905	13.30	51.30
7	Mekong River Delta	6,100,000	96.75	179.03
Total		**13,993,387**	**45.84**	**64.74**

Source: General Statistical Office, 2014. Calculation Results and Summary of the Project, 2017

The above figures show that, the overall mobile motive power being applied reached up 13,993,387 hp, though the output rate in individual region is increasing, its increased output rate is not so high due to the area of arable land being expanded and put to exploitation:

- Output over 100 agricultural labors: 45.84 hp
- Output over 100 ha of agricultural land: 64.74 hp

Below is the summarized data on the invested amount of mobile tractors and their corresponding output rates, by types, being utilized among regions nation-wide (**Table 2**).

The sizes of tractors being used by economic sectors vary by their cultivated land area scale, generally ranging from ≤ 28 hp for medium-sized tractor and ≤ 17 hp for two-wheel sized tractors or power tillers. The localities are advised to select proper sizes and types of motive power equipment being appropriate to local soil characteristics and cultivated field scales.

Table 3 Summary of stationary motive power sources being applied among regions Unit: horse power, hp

No.	Regions	Total stationary motive power output	Average output per 100 agric.'l labors	Average output per 100 ha of agric.'l land
1	Red River Delta	963,612	31.52	100.12
2	Midlands & North Mountains	980,460	22.85	12.68
3	North Central Coast	338,336	9.95	8.34
4	South Central Coast	321,232	16.47	9.54
5	Central Highlands	1,204,770	37.40	24.98
6	Southeast	999,825	13.62	52.56
7	Mekong River Delta	425,963	4.40	12.50
Total		**5,234,198**	**19.46**	**31.53**

Source: General Statistical Office, 2014. Calculation Results and Summary of the Project, 2017

*Excluding outputs from those engines installed on boats used for waterways transportation

About Stationary Motive Power

Due to increased needs of power sources for the operations on preliminary processing, preservation, water supply for crops, etc., a large amount of stationary motors has been invested by economic-sectors (electric motor, gasoline & diesel engine) with an overall output up to 5,234,198 hp nation-wide at a rate of 19.46 hp per 100 agricultural labors and 31.53 hp per 100 ha of agricultural land in which, most of motive power sources have been invested in the provinces of Red River Delta, Midlands & North Mountains, Central Highlands and Southeast (**Table 3**).

The total of both mobile and stationary motive power outputs being applied nation-wide is 19,277,585 hp with an average of 96.27 hp/100 ha of agricultural land and 65.3 hp/100 agricultural labors concentrating mostly in Central Highlands and Mekong River Delta - the localities where large production of commodities is existing (**Table 4**).

Machinery Attached to Motive Power Sources Used for Production and Processing of Agro-forestry Products

Investment rate of agricultural machinery and equipment for use in production and processing of agro-forestry products nation-wide is presented in **Table 5**.

It is seen that the amount of machinery and equipment applied for sowing, aqua-feed processing, combine harvesting is of at lowest level. The economic sectors generally concentrate their investment in the operations of water pumping, rice threshing, agro-forestry products processing - those which could contribute to ensuring crops productivity, generating employment and incomes for farmers.

Experiences Attained From the Development of Motive Power Sources and Their Attached Equipment for Production and Post-harvest Processing Activities

In the context of limited budget, the economic sectors are required to promote internal investment resources for effectively use their motive power sources and attachments so as to attain an effective model in production, trading based upon effectively application of their engineering machinery resources in their localities.

The above big evolvement was attained in the development of industries, small and craft industries, industry of agro-forestry products processing in close combination with deployment of concentrated-growing zones, expansion of consuming markets... is good references for the production regions in the country. This helps to exploit potentials in investment of equipment and machinery from economic-sectors and attract investors from foreign countries that, in turn, provide favorable conditions for the agriculture sector to develop much more mechanization models appropriate to regional production conditions.

The level of mechanized operations differs by regions depending on regional socio- economic conditions, crops and soil characteristics, water resources, etc. If adequate concerns from authorities at all level could be given to the engineering sector in services of agricultural production, crops and livestock productivity will increase, the labor transaction condition in agriculture and rural areas will be more favorable, from which farmers' incomes and living will be gradually improved.

On the Machinery Operation

Among the machinery being invested, tractor has been used prin-

Table 4 Summary of invested motive power output nation-wide

Unit: horse power, hp

No.	Regions	Total motive power output	Average output per 100 agric.'l labors	Average output per 100 ha of agric.'l land
1	Red River Delta	1,996,280	65.3	207.42
2	Midlands & North Mountains	2,990,380	69.7	38.68
3	North Central Coast	1,373,460	40.41	33.85
4	South Central Coast	895,145	45.9	26.58
5	Central Highlands	3,470,627	107.74	71.97
6	Southeast	1,975,730	26.92	103.86
7	Mekong River Delta	6,525,963	101.15	191.53
	Total	**19,227,585**	**65.30**	**96.27**

Source: General Statistical Office, 2014. Calculation Results and Summary of the Project, 2017

Table 5 Summary of stationary motive power sources being applied among regions

Unit: Piece

No.	Machine/Equip.'t	Quantity	Average/100 agric.'l households	Average/100 ha agric.'l land
1	Rice seeder, machine/implement	25,770	0.15	0.08
2	Insecticide sprayer	580,568	3.42	1.84
3	Water pump	2,169,868	12.76	6.86
4	Combine harvester	14,530	0.085	0.046
5	Windrow-type rice reaper	66,595	0.39	0.21
6	Paddy threshing machine	265,978	1.56	0.84
7	Dryer	63,639	0.37	0.20
8	Food processing machine	248,746	1.46	0.79
9	Wood processing equip.'t	277,021	1.63	0.88
10	Aqua-feed processing equip.'t	6,580	0.039	0.021
11	Animal-feed processing equip.'t	71,987	0.42	0.23

Source: General Statistical Office, 2014. Calculation Results and Summary of the Project, 2017 cipally for land preparation, in-field transportation (4-wheel medium-sized tractors and 2-wheel power tillers, small tractors) following the procedures as: ploughing, rotary tilling, soil puddling for summer crop, or, soil tilling combined with leveling. The cost for land preparation differs by region. If payment fee is based on paddy, the cost is roughly about 180-200 kg paddy/ha in general but it is lower if land is done by puddling plus leveling. To do land preparation ready for paddy transplanting, the total cost will be within 500.000-1.000.000 VNĐ/ha.

In addition to soil tillage, the tractor has been used in transportation of agricultural products and fertilizer, etc. The mechanization of land preparation reaches a high rate in the country. The table below summarizes the mechanization rates in land preparation in 7 production regions nation-wide.

Results in land tillage mechanization show that (**Table 6**), those regions where investment rate of motive power is high (RRD and MRD), mechanization in land preparation is also high, the highest level attained ranging from 84.7% to 96.14%. The Northern Mountains provinces are still facing difficulties and constraints in applying machine for land preparation.

II. Application of Stationary Motive Power Sources in Production, Preservation and Preliminary Processing of Agricultural Products

2.1. Utilization of Stationary Motive Power in Water Pumping Operation

According to preliminary statistical data, the present irrigation projects under exploitation include: 5,656 reservoirs; 8,512 dams; 5,194 electric pumping stations and irrigation culverts of different types together with other 10,698 projects. Over 23,000 dikes for flood prevention in early Autumn rice crop in Mekong Delta region and thousands of kilometers of canals and ditches with attached projects have been also constructed and exploited.

On water irrigation, supply and drainage: Presently, there are 75 big irrigation projects nation-wide together with 800 lakes and dams of large and medium sizes, over 3,500 lakes of over 1 million m^3 water capacities and dams of over 10 m high, more than 5,000 irrigation culverts of large sizes, over 10,000 pumping stations of big and medium sizes at a total of 24.8 million m^3/h capacities and thousands of other irrigation projects of medium and small sizes. The above system has a total capacity in providing direct irrigation for 3.45 million ha; creating sources in water supply for 1.13 million ha; 1.4 million ha in drainage; prevention of salty penetration for 0.87 million ha, improvement of 1.6 million ha of cultivated land being acidity infect-

Table 6 Land under annual crop planting being done by machine

No.	Regions	Annual crop planting area			Of which: rice planting area		
		Total, ha	Mechanized area, ha	Ratio, %	Total, ha	Mechanized area, ha	Ratio, %
	Country total	**7,232,979.20**	**4,753,536.80**	**65.72**	**4,107,310.40**	**3,499,935.10**	**85.21**
1	Red River Delta	632,121.95	599,779.30	94.88	564,667.46	542,852.22	96.14
2	Midlands & North Mountains	1,254,976.19	361,443.51	28.80	533,574.91	276,017.84	51.73
3	North Central Coast	847,534.66	462,633.28	54.59	450,879.76	360,805.65	80.02
4	South Central Coast	628,936.50	365,745.30	58.15	311,185.80	218,577.90	70.24
5	Central Highlands	1,201,124.70	759,446.60	63.23	268,074.50	213,680.70	79.71
6	Southeast	533,000.90	395,816.40	74.26	234,877.80	214,666.70	91.40
7	Mekong River Delta	2,135,284.30	1,808,672.40	84.70	1,744,050.20	1,673,334.10	95.95

Source: General Statistical Office, 2014. Results from the calculation and data analysis by the author, 2017

Table 7 Summary of areas under Irrigation and Drainage (I&D) system

No.	Regions	Land under annual crops planting			Of which: land under rice		
		Total, ha	Mechanized area, ha	Ratio, %	Total, ha	Mechanized area, ha	Ratio, %
	Nation-wide	**7,232,979.20**	**4,172,522.90**	**57.69**	**4,107,310.40**	**3,358,620.10**	**81.77**
1	Red River Delta	632,121.95	604,520.97	95.63	564,667.46	543,156.34	96.19
2	Midlands & North Mountains	1,254,976.19	434,813.81	34.65	533,574.91	357,279.74	66.96
3	North Central Coast	847,534.66	504,583.42	59.54	450,879.76	344,792.19	76.47
4	South Central Coast	628,936.50	356,750.10	56.72	311,185.80	175,501.90	56.40
5	Central Highlands	1,201,124.70	281,749.40	23.46	268,074.50	175,348.57	65.41
6	Southeast	533,000.90	258,272.90	48.46	234,877.80	171,011.90	72.81
7	Mekong River Delta	2,135,,284.3	1,731,832.30	81.11	1,744,050.20	1,591,529.50	91.25

Source: General Statistical Office, 2014. Results from the calculation and data analysis by the author, 2017 ed. The area under rice, vegetables, food and short-term industrial crops being irrigated has been constantly increasing over time.

On irrigation equipment investment: An amount of 2,169,868 pumping units of of all types were supplied nation-wide by the end of 2014, increased by 1.67 times in number as compared with that in 7 years ago. In average, 6.85 and 0.3 pumps have been invested over 100 hectares of agricultural land and of annual crops planting area, respectively (**Table 7**).

On the rate of mechanization in other operations:

- ***Crops care***: mechanization on crops care has been carried out over 60% of planted land area.

- ***Drying and preservation of agro-products are still experiencing at low level; in drying***: only 40-55% of total food output that needs to be dried has been done, attaining invested level of 0.53 dryers per 100 tons of food. Just only 7 million tons of rice have been under preservation and storage nation-wide; the stores for preservation are still lacking.

- ***Processing of agro-products and foodstuffs***: Processing of rice, animal feed, products from perennial crops like rubber, coffee, etc. has been carried out with high-tech processing lines and modern equipment. Preliminary processing of agro-products is developing at a rapid speed in quantity based on equipment and technologies of small and medium scales, attaining a rate of 1.5 machines per 100 households in food processing and roughly 0.5 machines in animal feed processing. Although the processing establishments are of small households or inter-households scales, their products have initially gained confidence in the markets.

2.2. On the Sector of Mechanical Manufacturing of Machinery for Agriculture and Rural Areas

Manufacturing of machinery for agriculture and rural areas is an urgent need at the present stage that actively affects the modernization process in agriculture, and contributes to increased international competition of the sector. Therefore, concerns should be given to the following issues for the sector development:

+ Conditions of production (crops, livestock, etc.);
+ Technological progresses;
+ Socio-economic development level of individual regions.

Presently, the two corporations principally engaged in mechanical manufacturing of machinery include: Vietnam Engine and Agricultural Machinery Corporation (VEAM) and Mechanization-Electrification-Construction Corporation - Joint Stock Company (AGRIMECO-JSC).

In addition to the two above big Corporations, there still have over 30 Mechanical Establishments under Ministry of Agriculture and Rural Development (MARD); more than 70 Enterprises and private Establishments throughout the country involved in production of agricultural machinery and equipment in services of agriculture and rural areas. The Industry and Trade Sector (the industrial sector specialized in manufacture of agricultural machinery, industrial machines in services of agriculture and rural areas) under Ministry of Trade and Industry (MOIT) is possessing 10 establishments: S.VEAM (in charge of fabricating engines, tractors), Tran Hung Dao Mechanical Engineering, NAKYNO (Tan Binh District, HCM City), Precision Mechanical Manufactory (Hanoi), FOMECO (Pho Yen Town, Thai Nguyen), etc.

On the domestic manufacturing capacity: The table below presents status about manufacturing capacity and the capability of domestic enterprises in meeting home demands on principal equipment till 2012 (**Table 8**) (based upon the Survey conducted by Ministry of Industry and Ministry of Agriculture and Rural Development).

Based upon the strategical orientation of the Government on developing mechanical sector, the economic-sectors have gradually made investment of equipment and associated technologies in production and post-harvest processing.

**** Constraints***: Farmers'incomes are still low leading to lack of capital in purchasing machinery, espe-

Table 8 Manufacturing capacity and the capability of domestic enterprises in meeting home demands on principal equipment till 2012

Products	Capability to meet the demand, %	Products	Capability to meet the demand, %
Gasoline and diesel engines:		Combine harvester	60
Diesel engine, 80 hp (incapable in manufg.)	50	Milling, polishing machines	100
Diesel engine, ≤ 25 hp		Equipment lines:	
+ 1 cylinder (cap. in manufg.: 80%)		+ Sugar, sugarcanes	90
+ 2 cylinders (incapable).		+ Animal feed	85
Tractors		+ Rubber latex processing	100
+ 4-wheeled type, 25 hp (cap. in manufg.: 80%)	50	+ Coffee processing	100
+ Crawler type, 75 hp (incapable)		Wood processing equipment (only those of low capacity and quality, still not meeting criteria for export)	100
+ 2-wheeled type, ≤ 18 hp (cap. in manufg.: 80%)	100		
		Aquaculture equipment	100
Electric motor	90	**Cultivating & water pumping machines**	100

cially those of high-tech processing lines. The consumer markets of agricultural engineering and machinery are still limited, especially, those provinces in Midlands and Northern Mountains regions in Central provinces.

**** Sector characteristics***: The capital as required in initial investment of the sector is high while derived profits are low, causing less attractive in calling foreign investment projects. Also, the sectoral production establishments are of small scales with self-sufficient operation, lack of specialization and inter-units cooperation, leading to low production investment efficiency. The leadership role of a professional Association has not worked effectively.

III. Estimation of Impact of Agricultural Mechanization on Agricultural Production in Vietnam

The aim in investing equipment and machinery in services of production and processing of agro-forestry products is, to contribute mainly to economic growth promotion.

In order to attain effectively economic growth, the following issues need to be considered:

+ Growth in means of production represented by energy being consumed;
+ Growth in labor resources (including technical labors);
+ Growth in science-technology and renovation of macro-management policy.

The first two components out of the three is the key one for the improvement of internal capacity to contribute to economic growth; these are factors of active and dynamic role.

To evaluate the effectiveness on investment of agricultural engineering equipment in pre-post harvest operations as well as in crops irrigation, the economists often use models of production function that reflect the relationship between the "output" and the selected input resources for the production process. Though other different methods could be used, the Cobb-Douglas production function has been selected in this study.

$Y = AX_1^{\beta 1}X_2^{\beta 2}X_3^{\beta 3}$ .....(1)

In which: A- Coefficient of freedom representing impact of the remaining factors in food production, $A = EXP(C)$;

Y: SLLTCH: Food grain output

X_1: DTLTCH: Factor representing food grain acreage;

X_2: LDNN: Factor representing agricultural labor;

X_3: TBMM: Factor representing machinery & equipment investment in production mechanization;

β_1; β_2; β_3: Exponents - regression coefficients in equations (2) or (3).

C: Coefficient in the program based on Eviews software.

Taking logarithm of the production function (1), the following equation is obtained:

$Ln(Y) = ln(A) + \beta_1{*}ln(X_1) + \beta_2{*}ln(X_2) + \beta_3{*}ln(X_3)$ .....(2)

Due to the Eviews software characteristics, the coefficient of freedom C is still not in logarithmic form, so, equation (2) takes the form:

$Ln(Y) = C + \beta_1{*}ln(X_1) + \beta_2{*}ln(X_2) + \beta_3{*}ln(X_3)$ .....(3)

In which: $ln(A) = C$ or $A = e^C$

1) Red River Delta (RRD)

Dependent Variable: Y
Method: Least Squares
Date: 23/9/16 Time: 11:45
Sample: 1995 2014
Included observations: 20

Variable	Coefficient	Std. Error	t-Statistic	Prob.
X_1	0.570564	0.157278	3.627738	0.0023
X_2	0.274784	0.111772	2.458437	0.0257
X_3	0.096022	0.021148	4.540357	0.0003
C	1.486708	1.895688	0.784258	0.4443

R-squared, R2	0.974694	Mean dependent var.	8.818978
Adjusted R-squared, R	0.969950	S.D. dependent var.	0.067703
S.E of regression	0.011736	Akaike info. criterion	-5.875393
Sum squared resid. (RSS)	0.002204	Schwarz criterion	-5.676246
Log Likelihood	62.75393	Hannan-Quinn criterion	-5.836517
F-statistic	205.4243	Durbin-Watson stat.	2.266730
Prob. (F-statistic)	0.000000		

Fig. 1 Variation of annual food output in RRD during past recent 20 years

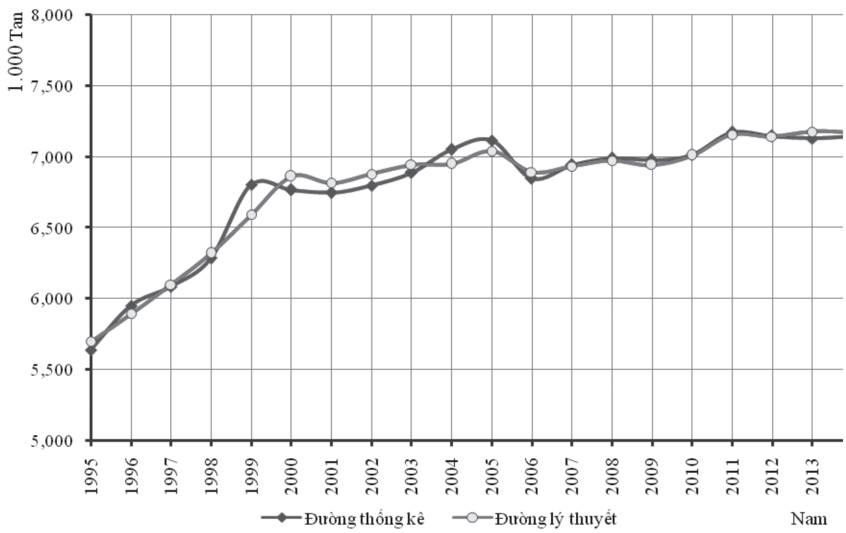

3.1. Results from data processing for several regions

1) Red River Delta (RRD)

$Ln(Y) = 1.487 + 0.571*Ln(X_1) + 0.275*Ln(X_2) + 0.096*Ln(X_3)$.....(4)

Equation (1) can be written in the canonical form:

$Y = 4.4225*X_1^{0.57056}X_2^{0.27478}X_3^{0.09602}$

In which: $A = e^{1.486708} = 4.4225$

Results from preliminary testing of statistical hypotheses shows that the predicted model based upon Cobb-Douglas production function is appropriate.

The graph below shows the fitness level between the two curves - one obtained from theoretical calculation and the other, from statistical data of annual food output in Red River Delta - is rather high (**Fig. 1**).

The variation of annual food output in Red River Delta by years is presented on the following graph:

2) Midlands and Northern Mountains Region

From Eq. (3), it is possible to write the regression function as follows:

$Ln(Y) = \mathbf{0.0129} + \mathbf{0.30525}*Ln(X_1) + \mathbf{0.3236}*Ln(X_2) + 0.4418*Ln(X_3)$ .....(5)

The equation can be written in the canonical form:

$Y = 1.01289*X_1^{0.30525}X_2^{0.32359}X_3^{0.4418}$ .....(6)

In which: $A = e^{0.012811} = 1.01289$

Results from preliminary testing of statistical hypotheses shows that the predicted model based upon Cobb-Douglas production function is appropriate.

The graph below shows the fitness level between the two curves - one obtained from theoretical calculation and the other, from statistical data of annual food output of the provinces in Midlands and Northern Mountains Region - is rather high (**Fig. 2**).

Preliminary test of statistical hypotheses:

- The t-Statistic value obtained from the table $|t\text{-Statistic}| > T_{(16;0.025)} = 2,119$ and the $|Prob| < 0.05$ is at the significance level of 5% indicating the regression coefficients β_1, β_2 and β_3 are different than 0, indicating that, factors X_1, X_2 and X_3 affect food production Y.

- At significance level of 5%, the F statistical value = 4,317.275 > $F_{0.05(k-1;n-k)}$ = 3.239 indicating the above predicted model based upon Cobb-Douglas production function is appropriate.

2) Midlands and Northern Mountains Region (MNM)

Dependent Variable: Y
Method: Least Squares
Data processing method: As above-mentioned
The results obtained are represented on the Table below.

Variable	Coefficient	Std. Error	*t*-Statistic	Prob.
X_1	0.305248	0.119098	2.562991	0.0208
X_2	0.323591	0.145799	2.219437	0.0413
X_3	0.441797	0.027087	16.31031	0.0000
C	0.012811	1.083340	0.011825	0.9907

Fig. 2 Variation of annual food output of the provinces in Midlands & Northern Mountains region during 1995-2014

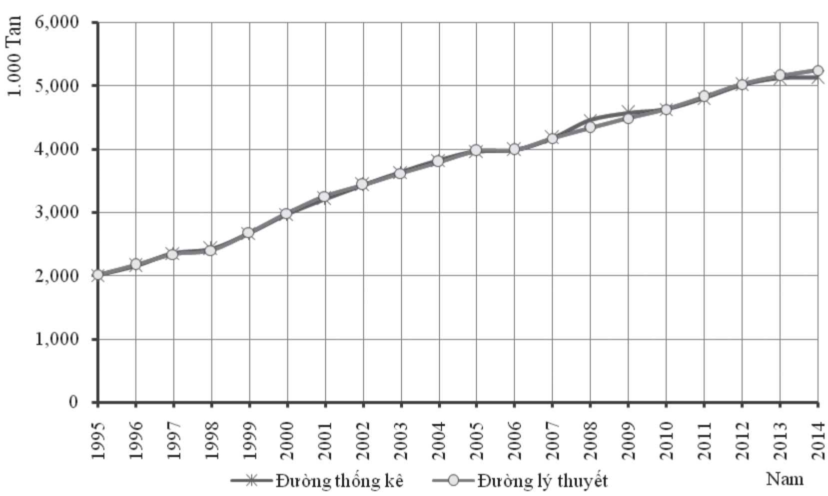

3) South Central Coast Region

From the equation as indicated above, it is possible to write the regression function as follows:

$Ln(Y) = 0.0036 + 0.5264*Ln(X_1) + 0.4135*Ln(X_2) + 0.1775*Ln(X_3)$ .....(7)

The equation can be written in the canonical form:

$Y = 1.00359*X_1^{0.52642}X_2^{0.41348}X_3^{0.17746}$ .....(8)

In which: $A = e^{0.00359} = 1.00359$

Results from preliminary testing of statistical hypotheses shows that the predicted model based upon Cobb-Douglas production function is appropriate.

The graph below shows the variation of annual food output in South Central Coast during past recent 20 years (1995-2014): **Fig. 3**.

From the graph it is seen that food output increases by time and there is a relevant fitness between theoretical calculation result and that obtained from statistical data.

4). Central Highlands

From the equation as indicated, the regression function can be written as follows:

$Ln(Y) = -1.538 + 0.533*Ln(X_1) + 0.2796*Ln(X_2) + 0.467*Ln(X_3)$ .....(9)

Or: $Y = 0.215*X_1^{0.533}X_2^{0.28}X_3 0.^{467}$ .....(10)

In which: $A = e^{-1.3816} = 0.215$

Results from preliminary testing of statistical hypotheses show that the predicted model based upon Cobb-Douglas production function is appropriate.

Again, the graph shows that, food output increases by time (1995-

Table 9 Contribution levels of production factors

Type	RRD			MNM			SCC			CH			MRD		
	GR, %	RC	CL, %	GR, %	RC	CL, %	GR, %	RC	CL, %	GR, %	RC	CL, %	GR, %	RC	CL, %
Food production	1.28														
Land, x_1	-0.53	0.571	-	2.03	0.305	12.13	-0.12	0.526	-	4.69	0.533	28.82	1.58	0.527	22.44
Agri. labor, x_2	2.28	0.275	48.96	1.40	0.324	8.87	1.25	0.413	18.13	3.91	0.280	12.60	3.15	0.114	9.70
Mechanization, x_3	10.83	0.096	81.23	9.61	0.442	82.99	13.71	0.177	85.39	11.56	0.467	62.31	8.06	0.337	73.14
Total		0.941	130.19		1.071	103.99		1.117	103.52		1.280	103.73		0.978	105.28

Note: GR = Growth rate, RC = Regres. coeff, CL = Contrib. level
Sources: Statistical data from related localities, 2014. Results from Author's calculation, 2017

2014) as presented on the following figure (**Fig. 4**).

The above graph shows that there is a relevant fitness between theoretical calculation result and that from statistical data.

5) Mekong River Delta (MRD)

From the above equation, the relationship between "Input" factors and food production "Output" could be written under the following form:

$$Ln(Y) = 1.373 + 0.5275*Ln(X_1) + 0.1142*Ln(X_2) + 0.3368*Ln(X_3) \quad .....(11)$$

Or: $$Y = 3.94736*X_1^{0.52745}X_2^{0.11422}X_3^{0.3368} \quad .....(12)$$

In which: $A = e^{1.373048} = 3.94736$

Results from preliminary testing of statistical hypotheses show that the predicted model based upon Cobb-Douglas production function is appropriate.

The graph below shows the progression of annual food output in MRD during past recent 20 years (1995-2014): (**Fig. 5**)

The above graph shows a rather close fitness between the result obtained from theoretical calculation and that derived from statistical data with a very low deviation level.

Detailed results on the contribution levels of input factors on food grain output at the provinces in five typical socio-economic regions (as presented below) are presented in **Table 9**, including:

+ Red river delta (RRD)
+ Midlands & Northern Mountains (MNM)
+ South Central Coast (SCC)
+ Central Highlands (CH)
+ Mekong river delta (MRD)

Remarks:

The table below presents the results as attained based upon data collected and calculation regarding the contribution levels of factors to agricultural production in related regions. Data from the table are useful as references for the comparison, selection for an effective investment of machinery and equipment adaptive to local conditions (**Table 10**).

The above results as obtained show that:

+ Land acreage for food plants growing affects greatly food production, i.e. machinery and equipment are under need at those localities where land area is available for carrying out mechanization of cultivating operations, especially, in the provinces of Midlands & Northern Mountains and Central Highlands.

+ The free coefficient representing influence levels of the factors on applying technical progresses, implementing mechanisms and policies relating to agricultural engineering sector in the provinces of Midlands and South Central Coast is of small

3) South Central Coast Region (SCC)

Dependent Variable: Y
Method: Least Squares
Included observations: 20
The results obtained are represented on the Table below

Variable	Coefficient	Std. Error	*t*-Statistic	Prob.
X_1	0.526423	0.242676	2.169239	0.0455
X_2	0.413482	0.194255	2.128556	0.0492
X_3	0.177464	0.015144	11.71820	0.0000
C	0.003588	2.126905	0.001687	0.9987

Fig. 3 Variation of annual food grain output (1995-2014)

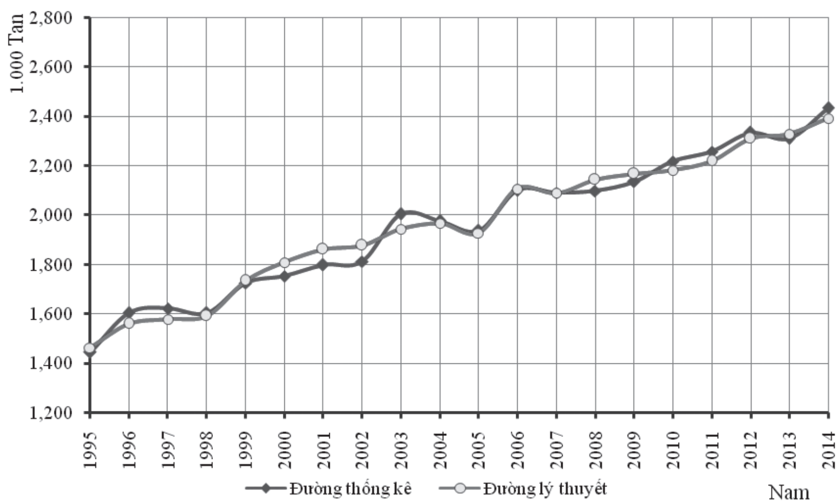

Table 10 Contribution levels of production factors

Influ. factors	RRD	MNM	SCS	CH	MRD
1 X_1 (DTLTCH)	0.571	0.305	0.526	0.533	0.527
2 X_2 (LDNN)	0.275	0.324	0.413	0.280	0.114
3 X_3 (TBMM)	0.096	0.442	0.177	0.467	0.337
4 A (Coeff.)	4.423	1.013	1.004	0.215	3.947
Total of X_i coeffs.	0.941	1.071	1.117	1.280	0.978

Note: x_1 = factor regarding land acreage for food plants growing; x_2 = factor regarding agricultural labor; x_3 = factor regarding equipment and machinery investment for mechanization; x_i = coefficient of regression function being calculated for related regions

number, proving that those above influences are still limited and the local authorities and adequate concern has not been given to the issue of raising labor productivity in production.

+ The three coefficient totals of individual regression functions for three regions of Central Highlands (1.280), South Central Coast (1.117), and Midlands & Northern Mountains (1.071) are all greater than 1; showing that, in order to ensure raising food output in the three above regions, investment of "INPUTS" factors need to be enhanced.

Conclusion - Recommendations

1. In general, the investment rates of motive power for agricultural production (in which, over 19.22 mil. hp invested for food plants production; 96.27 hp, over 100 ha of agricultural land, and 65.3 hp over 100 agricultural labors, averagely) are of high levels. With the active dynamism of the economic-sectors, mechanization of land preparation has reached from 65.7% to 85.2%; land area under irrigation and drainage from 58% to 82%, this shows initial efforts of Vietnam in the condition that the country is predicted as one among the few countries most vulnerable by climate change globally.
2. Although farmers' incomes are still limited, the above investment rates of equipment and machinery for production have affected production of the provinces in Midlands &Northern Mountains and Central Highlands (as shown by their influencing coefficients of 0.442 and 0.467, respectively). This proves the linkage among "INPUTS" factors ensuring raised food output is of practical significance with high scientific contents.
3. The model based on comprehensively calculating will provide a reference basis for related sectors to set up mechanisms and policies for developing mechanization in the process of agricultural modernization.

Hanoi, April 2017

4) Central Highlands (CH)

Dependent Variable: Y
Method: Least Squares
Data processing method: As above-mentioned
The results obtained are represented on the Table below.

Variable	Coefficient	Std. Error	*t*-Statistic	Prob.
X_1	0.532677	0.058398	9.121426	0.0000
X_2	0.279586	0.114796	2.435500	0.0269
X_3	0.467250	0.040893	11.42609	0.0000
C	-1.538158	0.658396	-2.336220	0.0328

Fig. 4 Variation of annual food grain output by time in Central Highlands (1995-2014)

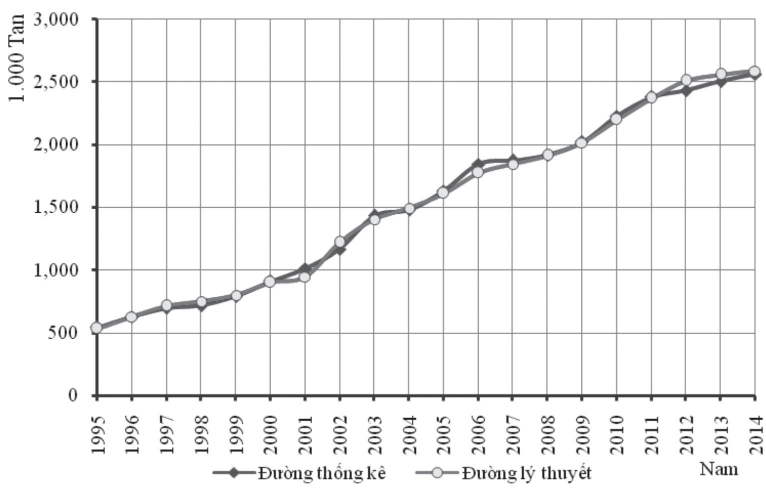

REFERENCES

1. General Statistical Office (2013). Survey Results on Agriculture, Rural Areas and Fishery of Vietnam from 2001 to 2011, published in 2013. Statistical Publishing House. Documents from Provincial Statistical Offices Surveys in 7 production regions.
2. Institute for Economic and Water Management (IWEM), Ministry of Agriculture and Rural Development. Current Status of Irrigation System in Vietnam. (Summary Documents, 2016).
3. Vietnam Engine and Agricultural Machinery (VEAM). Results on Implementation of Production Plan of Agricultural Engineering and Machinery for Agriculture and Rural Areas.

4. Pham Van Lang (2015). Evaluation Report on Current Status on Investment and Operation of Agricultural Engineering in Production and Preliminary Processing of Agro-Forestry Products in service of New Rural Construction Program in the Production Regions. Development Orientation up to 2025. The Report was presented at the "Conference on Promoting Mechanization in Agriculture to Create Driving Force for the Restructuring of Agriculture Sector" held by Ministry of Agriculture and Rural Development on 18 June, 2015 in Hanoi.
5. Pham Van Lang, Bui Quang Huy, Đo Thị Tam and Pham Hong Son. Evaluation of Agricultural Mechanization Level in Agricultural Production Areas. AMA-Japan, 3/2011.
6. Pham Van Lang. Development Orientation of Agricultural Engineering and Establishing Models for Application of Technical Progresses in the Provinces of Gia Lai and Hoa Binh. Scientific Report, 2016.
7. References Documents: Ly Hanh, Bach Le, Ma Thanh Lam, Chung Van Tai, Duong Van Dinh (2005). Analysis and Forecasting the level of Agricultural Machinery Investment in 2005 - 2015 in Cat Lam Province. Mechanized Agriculture Journal, 11 May, 2005 (translated by Vo Thanh Binh).

Other related References…

■■

5) Mekong River Delta (MRD)

Dependent Variable: Y
Method: Least Squares
Included observations: 20
The results obtained are represented on the Table below

Variable	Coefficient	Std. Error	*t*-Statistic	Prob.
X_1	0.527446	0.079746	6.614112	0.0000
X_2	0.114216	0.028582	3.996117	0.0010
X_3	0.336796	0.018087	18.62072	0.0000
C	1.373048	0.584504	2.349083	0.0320

Fig. 5 Variation of annual food output in MRD during past recent 20 years

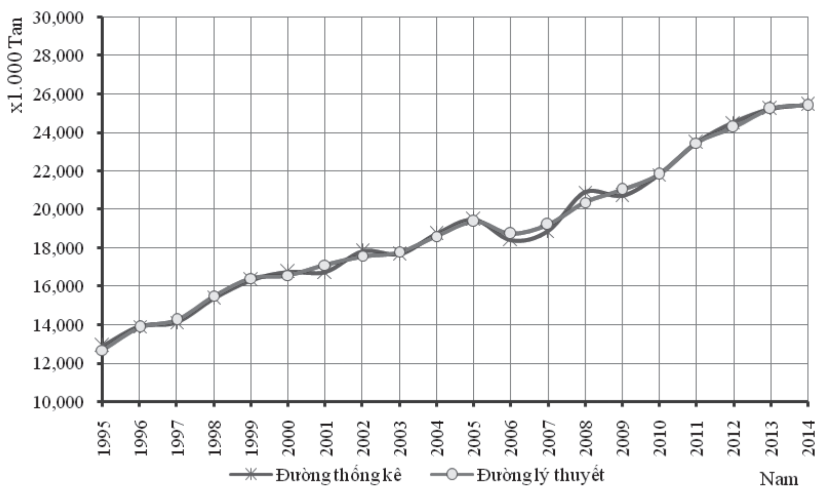

Co-operating Editors


B Kayombo


M F Fonteh


S A Ndindeng


S E Abdallah


A A K El Behery


Ahmad Addo

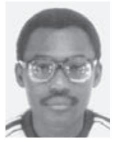
R J Bani


I K Djokoto


A N GITAU


D K Some


K Houmy


O A Oyelade


Umar B Bindir


J C Igbeka


E U-Odigboh


K C Oni


U L Opara


N G Kuyembeh


A H Abdoun


A B Saeed


A I Khatibu


S Tembo


H A Cetrangolo


I de A Nääs


A E Ghaly


E J Hetz


M A L Roudergue


R Aguirre


O Ulloa-Torres


Y M Mesa


P P Rondon


S G C Magaña


H Ortiz-Laurel


A I Luna Maldonado


G C Bora


M R Goyal


A K Mahapatra


S M Farouk


Daulat Hussain


M A Mazed


R Ali


Chetem Wangchen


M A Basunia


Minzan Li


Xiwen Luo


S M Ilyas


Surya Nath


Indra Mani


C R Mehta


A M Michael


B S Pathak


V M Salokhe

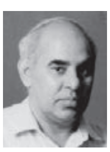
G Singh


S D Kulkarni


S R Verma


P Soni


Kamaruddin Abdullah


M Behroozi-Lar


Saeid Minaei


A Mahdavian


A M Abdul-Munaim


H Hasegawa


B A Snobar


J H Chung


In-Bok Lee


M Z Bardaie


Enkhbayar Gonchigdorj


M P Pariyar


H P W Jayasuriya


Alamgir A Khan


A Q A Mughal


M S Mirjat


N A Abu-Khalaf


R M Lantin


R P Venturina


S A Al-Suhaibani


A M S Al-Amri


S G Illangantileke


S F Chang


Suming Chen

Kamaruddin Abdullah
The Graduate School/Renewable Energy, Darma Persada University, Jl. Radin Inten II, Pondok Kelapa, East Jakarta, 13450, INDONESIA. TEL+64-21-8649051, kabdullah0997@yahoo.com

Mansoor Behroozi-Lar
Prof., Emeritus Tehran Uni. Agr. Eng., Ph. D., Jalal All Ahmad Nasim St. Nasim Danesh Complex Block #35, second floor Tehran, IRAN. Behroozil@Yahoo.com

Saeid Minaei
Assoc. Prof., Dept. of Agr. Machinery Eng., Tarbiat Modarres Univ., P.O.Box 14115-336, Tehran, IRAN. TEL+9821-44180537, minaee@modares.ac.ir

Alireza Mahdavian
Assistance Prof., Department of Biosystems Engineering, Tarbiat Modares Univ., P.o.Box 14115-336, Tehran -14977-13111, IRAN. TEL +98-912-3346506, al.mahdavian@gmail.com; a.mahdavian@modares.ac.ir

Ali Mazin Abdul-Munaim
Assistant Prof., Dept. of Agril. Machines and Equipments, College of Agric., Univ. of Baghdad, IRAQ. TEL+964-778-4561, old2a3y@yahoo.com

Hideo Hasegawa
Assoc. Prof., Institute of Science and Technology, Niigata University, 8050 Ikarashi 2-no-cho, Nishi-ku, Niigata 950-2181 JAPAN. +81-25-262-6690, hsgw@agr.niigata-u.ac.jp

Bassam A. Snobar
Prof., Univ. of Jordan, Faculty of Agriculture, Amman 11492, JORDAN. snobar@ju.edu.jo

Jong Hoon Chung
Prof., Dept. of Biosystems & Biomaterials Science and Eng., College of Agril. and Life Sciences, Seoul National Univ., Bldg 200 Rm 2216 1 Gwanangno, Gwanak-Gu, Seoul, 151-742, KOREA. TEL+82-2-880-4601, jchung@snu.ac.kr

In-Bok Lee
Prof., Laboratory of Aero-Environmental & Energy Engineering (A3EL), Dept. of Rural Systems Eng., College of Agril. & Life Sciences, Seoul National Univ., San 56-1, Shillim-dong, Gwanak-gu, Seoul-city, KOREA. TEL+82-2-880-4586, iblee@snu.ac.kr

Muhamad Zohadie Bardaie
Prof., Dept. of Agril. and Biosystems Eng., Univ. Putra Malaysia, 43400 upm, Serdang, Selangor, MALAYSIA. TEL+60-3-8946-6410

Enkhbayar Gonchigdorj
Director, School of Eng. & Technology, Mongolian University of Life Sciences, Ulaanbaatar, Zaisan, 17024, MONGOLIA. TEL+60-976-11-341554 enkhbayar@muls.edu.mn

Madan P. Pariyar
Consultant, Rural Development through Selfhelp Promotion Lamjung Project, German Technical Cooperation. P.O. Box 1457, Kathmandu, NEPAL.

Hemanatha P. W. Jayasuriya
College of Agril. and Marine Sciences, P.O. Box 34, PC 123Al-khod, Muscat Sultanate, OMAN. TEL+968-2414-1223, hemjay@squ.edu.om

Alamgir A. Khan
Research Engineer, Agricultural Mechanization Research Institute, Multan, PAKISTAN. alamgirakhtar@hotmail.com

A. Q. A. Mughal
Research Professor, Greenwich Univ., DK-10, Street 38t, Darakshan, DHA Phase-6, Karachi-75500, PAKISTAN. dr.aqmughal@greenwich.edu.pk

Muhammad Saffar Mirjat
Dean, Faculty of Agril. Eng., Sindh Agriculture Univ. Tandojam, PAKISTAN. TEL+92-221653160, drmirjat@hotmail.com

Nawaf A. Abu-Khalaf
Assistant Prof., Palestine Technical Univ. -Kadoorie (PTUK), P.O.Box 405, Hebron, West Bank, PALESTINE. TEL+972-2-2227-846/7, nawafu@hotmail.com

Reynaldo M. Lantin
Retired Professor, College of Engineering and Agro-Industrial Technology, University of the Philippines Los Banos, College, Laguna 4031, PHILIPPINES. TEL+63-49-536-2792, reylantin@gmail.com

Ricardo P. Venturina
PHILIPPINES.

Saleh Abdulrahman Al-suhaibani
Prof., Agril. Eng. Dept.,College of Agric., King Saud Univ., P.O. Box 2460 Riyadh 11451, SAUDI ARABIA. salsuhaibani@gmail.com

Ali Mufarreh Saleh Al-Amri
Prof., Dept. of Agril. Systems Eng., College of Agril. Sciences & Food, King Faisal Univ., P.O.Box 55035, Al-Ahsa, 31982 SAUDI ARABIA. aamri@kfu.edu.sa

Sarath G. Illangantileke
Prof., Sarath Ilangantileke, Consultant in Agric Engineering, Mechanization and Education, 4/567 Victoria Range Bungalows, Kengalla, SRI LANKA. sageilan@gmail.com

Sen-Fuh Chang
Adjunct Prof., Dept. of Bio-Industrial Mechatronics Eng., National Taiwan Univ., 136 choushan Road, Taipei, 106. TAIWAN. sfchang@ntu.edu.tw

Suming Chen
Prof., Dept. of Bio-Industrial Mechatronics Eng., National Taiwan Univ., 1, Section 4, Roosevelt Road, Taipei, TAIWAN. TEL+886-2-33665350, schen@ntu.edu.tw

Suraweth Krishnasreni
Emeritus Prof. 24/77 Baan Kasemsan 1, Soi Kasemsan 1 Rama 1 Rd., Wangmai, Pathumwan, Bangkok 10330, THAILAND, surawethk@gmail.com

Surin Phongsupasamit
President, Institute for Promotion of Teaching Science and Technology, 924 Sukumit Rd. Klong Toey Bangkok, THAILAND, surin1950@hotmail.com

Akkapol Senanarong
Agricultural Engineering Research Institue Department of Agriculture, 50 Phaholyothin Rd., Jatuchak Bangkok 10900, THAILAND, akkapol@ksc.th.com

Can Ertekin
Prof., Dpt. of Farm Machinery and Technologies Eng., Faculty of Agril., Akdeniz University, 07070, Antalya, TURKEY. ertekin@akdeniz.edu.tr

Imad Haffar
Managing Director, Palm Water Jumeirah Village (Slte Office Gate #10) Al Khail Road, P.O. Box 215122, Dubai, U.A.E. Tel+971-4-375-1196, imad.haffar@palmwater.ae

Nguyen Hay
Prof., President of Nong Lam Univ., Linh Trung Ward, Thu Duc District, Ho Chi Minh City, VIET NAM. nguyenhay@gmail.com

Pham Van Lang
VIET NAM. langvcd@yahoo.com


S Krishnasreni


S Phong-supasamit


A Senanarong


C Ertekin

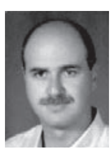
I Haffar


N Hay


P V Lang


T H Katardjiev


P Kic


J Müller


K P Ferentinos


Nick Sigrimis


E Gasparetto


W B Hoogmoed


Y Lobachevsky


M Martinov


J Ortiz-Cañavate


Brian G Sims

-EUROPE-

Tihomir Hristov Katardjiev
General Manager at Yogurtson Trade Ltd., Omachi 216-74, Ichikawa-shi, Chiba-ken 272-0801, Japan (BULGARIA). miro@yogurtson.com

Pavel Kic
Professor, Czech Univ. of Life Sciences Prague, Faculty of Eng. 16521 Prague 6-Suchdol, CZECH REPUBLIC. TEL+420-2-2438314 kic@tf.czu.cz

Joachim Müller
Prof. of the Univ. Hohenheim, Institute of Agril. Eng., Head of Agric.l Eng. in the Tropics and Subtropics, Univ. of Hohenheim, 70593 Stuttgart, GERMANY. TEL+49-711-459-22490, Joachim.mueller@uni-hohenheim.de

Konstantinos P. Ferentinos
Researcher, Dept. of Agricultural Engineering, Institute of Soil & Water Resources, Hellenic Agricultural Organization "Demeter", Ministry of Agriculture and Food of Greece, 61 Dimokratias Av., Athens 13561, GREECE. kpf3@cornell.edu

Nick Sigrimis
Prof., Agricultural University of Athens, Iera Odos 75, Athina 118 55, GREECE. TEL +30-6940940885, ns@aua.gr

Ettore Gasparetto
Former Professor of Agril. Mechanization, Dept. Agril. Eng., Univ. of Milano, Via Galileo Galilei 17, I-35121 Padova, ITALY. TEL+39-0250316619, ettore.gasparetto@unimi.it

W. B. Hoogmoed
Univ. Lecturer, Wageningen Univ., Farm Technology Group, P.O.Box 317, 6708 AA Wageningen NETHERLAND. willem.hoogmoed@wur.nl

Yakov Lobachevsky
Deputy Director of VIM, Federal State Budgetary Science Institution "Federal State Agro Engineering Center VIM", 1st Institutskiy passage, 5., Moscow -109428, RUSSIA. lobachevsky@yandex.ru

Milan Martinov
Prof., Faculty of Technical Sciences, Chair for Biosystems Eng., Novi Sad, SERBIA. TEL+ 381-21-485-2369, MilanMartinov@uns.ac.rs

Jaime Ortiz-Cañavate Puig-Mauri
Dpto. Ingenieria Rural Universidad Politécnica de Madrid, Esc. T. S. Ing. Agrónomos 28040-Madrid SPAIN. TEL+34-91-336-5852, jaime.ortizcanavate@upm.es

Brian G. Sims
FAO Agricultural Mechanization Consultant. 3 Bourneside Bedford MK41 7EG, U.K. BrianGSims@aol.com

Retirement Co-editors' Name List

Co-editor's name	Nationality	Inaugural year	Retired year
Adrian Moens	Netherlands	1972	1989
Bala Krishna Shrestha	Nepal	1972	1991
Chul Choo Lee	Korea	1972	2014
Chau Van Khe	Vietnam	1972	1980
Manbahadur Gurung	Bhutan	1972	2006
Merle L. Esmay	U. S. A.	1972	1990
Giuseppe Pellizzi	Italy	1973	2012
Mohamed A. Bedri	Sudan	1973	1987
Shahansha-Uddin Choudhury	Bangladesh	1973	1991
T. B. Muckle	U. K.	1973	1978
Chang Joo Chung	Korea	1975	2014
T. Touggaard Pedersen	Denmark	1975	1990
Bilash Kanti Bala	Bangladesh	1976	1982
George B. Hanna	Egypt	1976	1988
Jun Sakai	Japan	1976	2015
Siswadhi Soepardjo	Indonesia	1976	1985
Tieng-Song Peng Taiwan	Taiwan	1976	2015
Mohammad Ilyas	Pakistan	1977	1981
Amala Prasad Sharma	Fiji	1978	1981
Arumugam Kandiah	Ethiopia	1978	1989
Bherulal T. Devrajani	Pakistan	1978	2004
John Kilgour	U.K.	1978	2014
Satish Chandra	Fiji	1979	1990
Jitendra P. Mittal	Nigeria	1980	1993
Naresh Chandra Saxena	India	1980	1988
Paris Andereou	Lebanon	1980	1984
Wang Wanjun	China	1981	2012
Allah Ditta Chaudhry	Pakistan	1981	2015
Allan L. Phillips	U. S. A.	1981	2004
Julien G. Van Lancker	Brundi	1981	1989

Co-editor's name	Nationality	Inaugural year	Retired year
Suppiah Kathirkamathamby	Sri Lanka	1981	1991
Armed Hossain Mirdha	Mexico	1982	1991
A. A. Valenzuela	Chile	1982	2013
David Boakye Ampratwum	Ghana	1982	2011
Kshirode Chandra Roy	Bangladesh	1982	1985
M. H. Abdel Aziz	Saudi Arabia	1982	1991
Krishna Prakash Srivastava	Ethiopia	1983	1989
Muhammad Siddique Chaudhry	U. S. A.	1983	1991
Wimala Tissa Weerakoon	Zambia	1983	1985
Harry D. Henderson	Lebanon	1984	1985
Mohammad Afzal	Pakistan	1984	1994
A. P. Kaloyanov	Bulgaria	1985	2013
Soedjatmiko	Indonesia	1986	2014
Aalbert Anne Wanders	Netherlands	1988	2007
Ali Mahmoud El Hossary	Egypt	1988	2010
Chanchai Rojanasaroj	Thailand	1988	2011
Edward A. Baryeh	Zimbabwe	1988	2014
T. P. Ojha	India	1988	2015
Eltag S. Eldin Mahmoud	Sudan	1990	2011
Henrik Have	Denmark	1990	2009
Graeme Ross Quick	Australia	1995	2015
Rafiq ur Rehman	Pakistan	1995	2015
Abdulsamad Abdulmalik Hazza'a	Yemen	1999	2014
Yunus Pinar	Turkey	1983	2016
William J. Chancellor	U.S.A	1972	2017
Kunihiro Tokida	Japan	2016	2017
Shujun Li	China	2012	2018
Jan Pawlak	Poland	2002	2019
Oleg S. Marchenko	Russia	2003	2019

Back Issues

AGRICULTURAL MECHANIZATION IN ASIA, AFRICA AND LATIN AMERICA

(Vol.48, No.3, Summer, 2017-)

■■

INSTRUCTIONS TO AMA CONTRIBUTORS

The Editorial Staff of the AMA requests of articles for publication to observe the following editorial policy and guidelines in order to improve communication and to facilitate the editorial process:

Criteria for Article Selection

Priority in the selection of article for publication is given to those that –

a. are written in the English language;
b. are relevant: to the promotion of agricultural mechanization, particularly for the developing countries;
c. have not been previously published elsewhere, or, if previously published are supported by a copyright permission;
d. deal with practical and adoptable innovations by, small farmers with a minimum of complicated formulas, theories and schematic diagrams;
e. have a 50 to 100-word abstract, preferably preceding the main body of the article;
f. are printed, double-spaced, under 3,000 words (approximately equivalent to 6 pages of AMA-size paper) ; and those that
g. art: supported by authentic sources, reference or bibliography.
h. written in MS DOS format.

Rejected/Accepted Articles

a. As a rule, articles that are not chosen for AMA publication are not returned. At the earliest time possible, the writer(s) is advised whether the article is rejected or accepted.
b. When an article is accepted but requires revision/modification, the details will be indicated in the return reply from the AMA Chief Editor in which case such revision/modification must be completed and returned to AMA within three months from the date of receipt from the Editorial Staff.
c. The AMA does not pay for articles published.
d. Complimentary copies: Following the publishing, three successive issue are sent to the author(s).

Procedure

a. Articles for publication (original and one-copy) must be sent to AMA through the Co-operating Editor in the country where the article originates. (Please refer to the names and addresses of Co-operating Editors in any issue of the AMA). However, in the absence of any Co-operating Editor, the article needs to be sent to Co-operating Editor in the writer's neighboring country. Please note that it is AMA Chief Editor that decide whether publish each submitted paper on AMA or not. Even if Co-operating Editor found your manuscript suitable for publication on AMA, it can not the case with AMA Chief Editor.
b. Contributors of articles for the AMA for the first time are required to attach a passport size ID photograph (black and white print preferred) to the article. The same applies to those who have contributed articles three years earlier. In either case, ID photographs taken within the last 6 months are preferred.
c. The article must bear the writer(s) name, title/designation, office/organization, nationality and complete mailing address.

Format/Style Guidance

a. Article must be sent by E-mail with Word File and PDF File attached.
b. The data for graphs and photographs must be saved into piecemeal data and enclosed (attached) with the article.
c. Whether the article is a technical or popular contribution, lecture, research result, thesis or special report, the format must contain the following features:
(i) brief and appropriate title;
(ii) the writer(s) name, designation/title, office/organization; and mailing address;
(iii) an abstract following ii) above;
(iv) body proper (text/discussion);
(v) conclusion/recommendation; and a
(vi) bibliography
d. Tables, graphs and diagrams must be numbered. Table numbers must precede table titles, e.g., "Table 1 Rate of Seeding per Hectare". Such table number and title must be typed at the top center of the table. On the other hand, graphs, diagrams, maps and photographs are considered figures in which case the captions must be indicated below the figure and preceded by number, e.g., "Fig. 1 View of the Farm Buildings".
e. Papers are printed in black and white. Tables and figures must be made so as to be clearly understood in black and white.
f. **The data for the graph must also be included. (e.g. EXCEL for Windows)**
g. Tables and figures must be preceded by texts or discussions. Inclusion of such tables and figures not otherwise referred to in the text/discussion must be avoided.
h. Tables must be typed clearly without vertical lines or partitions. Horizontal lines must be drawn only to contain the sub-title heads of columns and at the bottom of the table.
i. Express measurements in the metric system and crop yields in metric tons per hectare (t/ha) and smaller units in kilogram or gram (kg/plot or g/row).
j. Indicate by footnotes or legends any abbreviations or symbols used in tables or figures.
k. Convert national currencies **in US dollars** and use the later consistently.
l. Round off numbers, if possible, to one or two decimal units, e.g., 45.5 kg/ha instead of 45.4762 kg/ha.
m. When numbers must start a sentence, such numbers must be written in words, e.g., Forty-five workers..., or Five tractors..."instead of 45 workers..., or, 5 tractors.

SUBSCRIPTION/ORDER FORM

AGRICULTURAL MECHANIZATION IN ASIA, AFRICA AND LATIN AMERICA (AMA)

Issued Quarterly

AMA has Achieved an IMPACT FACTOR!!

AMA has been read by those involved in agricultural machinery and industry all over the world since the first publishment in 1971. Thanks to many contributions from both the readers and writers, in 2012, we have achieved an Impact Factor, established by Thomson Reuters in U.S.A. AMA is the only Japanese agricultural machinery and industry related magazine which achieved an Impact Factor.

Subscription Rate (includes surface mail postage)

Annual (4 issues)........................... ¥8,000
Single copy....................................... ¥2,500

(Check one)
☐ Please send me/us an invoice
☐ I/We enclose remittance for ¥ ___________
☐ Please charge my/our credit card
☐ VISA
☐ MASTER Card. No. ___________________________

Exp. date ___________________________

Signature ___________________________

We deeply appreciate your payment by credit card (NO EXTRA CHARGE NEEDED).
We charge you extra 4,000 JPY when paid by check or wire transfer.

****

Name: ____

Firm: ____

Position: ____

Address: ____

(block letters)

FARM MACHINERY INDUSTRIAL RESEARCH CORP.
1-12-3 Kanda-Nishikicho, Chiyoda-ku, Tokyo 101-0054, Japan
Tel. +81-3-3291-3674, Fax. +81-3-3291-5717
URL: http://www.shin-norin.co.jp
E-Mail: ama@shin-norin.co.jp

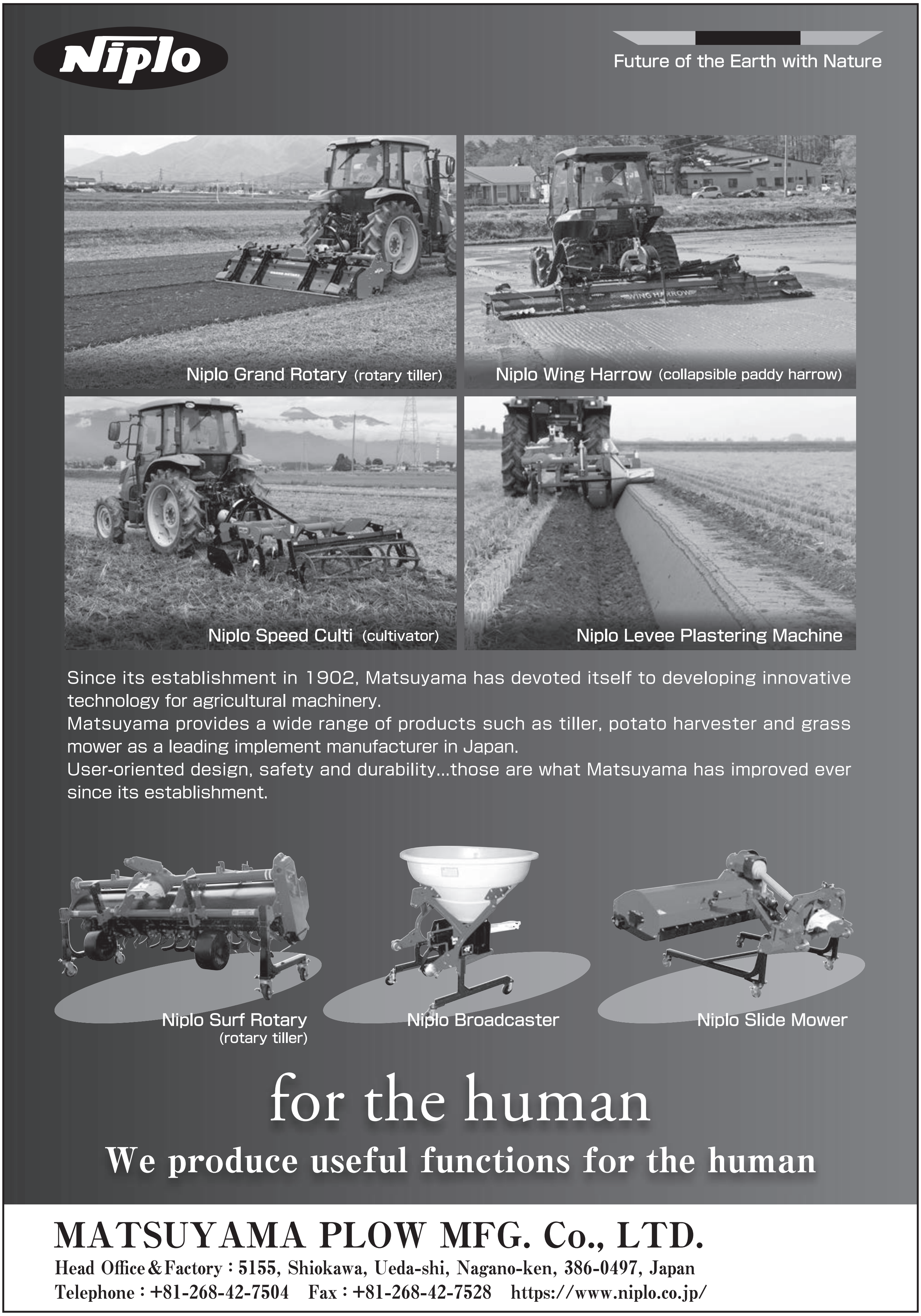
Niplo
Future of the Earth with Nature
Niplo Grand Rotary (rotary tiller)
Niplo Wing Harrow (collapsible paddy harrow)
Niplo Speed Culti (cultivator)
Niplo Levee Plastering Machine
Since its establishment in 1902, Matsuyama has devoted itself to developing innovative technology for agricultural machinery.
Matsuyama provides a wide range of products such as tiller, potato harvester and grass mower as a leading implement manufacturer in Japan.
User-oriented design, safety and durability...those are what Matsuyama has improved ever since its establishment.
Niplo Surf Rotary (rotary tiller)
Niplo Broadcaster
Niplo Slide Mower
for the human
We produce useful functions for the human
MATSUYAMA PLOW MFG. Co., LTD.
Head Office&Factory : 5155, Shiokawa, Ueda-shi, Nagano-ken, 386-0497, Japan
Telephone : +81-268-42-7504 Fax : +81-268-42-7528 https://www.niplo.co.jp/